
Morphological phylogeny of Megachilini and the evolution
of leaf-cutter behavior in bees (Hymenoptera: Megachilidae)

Victor H. Gonzalez, Grey T. Gustafson, & Michael S. Engel



Journal of Melittology

No. 85

ISSN 2325-4467

3 July 2019

On the cover: A female of *Megachile* sp. preparing to take a freshly cut coinvine [*Dalbergia ecastaphyllum* (L.) Taub. (Fabaceae: Faboideae: Dalbergieae)] leaf section back to her nest (Frenchman's Forest Natural Area, Palm Beach County, Florida; photograph by Bob Peterson; used with permission).

Journal of Melittology

Bee Biology, Ecology, Evolution, & Systematics

The latest buzz in bee biology

No. 85, pp. 1–123

3 July 2019

Morphological phylogeny of Megachilini and the evolution of leaf-cutter behavior in bees (Hymenoptera: Megachilidae)

Victor H. Gonzalez^{1,2}, Grey T. Gustafson^{2,3}, & Michael S. Engel^{2,3,4}

Abstract. A unique feature among bees is the ability of some species of *Megachile* Latreille *s.l.* to cut and process fresh leaves for nest construction. The presence of a razor between the female mandibular teeth (interdental laminae) to facilitate leaf-cutting (LC) is a morphological novelty that might have triggered a subsequent diversification in this group. However, we have a limited understanding of the phylogeny of this group despite the large number of described species and the origins and patterns of variations of this mandibular structure are unknown. Herein, using a cladistic analysis of adult external morphological characters, we explored the relationships of all genera of Megachilini and the more than 50 subgenera of *Megachile s.l.* We coded 272 characters for 8 outgroups and 114 ingroup species. Depending on the weighting scheme (equal or implied weighting), our parsimony analyses suggested the monophyly of *Megachile s.l.* and that either *Noteriades* Cockerell or the clade *Coelioxys* Latreille + *Radoszkowskiana* Popov is the extant sister group of all other Megachilini. In addition, we conducted Bayesian total-evidence tip-dating analyses to examine other possible hypotheses of relationships and patterns of variation of the interdental lamina. Our analyses suggest that interdental laminae developed asynchronously from two different structures in the mandible, and differ in their phenotypic plasticity. Character correlation tests using phylogenetic pairwise comparisons indicated that the presence of interdental lamina is not associated with head size, mandible size and shape, and pubescence on the adductor interspace. We discuss the implications of our findings for the classification of Megachilini and the development of novel evolutionary, ecological, and functional hypotheses on this behavior. New taxa established are **Pseudoheriadini** Gonzalez & Engel, new tribe, **Ochreriadini** Gonzalez & Engel, new tribe, **Cremnomegachile** Gonzalez & Engel, new genus, **Rozenapis** Gonzalez & Engel, new genus, and **Saucrochile** Gonzalez & Engel, new genus, along with the following **new combinations**: *Cremnomegachile dolichosoma* (Benoist), new combination, *Rozenapis ignita* (Smith), new combination, and *Saucrochile heriadiformis* (Smith), new combination.

¹ Undergraduate Biology Program, Haworth Hall, 1200 Sunnyside Avenue, University of Kansas, Lawrence, Kansas 66045, USA (victorgonzab@gmail.com).

² Department of Ecology & Evolutionary Biology, Haworth Hall, 1200 Sunnyside Avenue, University of Kansas, Lawrence, Kansas 66045, USA (gtgustafson@gmail.com).

³ Division of Entomology, Natural History Museum, 1501 Crestline Drive – Suite 140, University of Kansas, Lawrence, Kansas 66045-4415, USA (msengel@ku.edu).

⁴ Division of Invertebrate Zoology, American Museum of Natural History, Central Park West at 79th Street, New York, New York 10024-5192, USA.

doi: <http://dx.doi.org/10.17161/jom.v0i85.11541>

CONTENTS

Abstract	1
Introduction	3
Diversity of Megachilidae	6
Diversity and Phylogeny of Megachilini	7
What is the Genus <i>Megachile</i> ?	7
Fossil Record	9
Material and Methods	10
Morphological Phylogeny of Megachilini	10
Taxon sampling	10
Morphological data	11
Data compilation	11
Data characterization	26
Phylogenetic analyses	26
Phylogenetic signal of morphological characters	28
Origin of the Interdental Lamina in the Female Mandible	28
Evolutionary Origins of the Interdental Lamina	29
Molecular data	29
Combined data	30
Phylogenetic analyses	30
Patterns of variation of the interdental lamina	33
Results	33
Morphological-based Phylogeny of Megachilini	33
Phylogenetic signal	34
Origin and Evolution of the Interdental Lamina	35
Combined phylogenies	35
Types of interdental lamina	36
Evolution of the interdental lamina	39
Discussion	40
Phylogenetic Relationships within Megachilini	40
Monophyly of subgenera of <i>Megachile s.l.</i>	43
Phylogenetic signal of morphological characters	44
Origins and Patterns of Variation of the Interdental Lamina	45
Origin of Leaf-cutting Behavior	45
Classificatory Implications	48
Family Megachilidae	48
Tribe Megachilini	50
Conclusions and Future Directions	54
Limitations of the Study	55
Descriptions of New Taxa	56
Key to extant tribes of Megachilinae	56
Pseudoheriadini Gonzalez & Engel, new tribe	57
Ochrieriadini Gonzalez & Engel, new tribe	58
<i>Cremnomegachile</i> Gonzalez & Engel, new genus	58
<i>Rozenapis</i> Gonzalez & Engel, new genus	60
<i>Saucrochile</i> Gonzalez & Engel, new genus	62
Acknowledgements	63
References	63
Appendices 1–7	72

INTRODUCTION

A unique behavior among bees is the ability to cut and process fresh leaves for nest construction. Using their mandibles, the females cut and collect circular to elliptical leaf pieces, leaving distinct excision patterns along the margin of leaves. The bees then use these leaf pieces to line and separate the brood cells, which they build in the ground or inside pre-existing cavities (e.g., Michener, 1953). This leaf-cutter (LC) behavior is exclusive to a group of solitary bees in the genus *Megachile* Latreille (Groups 1 and 3 of Michener, 2000, 2007), the most ecologically and morphologically diverse group of the family Megachilidae with a problematic taxonomy (Fig. 1C–G). This genus includes a number of introduced species (e.g., Cane, 2004; Rasmussen *et al.*, 2012), many highly promising pollinators, and *Megachile (Eutricharaea) rotundata* (Fabricius), the most intensively managed and produced solitary bee in the world for the production of alfalfa (Pitts-Singer & Cane, 2011).

A good knowledge of LC behavior is essential to gain a better understanding of species' biologies, predict species distributions, and improve current management practices for commercial and conservation purposes (Sinu & Bronstein, 2018). However, limited information is available on which species of plants are used by LC bees and by which bee species. In addition, the majority of records are from common bees in urban or agricultural areas (MacIvor, 2016; Kambli *et al.*, 2017; Sinu & Bronstein, 2018). Such limitations are surely a reflection of the challenges associated with finding nests, identifying plants from leaf fragments, and LC bees' taxonomic problems (Michener, 2007; Gonzalez *et al.*, 2013). Significantly, less information is yet available on the evolutionary history of this behavior and the mandibular structures involved in leaf cutting.

Unlike other bees, megachilids do not line their cells with hydrophobic secretions of the Dufour's gland; instead, they rely on the physicochemical properties of the foreign material used for nesting (Williams *et al.*, 1986). In the case of LC bees, certain phytochemicals (e.g., saponins) might increase larval mortality (Horne, 1995), while others (e.g., flavonoids, phenols, terpenoids) might decrease it by providing protection against microbes (MacIvor, 2016; Sinu & Bronstein, 2018). Therefore, it is not surprising that available data suggest that LC bees are highly selective in their plant and leaf choices, avoiding latex-producing plants, and preferring species with glabrous leaves, particularly in the families Fabaceae and Rosaceae (Michener, 1953; Kambli *et al.*, 2017; Sinu & Bronstein, 2018).

The female mandible of LC bees varies considerably in its overall length and shape, as well as in the number and shape of its teeth (Fig. 2). It also has a distinct lamina in one or more spaces between the teeth, which authors have called 'interdental lamina' (Pasteels, 1965) or 'cutting edges' (Michener, 1962). Doubtless, this structure is an evolutionary novelty among bees because it is unique to this group and its appearance might have triggered a subsequent diversification within LC bees. Presently, the total number of LC bees accounts for about 57% of the species in Megachilini (Michener, 2007).

The presence or absence of this interdental lamina, as well as its size and shape, varies among species and species groups. Available information indicates that such variations correlate with different modes of leaf-cutting behavior and have been useful in the taxonomy of the group. Species with a lamina that entirely fills the space between teeth generally exhibit extensive LC behavior; their brood cells are entirely made of smooth-margined leaf pieces (e.g., Kambli *et al.*, 2017; Gonzalez *et al.*, 2018).

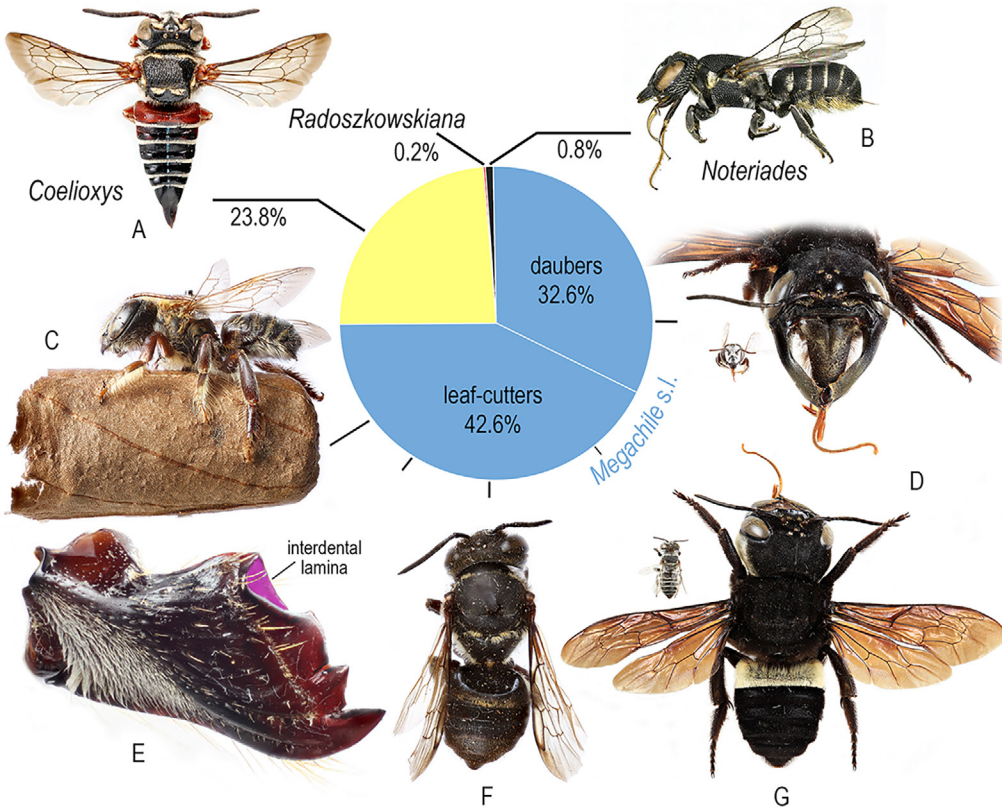


Figure 1. Species richness of currently recognized genera in the bee tribe Megachilini. **A.** Dorsal habitus of a female of *Coelioxys* sp. **B.** Lateral habitus of a female of *Noteriades spinosus* Griswold & Gonzalez. **C.** Male of *Megachile (Zonomegachile) kalina* Gonzalez, Griswold, & Engel on top of a brood cell built with leaf pieces. **D.** Facial habitus of leaf-cutter *M. (Eutricharaea) minutissima* Radoszkowski (left) and dauber bee *M. (Callomegachile) pluto* (Smith) (right). **E.** Outer surface of the female mandible of *M. (Leptorachis) laeta* Smith, a leaf-cutter bee, showing interdental lamina in pink. **F.** Dorsal habitus of *M. (Rhyssomegachile) kartaboensis* Mitchell. **G.** Dorsal views of *M. (E.) minutissima* (upper left) and *M. (C.) pluto* (right). Photographs are not at the same scale, except for the large and small species compared in figures D and G.

In contrast, species with incomplete lamina (not entirely filling spaces between teeth) or without it, have more limited LC behavior, with their brood cells made of a combination of mud and leaf or petal pieces, which are irregularly cut, often with serrate margins (Michener, 2007; Soh, 2014). The absence of this lamina in the mandible of some species that still exhibit LC behavior indicates that other structures are also involved in leaf cutting. Similarly, the morphological diversity of the mandible also suggests different mechanical solutions to diverse functional problems. However, no one has yet attempted to understand the origins and patterns of variations of these mandibular structures using a phylogenetic framework. To date, the phylogenetic relationships among the four genera of Megachilini (*Coelioxys* Latreille, *Megachile* s.l., *Noteriades* Cockerell, and *Radoszkowskiana* Popov), as well as that of the more than 50 subgenera of *Megachile* s.l., are largely unexplored. Besides an unpublished dissertation (Gonzalez, 2008), the only phylogenetic hypothesis available is that of Trunz *et al.* (2016) using molecular data.



Figure 2. Leaf excisions and a sampling of the morphological diversity among the female mandible of leaf-cutter bees. **A.** Leaves of *Rosa* sp. (Rosaceae) from Lesvos, Greece. **B.** Fossil leaf cut (Fabaceae) from Eckfeld Maar, Germany (~43 Ma). **C–J.** Outer view of the mandible showing interdentary laminae in green (odontogenic) and pink (ctenogenic). **C.** *Megachile* (*Chrysosarus*) *parsonsiae* Schrottky. **D.** *M.* (*Rhyssemegachile*) *simillima* Smith. **E.** *M.* (*Pseudocentron*) *pruina* Smith. **F.** *M.* (*Zonomegachile*) sp. **G.** *M.* (*Moureapis*) *maculata* Smith. **H.** *M.* (*Melanosarus*) *xylocopoides* Smith. **I.** *M.* (*Acentron*) *albitarsis* Cresson. **J.** *M.* (*Leptorachis*) *petulans* Cresson. Abbreviations: Mt = mandibular tooth.

Several authors have recorded fossilized dicotyledonous leaves with distinctive cuts along their margins, similar to those caused by LC bees (Figs. 2A, B). Those trace fossils are from deposits in Europe, North and South America, and the oldest is approximately 60 Ma (e.g., Labandeira, 2002; Wedmann *et al.*, 2009; Michez *et al.*, 2012). Comparative analyses of the ellipse eccentricity between leaf discs of brood cells of living species and fossil excisions, support the attribution of these trace fossils to LC bees (Sarzetti *et al.*, 2008). However, molecular analyses using a node-dating approach,

which places the oldest fossil to the youngest internal node and thus imposes the age of the fossil as a minimum age constraint, suggest that LC bees originated around 20–25 Ma (Litman *et al.*, 2011; Trunz *et al.*, 2016). Other dating approaches might be useful for investigating this temporal discrepancy, such as Bayesian total-evidence tip dating, which utilizes morphological data to infer the placement of fossils within the phylogeny (as terminals or ‘tips’) in order to calibrate the tree. Therefore, tip-dating does not require the *a priori* constraint of taxa to nodes in order to generate age estimates, and allows the use of all available fossils within a group, extending age estimates beyond the minimum age for clades (Ronquist *et al.*, 2012a). Unfortunately, despite the existence of fossil megachilids, such analyses are not yet available for these or any other group of bees.

Considering the biological importance of the LC behavior in the evolution and diversification of this group of pollinators, we set the following goals: First, to explore the relationships of the genera of Megachilini and the subgenera of *Megachile s.l.* using adult morphological data. Second, to determine the possible origins of the interdental lamina in the female mandible. Third, to explore possible patterns of variation of the interdental lamina. Fourth, to examine the implications of our phylogenetic results on the classification of Megachilidae and Megachilini. In addition, to examine other possible patterns of variation of the interdental lamina, we conducted preliminary Bayesian total-evidence tip-dating analyses. We conducted two sets of analyses aimed at obtaining more accurate divergence time estimates because available analyses (*e.g.*, Litman *et al.*, 2011; Trunz *et al.*, 2016) employed a node-dating approach to estimate the origin of LC bees. Thus, we first conducted a phylogenetic analysis of all tribes in Megachilidae and then used the divergence-time estimates generated from that analysis to inform priors for the phylogenetic analysis of the genera of Megachilini. In the following sections, we provide an overview of the diversity, fossil record, and phylogeny of megachilids, highlighting outstanding problems in their classification. Unless otherwise indicated, we followed Michener’s (2000, 2007) subgeneric classification of *Megachile s.l.* to facilitate comparisons (Appendix 1).

Diversity of Megachilidae

Megachilidae are the third largest bee family containing more than 4100 species worldwide (Michener, 2007; Ascher & Pickering, 2018). Megachilids utilize a high diversity of nesting materials and substrates. For example, they use mud, petals, leaves (intact pieces or macerated to a pulp), resins, gravel, and plant trichomes to build their brood cells in the soil, attached to twigs, under surfaces of rocks, or inside pre-existing cavities including man-made constructions (*e.g.*, Rozen *et al.*, 2010; Gonzalez & Griswold, 2013). The most recent higher-level classificatory proposal for the family (Gonzalez *et al.*, 2012) recognizes four subfamilies and nine tribes, three of which are extinct (Ctenoplectrellini, Glyptapini, and Protolithurgini). Morphological (Gonzalez *et al.*, 2012) and molecular data (Litman *et al.*, 2011) support the monophyly of these tribes, except that of Osmiini, which has long been suspected to be paraphyletic (*e.g.*, Engel, 2001; Michener, 2007; Praz *et al.*, 2008). In these morphological and molecular analyses, either Megachilini or Megachilini + Dioxyini renders Osmiini paraphyletic. The phylogenetic relationships of Dioxyini are also still not clear. This small monophyletic group of cleptoparasitic bees (~36 spp.) appeared as sister of *Aspidosmia* Brauns (Aspidosmiini) in the molecular analysis, but in the morphological analysis it was the sister group of Megachilini.

Diversity and Phylogeny of Megachilini

Megachilini contain about half of the species of the family (~2000 spp.: Michener, 2007; Ascher & Pickering, 2018). The most widely used classificatory proposal for bees worldwide (Michener, 2007) recognizes a free-living genus *Megachile*, and two cleptoparasitic genera, *Coelioxys* (Fig. 1A) and *Radoszkowskiana*. Gonzalez *et al.* (2012) transferred from the Osmiini another free-living genus, *Noteriades* (Fig. 1B). All genera of Megachilini seem monophyletic, except for *Megachile*.

Coelioxys is cosmopolitan in distribution and includes about 470 species grouped in 15 subgenera in the classification of Michener (2007), but several Neotropical taxa synonymized by him are still recognized by some authors (*e.g.*, Moure *et al.*, 2007). *Coelioxys* are commonly collected bees and frequently found parasitizing other megachilids and some apids. Multiple authors have studied their behavior and immatures (references in Michener, 2007). *Radoszkowskiana* includes only four species restricted to the Palearctic region, which are morphologically and behaviorally similar to *Coelioxys* (Rozen & Kamel, 2007). Rocha Filho & Packer (2017) explored phylogenetic relationships among the subgenera of *Coelioxys*.

Noteriades includes 16 species that occur across tropical and subtropical regions of sub-Saharan Africa, India, and Southeast Asia. The biology of this group of bees is unknown (Griswold & Gonzalez, 2011). Species are small, heriadiform or hoplitiiform in body shape, and non-parasitic considering the presence of a metasomal scopa. Griswold (1985) first suggested the close relationship of this genus with Megachilini, which molecular (Praz *et al.*, 2008; Litman *et al.*, 2011) and morphological analyses (Gonzalez *et al.*, 2012) supporting his conclusion.

Remaining species of Megachilini (~1500 spp.) are in *Megachile*, a genus that includes both LC bees and species that primarily use mud or resins as nesting materials. The genus occurs in a wide diversity of habitats on all continents, ranging from lowland tropical rain forests, deserts, to high elevation environments. In appearance, species of *Megachile* range from nearly bare, elongate, parallel-sided bees to robust, setose bees resembling some smaller bumble bee species; their body length ranges from about 4 mm in *M. (Eutricharaea) minutissima* Radoszkowski, to nearly 40 mm in *M. (Callomegachile) pluto* Smith, the longest bee in the world (Figs. 1D, G). As we briefly describe below, the taxonomy of *Megachile* is problematic and its phylogenetic relationships largely unexplored.

What is the Genus *Megachile*?

The concept of *Megachile* has changed multiple times since its conception. Latreille (1802) proposed *Megachile* for the European species *Apis centuncularis* Linnaeus, and it initially included not only species of this genus as currently defined, but also species that now belong to different tribes of Megachilidae. Later, Lepeletier de Saint Fargeau (1841) proposed the genus *Chalicodoma* for another European species, *Apis muraria* Olivier. During the second half of the 1800's, as well as during the first decades of the 1900's, several authors (*e.g.*, Smith, 1865; Thomson, 1872; Provancher, 1882; Meunier, 1888; Friese, 1899; Robertson, 1901, 1903; Cockerell, 1907, 1922; Mitchell, 1924) proposed a number of generic or subgeneric names for closely allied taxa to *Megachile* from different regions of the world. Until the late 1800's, most authors recognized both *Megachile* and *Chalicodoma* as morphologically and biologically distinct groups, the first consisting of LC bees and the second of species that use mud or resins to build

their nests (e.g., Gerstaecker, 1869; Radoszkowsky, 1874; Taschenberg, 1883). However, Dalla Torre (1896) appears to be the first to have treated *Chalicodoma* as a subgenus of *Megachile*, a position followed by Friese (1898, 1899, 1909, 1911a, 1911b). The latter author (Friese, 1911a) also recognized two previously described taxa, *Thaumatossoma* Smith and *Stellenigris* Meunier, as genera closely related to *Megachile*.

Mitchell (1933) also considered *Megachile* in a broad sense following earlier authors. He regarded *Thaumatossoma* and other generic names proposed until then as subgenera of *Megachile*, including some that Friese (1911a, 1911b) did not mention. In subsequent years, Mitchell (1935a, 1935b, 1936a, 1936b, 1937a, 1937b, 1937c, 1943) proposed several new taxa from the Western Hemisphere and revised their species in a series of monographs that stand until today as major or only resources of regional identification for these bees.

Based on the generic concepts previously used and the discovery of some morphological features that correlated with nesting behavior, Michener (1962, 1965) divided *Megachile* into three genera (*Chalicodoma*, *Creightonella* Cockerell, and *Megachile*). *Chalicodoma* included Eastern Hemisphere species with a strongly convex and rather parallel-sided metasoma and female mandibles without interdental laminae (Figs. 1D, G); those morphological features are associated with narrow burrows and the use of mud or resin as nesting materials. In contrast, *Megachile* included a cosmopolitan group of bees with a flattened metasoma and female mandibles with interdental laminae, features that allow them to cut and use leaf or petal pieces for constructing cells in wider burrows. *Creightonella* combined features of both genera, a female mandible with interdental laminae to cut leaves, and a strongly convex, parallel-sided metasoma. *Creightonella* included a relatively small number of species (50 spp.) restricted to the Eastern Hemisphere. Pasteels (1965) also independently developed the same classificatory scheme of Michener (1962, 1965) when considering the African fauna. Both authors, C.D. Michener and J.J. Pasteels, not only described several subgenera within *Megachile* and *Chalicodoma*, but also rendered as subgenera a few other generic names proposed at the time.

In 1980, when T.B. Mitchell revised the LC bees from the Western Hemisphere, he adopted the multigeneric proposal of Michener (1962, 1965) in recognizing three genera. However, he further divided *Megachile* into six genera, each with multiple subgenera. Although he was not concerned with the Eastern Hemisphere fauna, he made an effort to summarize and place this fauna within his classificatory scheme, which was not widely adopted (Appendix 1).

Despite having divided *Megachile* into three genera in the 1960's, Michener (2000, 2007) no longer recognized them when treating the world fauna because of the exceptions and intergradations he later observed in the main morphological features, as well as for almost all other features he had previously used to characterize these groups. In particular, *Megella* Pasteels and *Mitchellapis* Michener represented major problems within his system. Although Pasteels (1965) and Michener (1965) initially placed both taxa in *Megachile*, they exhibit features of both *Megachile* and *Chalicodoma*. For example, typical *Megachile* characteristics are the interdental laminae in the female mandible and the apex of the female sixth sternum with a fringe of short, dense plumose setae. Features typical of *Chalicodoma* include the elongate, parallel-sided body, apex of the female tibiae with a distinct, sharp spine, and the presence of setae on the lateral margins of the male eighth sternum. Michener (2000, 2007) also synonymized certain subgeneric names that authors created for unusual species and organized the more than 50 subgenera into three informal groups, which corresponded to each genus that

he previously recognized in the 1960's. That is, Groups 1, 2, and 3, are equivalent to the genera *Megachile*, *Chalicodoma*, and *Creightonella*, respectively, in Michener's (1962, 1965) earlier classification (Appendix 1). Because of the presence of marginal setae on the eighth sternum of the male, Michener (2000, 2007) placed these two "problem" taxa (*Mitchellapis* and *Megella*) in Group 2 (*Chalicodoma*), not in Group 1 (*Megachile*) as he (Michener, 1965) and Pasteels (1965) initially assigned them. Another subgenus that also bridged the gap between *Megachile* and *Chalicodoma* was *Chelostomoda* Michener. Michener (1962) described this group as a subgenus of *Chalicodoma* even though it also possesses interdental laminae as in *Megachile*.

Today, there is no consensus in the classification of *Megachile*. Some authors still follow Michener's earlier classification (Michener, 1962, 1965) in recognizing the genera *Chalicodoma*, *Creightonella*, and *Megachile*, including several subgenera that were proposed for species with aberrant or unusual morphologies and that Michener (2000, 2007) synonymized (e.g., Silveira *et al.*, 2002; Durante & Abrahamovich, 2006; Moure *et al.*, 2007; Ornos *et al.*, 2007). Other authors (Trunz *et al.*, 2016) recognize a few other taxa at the generic level, as they were initially proposed (*Gronoceras* Cockerell and *Heriadopsis* Cockerell) or were suggested by Michener (2007) as an alternative classification (*Matangapis* Baker & Engel). The species-level systematics of *Megachile s.l.* (*sensu* Michener 2000, 2007) is also problematic and thus species identifications are challenging in most groups. Taxonomic revisions for the majority of the subgenera are not available, keys to species are lacking, and many species have not been properly associated with any of the known subgenera (Michener, 2000, 2007). Even in North America, many species are still known from a single sex or from a small number of specimens (Sheffield & Westby, 2007; Gonzalez *et al.*, 2013, 2018).

The phylogenetic relationships among the genera of Megachilini, as well as the subgenera of *Megachile s.l.*, are largely unexplored. Michener (2000, 2007) suggested that *Coelioxys* might render *Megachile s.l.* paraphyletic because it shares some morphological traits, particularly with *Chelostomoides* Robertson. Likewise, the recent inclusion of *Noteriades* in Megachilini might also render *Megachile s.l.* paraphyletic considering that this genus shares the presence of arolia (a rare feature in Megachilini, typical of Osmiini) with *Matangapis* and *Heriadopsis*. An unpublished dissertation (Gonzalez, 2008) explored the relationships within Megachilini using morphological data but did not include *Noteriades*. Similarly, the positions of *Matangapis* and *Heriadopsis* were unclear in a recent molecular analysis (Trunz *et al.*, 2016), as both taxa nested in a clade consisting of *Coelioxys* and *Radoszkowskiana*. Doubtless, species-level revisionary studies and phylogenetic analyses are required to develop a more stable taxonomy and phylogeny-based classification of *Megachile s.l.*

Fossil Record

Engel (1999, 2001), Engel & Perkovsky (2006), and Michez *et al.* (2012) summarized the fossil record for Megachilidae. The extinct tribes Protolithurgini, Ctenoplectrellini, and Glyptapini contain several species in five genera (*Protolithurgus* Engel, *Ctenoplectrella* Cockerell, *Glaesosmia* Engel, *Friccomelissa* Wedmann *et al.*, and *Glyptapis* Cockerell) all from the Eocene (33.9–56 Ma) and many in Baltic amber. The first tribe is sister to all Lithurginae while the remaining two are sisters to all Megachilinae, except Aspidosmiini which might render Ctenoplectrellini paraphyletic (Gonzalez *et al.*, 2012). For Megachilini, most records are trace fossils of dicotyledonous leaves with excisions along the margins, similar to those caused by LC bees of the genus *Megachile s.l.* (Wed-

mann *et al.*, 2009; Engel & Perkovsky, 2006; Sarzetti *et al.*, 2008). Body compressions are few and have not been associated to any subgenus. *Megachile glaesaria* Engel, from the Miocene Dominican amber (*ca.* 17 Ma), is the best-preserved fossil of Megachilini. Engel (1999) noted the close resemblance of this species to some species of the extant North American *Chelostomoides*. However, he placed it in its own subgenus, *Chalicodomopsis* Engel, because of the presence of a small inner tooth in the pretarsal claws and some wing features, which are present in both Megachilini and Anthidiini. He also suggested that *M. glaesaria* might be a basal member of the Group 2 of subgenera or sister to all Megachilini. To date, the phylogenetic position of *M. glaesaria* is unknown.

MATERIAL AND METHODS

Morphological Phylogeny of Megachilini

TAXON SAMPLING: We used eight taxa as outgroups based on the phylogeny of Gonzalez *et al.* (2012) and 114 species of Megachilini as follows: one species of *Noteriades*, one species of *Radoszkowskiana*, three species of *Coelioxys*, and 109 species of *Megachile s.l.* The latter genus is represented by species of 57 subgenera that included those recognized by Michener (2007), the fossil species *M. glaesaria* (Engel, 1999), and four recently described taxa by Baker & Engel (2006), Engel & Baker (2006), Engel & Gonzalez (2011), and Gonzalez & Engel (2012) (Appendix 2). For each subgenus of *Megachile s.l.*, we included the type species and, to maximize variation, when available at least one morphologically divergent species from it, or species separated subgenerically but synonymized by Michener (2000, 2007), Gonzalez *et al.* (2010), Gonzalez & Engel (2012), and Gonzalez (2013). About half of the subgenera are represented by one species because they either are monotypic (10 subgenera) or seemed morphologically uniform (20 subgenera). The only three subgenera of *Megachile s.l.* that we were not able to examine are *Austrosarus* Raw, *Neochalicodoma* Pasteels, and *Stellenigris* Meunier. However, Gonzalez & Engel (2012) and Gonzalez (2013) considered the first as a synonym of *Chryosarus* Mitchell and the second as a synonym of *Pseudomegachile* Friese, subgenera represented by several species in our analyses. The identity and correct taxonomic placement of *Stellenigris* is a mystery. Michener (2000, 2007) suggested that it might belong to large species of the Group 2 of *Megachile s.l.*, but the type specimen of *Stellenigris vandeveldeii* Meunier, 1888, is probably lost or perhaps destroyed, along with other insects described by F. Meunier (Engel, 2007).

Most specimens studied are in the Snow Entomological Collection, University of Kansas Natural History Museum, although we borrowed specimens of a few rare species from the following institutions (names of the people who kindly arranged these loans are in parentheses): Academy of Natural Sciences of Drexel University, Philadelphia, PA (D. Otte, J. Weintraub); American Museum of Natural History, New York (J.G. Rozen, Jr.); Bee Biology and Systematics Laboratory, USDA-ARS, Utah State University, Logan, UT (T. Griswold, H. Ikerd); the Natural History Museum, London, UK (D. Notton); Department of Terrestrial Invertebrates, Western Australian Museum, Welshpool (T. Houston); Illinois Natural History Survey, Urbana, Illinois, USA (P. Tinerella); Museum of Comparative Zoology, Harvard University, Cambridge, MA (P. Perkins, R.L. Hawkins); Musée Royal de L'Afrique Centrale, Tervuren (A. Pauly, E. De Coninck); Museum für Naturkunde der Humboldt-Universität, Berlin, Germany (F. Koch, V. Ritcher); North Carolina State University Insect Museum, Raleigh, NC (Rob Blinn); Oxford University Museum of Natural History, Oxford, UK (J. Hogan); and United States

National Museum of Natural History, Washington, D.C. (D. Furth, B. Harris).

MORPHOLOGICAL DATA: Morphological terminology generally follows that of Michener (2000, 2007) and Engel (2001), except for 'torulus' and 'interdental lamina', which we use herein instead of 'antennal socket' and 'cutting edge'. The first term is in broader application across Hymenoptera while the second describes more accurately the laminae between the teeth of the female mandible that characterizes the majority of LC bee species. 'Cutting edges' have widely been used in the taxonomic literature of *Megachile s.l.* (e.g., Michener, 1962, 2007) but these terms are functionally and structurally ambiguous. They imply that these are the only structures used in cutting leaves and do not inform on their shape nor on their location in the mandible. The absence of interdental laminae in some species of *Megachile s.l.* (e.g., *Chrysosarus*) that also cut leaves or even petals [e.g., *M. (Megachile) montivaga* Cresson] (e.g., Zillikens & Steiner, 2004; Torretta *et al.*, 2014; Orr *et al.*, 2015) clearly indicates that these are not the only mandibular structures involved in leaf cutting. For example, the upper and lower margins of each tooth are sometimes thin and sharp, and they might function as razors even when the interdental laminae are present. Thus, as initially proposed by Pasteels (1965), the term interdental laminae seems more appropriate than cutting edges to describe the laminae between the teeth. Terminology for the mandible, proboscis, and female's sting apparatus and associated sterna follows Michener & Fraser (1978), Winston (1979), and Packer (2003, 2004), respectively.

DATA COMPILATION: We conceptualized and scored the majority of character statements from searching on all parts of the body of both male and female sexes, including the labiomaxillary complex, mandible, and genitalia with its associated terga and sterna. We also took and modified some character statements from the cladistic analyses of Roig-Alsina & Michener (1993) and Gonzalez *et al.* (2012). During the conception and formulation of character statements, the following comparative studies and taxonomic revisions were useful for character selection as they mentioned or discussed morphological features of taxonomic importance: Michener (1962, 1965, 2000, 2007), Michener & Fraser (1978), Winston (1979), Mitchell (1980), and Roig-Alsina & Michener (1993).

We examined and measured morphological features using Olympus SZ60 and SZX12 stereomicroscopes with an ocular micrometer. We cleared the labiomaxillary complex and genitalia with 10% KOH at room temperature for about 24h. Then, we washed them with 70% ethanol before storing them in glycerin. To document character states, we prepared line illustrations as well as photomicrographs, which we took with a Canon 7D digital camera attached to an Infinity K-2 long-distance microscope lens, and assembled with Zerene Stacker™ software package. We processed final figures with Adobe Photoshop® CC.

We built a data matrix in WinClada (Nixon, 1999) and scored 272 characters (Appendix 3). However, we were not able to code all characters for all species because some taxa are known only from the type specimen and we could not dissect them, and in other cases, they are only known from one sex. Unless we suspected sexual dimorphism, we took characters from the available sex. We only used continuous characters, such as proportions or measurements, when we found distinct gaps in the measured variable among the examined specimens. To avoid duplication, we coded only in the female those characters that are unequivocally present in both sexes (e.g., labiomaxillary complex).

To facilitate further comparisons, we formulated character statements following Sereno (2007), in which the most general locator is positioned first (e.g., antennal scape), followed by a variable (e.g., length), a variable qualifier (e.g., length relative to torulocellar distance), and mutually exclusive character states, the latter following a colon.

In some cases, we added a secondary or tertiary locator to clarify the position of the primary locator.

The following are the descriptions of the character statements used in the generic-level analysis of Megachilini. We indicated the original author of a character statement and used the following abbreviations F, OD, PW, Mt, S, and T for flagellomere, median ocellus diameter, one puncture width, mandibular tooth, and metasomal sterna and terga, respectively.

Female

Head

1. Subantennal area (*i.e.*, clypeoantennal distance), length relative to vertical diameter of torulus (Gonzalez *et al.*, 2012: char. 4): 0 = short, equal to or shorter than; 1 = long, $\geq 1.2\times$.
2. Anterior tentorial pit, location (Roig-Alsina & Michener, 1993: char. 2): 0 = at the intersection of subantennal and epistomal sulci; 1 = on epistomal sulcus, below intersection with subantennal sulcus.
3. Anterior tentorial pit, shape: 0 = rounded, about as long as broad; 1 = elongate, about twice as long as broad.
4. Interantennal area (*i.e.*, intertorular distance), length relative to torulorbital distance (Gonzalez *et al.*, 2012: char. 9): 0 = equal to or shorter than; 1 = greater than.
5. Antenna, scape, length (excluding basal bulb) relative to torulocellar distance: 0 = equal to or shorter than; 1 = long, $\geq 1.2\times$.
6. Antenna, pedicel, length relative to length of F1 (modified from Gonzalez *et al.*, 2012: char. 13): 0 = short, at most as long as; 1 = long, $\geq 1.5\times$. In character state 1, the pedicel is often about as long as or longer than length of F1 and F2 combined.
7. Antenna, F1, length relative to F2: 0 = 1.5–2.0 \times longer than; 1 = about as long as; 2 = shorter than.
8. Vertex, integument, with fine, shining longitudinal line from ocelli to its posterior margin: 0 = absent; 1 = present.
9. Paraocular carina (Roig-Alsina & Michener, 1993: char. 4): 0 = absent; 1 = present.
10. Preoccipital carina (Gonzalez *et al.*, 2012: char. 18): 0 = absent; 1 = present.
11. Preoccipital carina, dorsal edge of head behind vertex (modified from Gonzalez *et al.*, 2012: char. 19): 0 = present; 1 = absent.
12. Ocelloccipital area, length relative to OD (Gonzalez *et al.*, 2012: char. 20): 0 = short, 1.0–3.0 \times ; 1 = long, $\geq 3.1\times$.
13. Hypostomal area, short transverse carina: 0 = absent; 1 = present. This short carina encloses a small, shiny, depressed area, behind the mandible and is present in the female of *Melanosarus* Mitchell.
14. Hypostomal carina, posterior portion, tooth or strong protuberance: 0 = absent; 1 = present, distinct. In most species, the hypostomal carina gently curves from the base of the mandible (ventral portion) to behind the head (posterior portion), but in some species a distinct tooth or strong protuberance develops where the ventral portion flexes upwards behind the head.
15. Hypostomal carina, ventral portion, orientation relative to margin of mandibular socket (Gonzalez *et al.*, 2012: char. 21): 0 = directed to medial margin; 1 = curving towards posterior margin (Griswold & Gonzalez, 2011: fig. 13).
16. Supraclypeal area, lower portion, shape (modified from Gonzalez *et al.*, 2012: char. 8): 0 = flat, elevated or modified, not strongly convex in profile; 1 = strongly convex in profile.
17. Clypeus, width relative to mid length: 0 = short, $\geq 3.0\times$; 1 = long, $\leq 2.8\times$.
18. Clypeus, basal portion, shape: 0 = flat or convex, not greatly elevated or ornate; 1 = greatly elevated and ornate.
19. Clypeus, disc, shape: 0 = flat or convex, not elevated; 1 = elevated with flat median section.
20. Clypeus, distal margin, degree of projection over labroclypeal articulation (Gonzalez *et al.*, 2012: char. 1): 0 = not projected, articulation clearly visible (Fig. 1D; Engel & Gonzalez, 2011:

- fig. 8); 1 = slightly projected, articulation not visible (Gonzalez & Engel, 2012: fig. 4); 2 = strongly projected, articulation not visible (Eardley, 2012: fig. 43a). In species having character state 2, the strongly projected distal margin makes the clypeus hexagonal in shape, as in *Chalicodoma*. The clypeus of *M. (Schrottkyapis) assumptionis* Schrottky has a bifid median process strongly produced over the labrum (Silveira *et al.*, 2002: fig. 11.25); however, the apicolateral margins of the clypeus slightly cover the base of labrum; thus, we coded this species as having character state 1.
21. Clypeus, complete longitudinal median carina: 0 = absent; 1 = present (Pasteels, 1965: fig. 1059).
 22. Clypeus, pubescence, density: 0 = sparse throughout, integument visible among setae; 1 = dense throughout, integument not visible among setae; 2 = dense on sides of clypeus, sparse to absent on disc (Eardley, 2013: fig. 66a).
 23. Clypeus, disc, abundant, erect, short and partially hooked or wavy setae: 0 = absent; 1 = present (Durante & Abrahamovich, 2006: figs. 1–3; Gonzalez & Griswold, 2013: fig. 5E). These modified setae are associated with the passive collection of pollen from nototribic flowers.
 24. Labrum, shape: 0 = rectangular, base as wide as apex, lateral margins parallel to each other (Mitchell, 1980: fig. 48); 1 = subtriangular, base $\geq 1.5\times$ apical width, lateral margins converging apically (Mitchell, 1980: fig. 30).
 25. Labrum, disc, pubescence: 0 = absent; 1 = present.
 26. Labrum, disc, type and length of setae: 0 = consisting only of long ($\geq 1.0\times$ OD), erect setae; 1 = consisting of two types of setae, minute, yellowish, appressed setae, and long ($\geq 1.0\times$ OD), erect setae; 2 = consisting only of minute, yellowish, appressed setae.
 27. Labrum, midapical or subapical protuberance: 0 = absent; 1 = present.
 28. Mandible, length relative to length of compound eye in lateral view: 0 = short, $\leq 0.7\times$; 1 = long, $\geq 0.9\times$ (Fig. 1D; Engel & Gonzalez, 2011: fig. 8).
 29. Mandible, outer surface, median root of outer ridge: 0 = absent; 1 = present, extending towards abductor swelling (Gonzalez & Engel, 2012: fig. 5).
 30. Mandible, outer surface, upper root of outer ridge: 0 = absent; 1 = present, extending towards acetabulum and joining acetabular carina (Fig. 2F).
 31. Mandible, outer surface, secondary transverse ridge: 0 = absent; 1 = present, distinct. King (1994: fig. 8) recognized and illustrated this ridge, which is dorsal and parallel to the acetabular groove. In some species, such as *M. (Litomegachile) brevis* Say, the acetabular interspace is elevated, flattened or evenly convex, with a distinct edge delimiting the superior margin of the acetabular groove. However, we coded these species as having character state 0 because this is an edge, not a ridge.
 32. Mandible, transverse ridge, basal portion joining acetabular carina: 0 = absent; 1 = present (King, 1994: fig. 8).
 33. Mandible, apex, width relative to base in lateral view: 0 = narrow, equal to or narrower than (Engel & Gonzalez, 2011: fig. 8); 1 = broad, $\geq 1.5\times$ (Figs. 2C–J).
 34. Mandible, distal margin, axis: 0 = straight or nearly so, not strongly oblique (Figs. 2C–J); 1 = strongly oblique as in *Chalicodoma* and *Chalicodomoides* Michener (Michener, 2007: fig. 84–12d).
 35. Mandible, outer surface, apex, type of integument: 0 = smooth and shiny, or nearly so, between punctures (Figs. 2C–J; Gonzalez & Engel, 2012: fig. 33); 1 = microreticulate to finely punctate (Fig. 3A; Engel & Gonzalez, 2011: fig. 24).
 36. Mandible, outer surface, apex of acetabular mandibular groove, distinct tuft or brush of long golden setae: 0 = absent; 1 = present (Fig. 2F). In some species, such as *M. (Paracella) semioenustella* Cockerell, another brush is also present at the apex of the outer groove. In species with a well-developed outer premarginal fimbria, such as *M. (Hackeriapis) ferox* Smith, the apices of the acetabular and outer grooves often appeared as having brushes; however, the setae on these areas are about the same length and density as those on the outer premarginal fimbria. Thus, we coded these species as having character state 0.
 37. Mandible, outer premarginal impressed fimbria (Gonzalez *et al.*, 2012: char. 39): 0 = reduced or absent (Fig. 2E); 1 = present, distinct (Fig. 3E; Michener & Fraser, 1978: fig. 29).

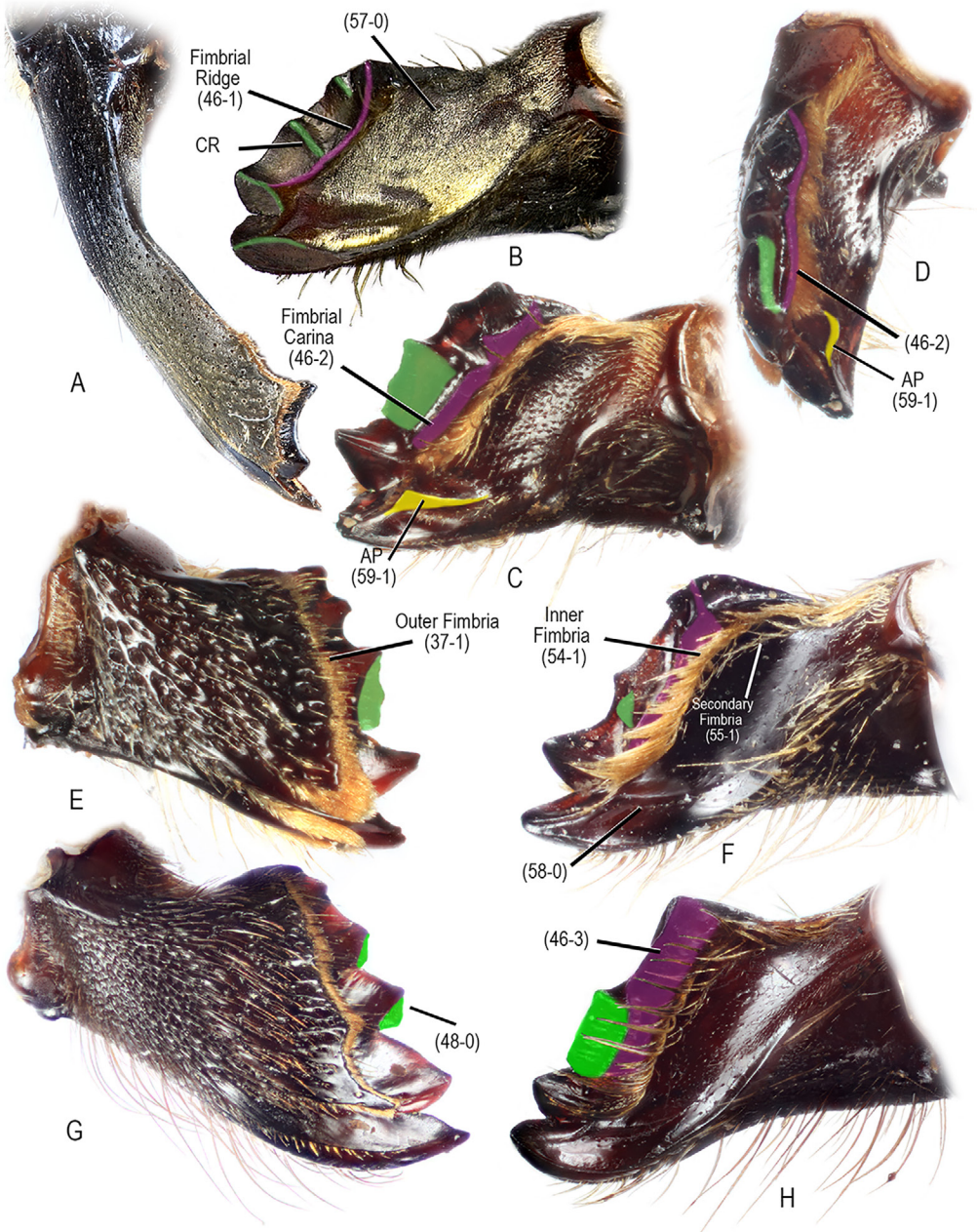


Figure 3. Female mandible of *Megachile* Latreille s.l. in outer (A, E, G), frontal (D), and inner views (B, C, F, H). **A.** *Megachile* (*Callomegachile*) *pluto* Smith. **B.** *M.* (*Callomegachile*) sp. **C–E.** *M.* (*Chelostomoda*) *spissula* Cockerell. **F.** *M.* (*Rhysomegachile*) *simillima* Smith. **G.** *M.* (*Creightonella*) *frontalis* (Fabricius). **H.** *M.* (*Pseudocentron*) *pruina* Smith. Interdentary laminae highlighted in green (odontogenic) and pink (ctenogenic). Abbreviations: CR = corono-radicular ridge; AP = adductor apical ridge.

38. Mandible, outer surface, acetabular interspace, shape: 0 = not conspicuously flattened or depressed, gently curving towards base of mandible (Fig. 3A); 1 = clearly flattened or depressed, such as outer surface of mandible has a distinguishable basal, lateral surface, and

- a distal, anterior surface (Fig. 1E). Character state 1 is typical of most Group 1 of subgenera of *Megachile s.l.*
39. Mandible, tooth count: 0 = two; 1 = three; 2 = four to six; 3 = lower distal margin with one or two large teeth, upper portion edentate or nearly so, or with very small teeth (Michener, 2007: fig. 84-12d, e). In some species, the upper distal margin is incised, resulting in a 5- or 6-toothed mandible (e.g., Figs. 2D, H), with the upper teeth closer than other teeth. We coded these species as having character state 2.
 40. Mandible, Mt_1 , width relative to basal width of Mt_2 : 0 = $\leq 1.4\times$ (Figs. 2C–H); 1 = $\geq 1.5\times$ (Fig. 2I).
 41. Mandible, third dental interspace, length relative to combined length of first and second interspaces: 0 = short, $\leq 1.5\times$ or absent; 1 = long, about $2.0\times$ (Michener, 2007: fig. 84-11f).
 42. Mandible, upper distal margin, shape: 0 = rounded or pointed with apex anteriorly directed; 1 = pointed, subtriangular, and with apex dorsally directed.
 43. Mandible, upper tooth, shape: 0 = acute or right angular (Fig. 2I); 1 = rounded or truncate, not incised (Fig. 2G); 2 = rounded or truncate, incised (Fig. 2H).
 44. Mandible, upper margin near distal margin, tooth or projection: 0 = absent; 1 = present.
 45. Mandible, upper margin near mandibular base, tooth or projection: 0 = absent; 1 = present (Michener, 1965: fig. 664).
 46. Mandible, inner surface preapically: 0 = without a distinct fimbrial ridge or carina; 1 = with a distinct fimbrial ridge running somewhat parallel to the mandibular margin (Fig. 3B); the surface between this ridge and the mandibular margin is sloping; 2 = with a distinct fimbrial carina running parallel to the mandibular margin, usually posterior to the bases of teeth and not apically extended into a lamina; the surface formed between this carina and the mandibular margin somewhat perpendicular (Figs. 3C, D, F); 3 = with a distinct lamina projecting beyond bases of upper teeth (Figs. 2E, 3H).
 47. Mandible, second interspace, interdental lamina: 0 = absent; 1 = present (Fig. 2H).
 48. Mandible, second interspace, type of interdental lamina: 0 = incomplete, not filling interspace (Fig. 3G); 1 = complete, filling interspace.
 49. Mandible, second interspace, origin of interdental lamina: 0 = not arising from inferior border of third tooth and thus interpreted as an apical extension of the fimbrial carina (ctenogenic laminae, see results); 1 = arising from the inferior border of third tooth (odontogenic laminae, Figs. 3C–D). In *M. assumptionis* and *M. (Stelodides) euzona* Pérez, a very small laminar projection (not visible in frontal view) arises from the inferior border of Mt_3 , and thus suggesting an incomplete interdental lamina; however, we coded these species as having character state 0. In *M. (Tylomegachile) orba* Schrottky and *M. (Tylomegachile) simplicipes* Friese, the interdental laminae of the second and third interspaces are presumably fused; however, a frontal view of the mandibular margin reveals that these laminae are in different planes. This suggests that the interdental lamina of the second interspace arises from the third tooth and thus we coded these species as having character state 1.
 50. Mandible, second interspace, interdental lamina fused with third tooth, thus resulting in a broad, thin tooth with a more or less truncate margin: 0 = absent; 1 = present. Character state 1 is a putative synapomorphy of *Amegachile* Friese (Michener, 2007: fig. 84-11e).
 51. Mandible, third interspace, interdental lamina: 0 = absent; 1 = present (Fig. 3G).
 52. Mandible, third interspace, type of interdental lamina: 0 = incomplete, not filling interspace; 2 = complete, filling interspace.
 53. Mandible, third interspace, origin of interdental lamina: 0 = not arising from inferior border of fourth tooth and thus interpreted as an apical extension of the fimbrial carina; 1 = arising from inferior border of fourth tooth. In *M. semivenustella*, in addition to a complete interdental lamina, there seems to be a small, incomplete interdental lamina arising from Mt_4 ; thus, we coded this species as having both character states.
 54. Mandible, inner surface, inner fimbria, length relative to apical mandibular margin (Gonzalez *et al.*, 2012: char. 36): 0 = short, restricted to upper margin (Michener & Fraser, 1978: fig. 25); 1 = long, extending across entire margin (Fig. 3F).
 55. Mandible, inner surface, secondary fimbria: 0 = absent; 1 = present (Fig. 3F).
 56. Mandible, adductor interspace, setae (Gonzalez *et al.*, 2012: char. 37): 0 = absent; 1 = present

(Figs. 3B, C).

57. Mandible, adductor interspace, length of setae relative to OD: 0 = short, $\leq 0.2\times$; 1 = long, $\geq 0.4\times$.
58. Mandible, adductor interspace, longitudinal, impressed line below adductor apical ridge marked with a series of setae: 0 = absent (Fig. 3F); 1 = present.
59. Mandible, strong adductor apical ridge (Gonzalez *et al.*, 2012; char. 34): 0 = absent; 1 = present (Fig. 3C).
60. Labium, glossa (in repose), length: 0 = short, not reaching metasoma; 1 = long, reaching metasoma.
61. Labium, prementum, subligular process, shape (modified from Gonzalez *et al.*, 2012; char. 48): 0 = elongate, long and narrow, styliiform (Winston, 1979: fig. 12f); 1 = broad, apex truncated or nearly so (Winston, 1979: fig. 38); 2 = broad, with pointed apex (Winston, 1979: fig. 28).
62. Labium, first palpomere, length relative to length of second palpomere: 0 = short, $\leq 0.5\times$; 1 = long, $\geq 0.8\times$.
63. Labium, first palpomere, length relative to width: 0 = $\leq 3.5\times$; 1 = $\geq 4.0\times$.
64. Labium, first palpomere, distinct brush of setae on midbasal concavity (Gonzalez *et al.*, 2012; char. 51): 0 = absent; 1 = present (Winston, 1979: fig. 11a).
65. Labium, third palpomere, axis relative to second palpomere: 0 = on same plane; 1 = at an angle.
66. Maxilla, stipes, dististipital process (Roig-Alsina & Michener, 1993; char. 31): 0 = absent or reduced (Winston, 1979: fig. 7a); 1 = present, elongated, almost joining stipital sclerite.
67. Labium, glossa, shape: 0 = not broadened or ligulate; 1 = broadened or ligulate (Michener, 1965: fig. 716).
68. Maxilla, palpomere count, including basal palpomere (modified from Gonzalez *et al.*, 2012; char. 60): 0 = two or three; 1 = four or five.
69. Maxilla, palpi, setae length relative to palpomere diameter: 0 = short, $\leq 2.0\times$; 1 = long, $\geq 2.1\times$.
70. Maxilla, second palpomere, length relative to width: 0 = short, $\leq 1.6\times$; 1 = long, $\geq 2.0\times$.
71. Maxilla, third palpomere, length relative to width: 0 = short, $\leq 2.6\times$; 1 = long, $\geq 3.0\times$.
72. Maxilla, lacinia, apical setae, length and thickness setae relative to setae on medial margin: 0 = similar in length and thickness; 1 = distinctly longer and thicker.
73. Hypostoma, paramandibular process (Gonzalez *et al.*, 2012; char. 22): 0 = short or absent; 1 = present, long (Gonzalez *et al.*, 2012: fig. 6).
74. Hypostoma, paramandibular carina, shape and length relative to distance between paramandibular process and hypostomal carina (modified from Gonzalez *et al.*, 2012; char. 23): 0 = short, half or less; 1 = long, ending at hypostomal carina; 2 = long, not reaching hypostomal carina, usually curving upwards or downwards; 3 = long, reaching posterior component of the hypostomal carina and forming a strong lobe.

Mesosoma

75. Pronotal lobe, shape (Gonzalez *et al.*, 2012; char. 61): 0 = rounded, without carina or strong lamella; 1 = with strong carina or border; 2 = with conspicuously broad, thin lamella.
76. Omaular carina (Gonzalez *et al.*, 2012; char. 65): 0 = absent; 1 = present.
77. Mesepisternum, punctation: 0 = finely or coarsely punctate, not forming strong rows with distinct shining ridges among them; 1 = coarsely punctate, forming strong rows with distinct shining ridges among them.
78. Mesoscutum, anterior margin in profile, shape and sculpturing (Gonzalez *et al.*, 2012; char. 69): 0 = rounded, without distinctly different surface sculpture; 1 = truncate, perpendicular, or nearly so, shinier and less punctate than dorsal portion.
79. Mesosoma, dorsum, yellow or reddish maculations: 0 = absent; 1 = present.
80. Mesoscutum, disc, length and density of setae: 0 = consisting only of long setae ($\geq 3.0\text{--}4.0\times$ OD), integument barely visible; 1 = consisting only of very short setae ($\leq 0.5\times$ OD), integument sparsely covered to almost bare; 2 = consisting only of short setae ($1.5\text{--}2.0\times$ OD), integument visible or partially obscured among setae; 3 = consisting of two types of setae, minute, yellowish, appressed setae, and erect longer setae ($2.0\times$ OD); 4 = consisting of semi-erect or appressed yellowish tomentum uniformly covering the integument.

81. Mesoscutum, notaulus line, fascia: 0 = absent; 1 = present.
82. Mesoscutum, parapsidal line, length relative to length of tegula in dorsal view (Gonzalez *et al.*, 2012: char. 72): 0 = long, $\geq 0.4\times$; 1 = short, $\leq 0.3\times$ or absent.
83. Mesoscutum, disc, punctation, density and size: 0 = finely and closely ($\leq 1.0\text{--}2.0\times$ PW) punctate, punctures ($\leq 0.2\times$ OD) not in row; 1 = coarsely and densely punctate, punctures ($\geq 0.5\times$ OD) arranged in rows, thus giving a striate or wrinkled appearance (Engel & Gonzalez, 2011: fig. 37); 2 = coarsely and densely punctate, punctures ($\geq 0.5\times$ OD) not arranged in rows.
84. Mesoscutal-mesoscutellar suture, white fascia: 0 = absent; 1 = present.
85. Preaxilla (below posterolateral angle of mesoscutum), incline and pubescence (Gonzalez *et al.*, 2012: char. 73): 0 = sloping, with setae as long as those on adjacent sclerites (Gonzalez *et al.*, 2012: fig. 10); 1 = vertical, usually nearly aetose (Gonzalez *et al.*, 2012: fig. 11).
86. Axilla, posterior margin, shape (modified from Gonzalez *et al.*, 2012: char. 74): 0 = rounded, not projected in acute angle or spine; 1 = weakly projected, not reaching posterior transverse tangent of mesoscutellum; 2 = strongly projected into acute angle or spine, surpassing posterior transverse tangent of mesoscutellum (Michener, 2007: fig. 84-6a).
87. Axilla, lateral surface, shape: 0 = not depressed; 1 = depressed, partially or entirely hidden by dorsal surface.
88. Axilla, lateral surface, sculpturing and pubescence: 0 = similarly punctate and setose as on its dorsal surface; 1 = smooth and shiny, aetose; 2 = micropunctate to strongly imbricate on at least its ventral half, dull, aetose or with sparse setae.
89. Axillar fossa, depth: 0 = shallow, surface behind it subhorizontal, without a high mesoscutellar crest between it and metanotum (Fig. 4A); 1 = deep, its posterior surface usually ascending to strong mesoscutellar crest between fossa and metanotum (Fig. 4B).
90. Mesoscutellum, shape in profile: 0 = flat or convex, forming relatively uninterrupted surface with metanotum, thus without a distinct posterior surface; 1 = elevated from metanotum, with a distinct posterior surface.
91. Metanotal pit: 0 = absent; 1 = present, distinct (Fig. 4B).
92. Metanotum, sublateral length relative to midlength: 0 = about as long as; 1 = narrower than.
93. Metanotum, degree of visibility given by mesoscutellum in dorsal view (modified from Roig-Alsina & Michener, 1993: char. 74): 0 = entirely or partially hidden; 1 = fully exposed (Fig. 4C).
94. Metanotum, median tubercle or spine (Michener, 1996: char. 7): 0 = absent; 1 = present (Michener, 2007: fig. 83-1).
95. Propodeal triangle (= metapostnotum), pubescence (Roig-Alsina & Michener, 1993: char. 79): 0 = present; 1 = absent.
96. Propodeum, shape in profile (Roig-Alsina & Michener, 1993: char. 73): 0 = largely vertical; 1 = entirely slanting or with slanting dorsal portion rounding onto vertical portion.
97. Propodeal pit, shape (Gonzalez *et al.*, 2012: char. 87): 0 = rounded or elongate, but not linear; 1 = linear.
98. Legs, color: 0 = dark brown to black, concolor with remaining areas of mesosoma; 1 = reddish or orange, contrasting with dark brown to black mesosoma.
99. Metatibia, outer surface, strong tubercles or spicules that do not end in setae or bristles (Gonzalez *et al.*, 2012: char. 102): 0 = absent; 1 = present (Michener, 2007: fig. 80-3b).
100. Mesotibia, outer surface, apically with acute angle and distinct notch anteriorly (Gonzalez *et al.*, 2012: char. 92): 0 = absent; 1 = present (Gonzalez *et al.*, 2012: fig. 14).
101. Mesotibia, outer surface, long, acute medial spine on apical margin: 0 = absent; 1 = present (Fig. 4D).
102. Mesotibia, outer surface, distinct longitudinal carina on apical one-fourth: 0 = absent; 1 = present (Fig. 4E). This carina joins the distal margin of the tibia, sometimes in a sharp angle, and thus appearing as a spine [*e.g.*, *M. (Amegachile) bituberculata* Ritsema]; however, there is always a concave, bare area posterior to this carina, which is absent in taxa that possess a true spine. In some species, this carina and the distal margin of tibia form a distinct spatulate or spoon-like process, easily visible in posterior view. This carina is apically notched in *Melanosarus*.
103. Mesotibia, outer surface, area behind longitudinal carina, setae: 0 = present; 1 = absent.

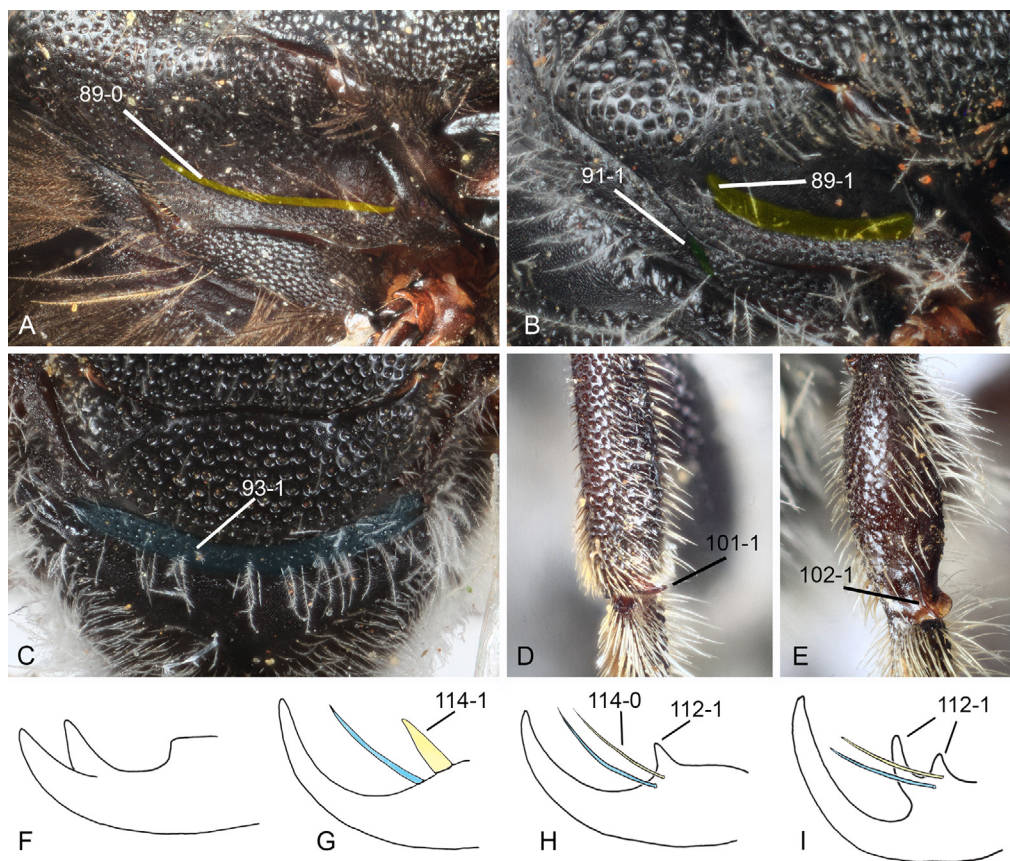


Figure 4. Some female morphological features used in the phylogenetic analysis. **A, B.** Lateral view of axilla. **C.** Dorsal view of mesoscutellum and metanotum. **D, E.** Outer view of apex of mesotibia. **F–I.** Pretarsal claws. *Megachile (Melanosarus) xylocopoides* Smith (A); *M. (Stenomegachile) dolichosoma* Benoist (B, C); *M. (Chelostomoides) rugifrons* (Smith) (D); *M. (Megachiloides) pascoensis* Mitchell (E); *Dioxys productus* (Cresson) (F); *M. (Acentron) albitarsis* Cresson (G); *M. (Hackeriapis) ferox* Smith (H); *M. (Schizomegachile) monstrosa* Smith (I).

104. Mesotibia, outer surface, posterodistal margin projected into a distinct spine: 0 = absent; 1 = present (Gonzalez & Engel, 2012: fig. 7). In *M. (Lophanthedon) dimidiata* (Smith) the projection is small and sometimes absent. We coded this species as having character state 0.
105. Mesotibia, outer surface, tuft of stiff setae on posterodistal margin: 0 = absent; 1 = present.
106. Metatibia, basitibial plate (Roig-Alsina & Michener, 1993: char. 84): 0 = absent; 1 = present.
107. Metatibia, scopa consisting of uniformly dispersed long setae on outer surface: 0 = absent; 1 = present.
108. Metatibia, spurs, shape: 0 = pointed, straight or gently curving apically; 1 = pointed, straight with apex strongly curved inward; 2 = not pointed, parallel-sided and with apex blunt.
109. Metabasitarsus, length relative to length of tibia: 0 = short, $\leq 0.5\times$; 1 = long, $\geq 0.8\times$.
110. Metabasitarsus, length relative to width (modified from Roig-Alsina & Michener, 1993: char. 90): 0 = $\geq 3.0\times$; 1 = $\leq 2.8\times$.
111. Pretarsal claws, shape (Roig-Alsina & Michener, 1993: char. 99): 0 = simple (Fig. 4G–I); 1 = bifurcate (Fig. 4F).
112. Pretarsal claws, one or two basal projections: 0 = absent; 1 = present (Figs. 4H, I).
113. Pretarsal claws, seta count: 0 = one; 1 = two.
114. Pretarsal claws, thickness and length of setae relative to each other: 0 = similar thickness,

one of them at least half length of the other (Fig. 4H, I); 1 = one conspicuously shorter and stouter than the other (Fig. 4G).

115. Propretarsus, arolium (Roig-Alsina & Michener, 1993: char. 98): 0 = reduced or absent; 1 = present.
116. Forewing, first submarginal cell, length relative to second as measured on posterior margin (modified from Gonzalez *et al.*, 2012: char. 116): 0 = equal to or shorter than; 1 = longer than.
117. Forewing, basal vein (M), location relative to cu-a (modified from Gonzalez *et al.*, 2012: char. 118): 0 = posterior to; 1 = confluent with, or basal to.
118. Forewing, 2m-cu (second recurrent vein), location relative to 2rs-m (second submarginal crossvein) (Michener, 1996: char. 12): 0 = basal to (Michener, 2007: fig. 81-1b); 1 = confluent with, or distal to (Michener, 2007: fig. 82-1).
119. Forewing, pterostigma, length relative to width (Gonzalez *et al.*, 2012: char. 112): 0 = long, $\geq 2.1\times$; 1 = short, $\leq 2.0\times$.
120. Forewing, coloration: 0 = entirely hyaline, yellowish, or dusky; 1 = apical half dusky, contrasting with hyaline or yellowish basal half; 2 = yellowish wing base with dusky costal margin.
121. Hind wing, second abscissa of vein M+Cu, length relative to length of cu-a (Gonzalez *et al.*, 2012: char. 122): 0 = short, $\leq 3.0\times$; 1 = long, $\geq 3.1\times$.
122. Hind wing, jugal lobe, length relative to length of vannal lobe (each lobe measured from wing base to apex) (modified from Roig-Alsina & Michener, 1993: char. 105): 0 = $\leq 0.5\times$; 1 = $\geq 0.6\times$.

Metasoma

123. Metasoma, shape: 0 = strongly convex dorsally, more or less parallel-sided as in *Chalicodoma* and *Chalicodomoides* (Michener, 2007: fig. 84-9); 1 = not parallel-sided, cordate, triangular, and rather flattened as in *Megachile s.str.* (Michener, 2007: fig. 84-8); 2 = as in *Coelioxys* (Michener, 2007: fig. 84-2).
124. T1, junction of anterior and dorsal surfaces, shape (Gonzalez *et al.*, 2012: char. 125): 0 = rounded; 1 = angled; 2 = carinate.
125. T1, disc in profile and posterior margin in dorsal view, shape (Gonzalez *et al.*, 2012: char. 124): 0 = flattened, posterior margin rounded, anterior and dorsal surfaces indistinguishable; 1 = convex, posterior margin straight or nearly so, with distinct anterior and dorsal surfaces.
126. T1, pubescence, length, density, and color relative to those on T2 and T3: 0 = about the same length, density, and/or color, not contrasting notoriously with these terga; 1 = not of the same color, distinctly longer (2.0–3.0 \times) and denser.
127. T1, dorsal surface, length relative to length of T2 (measured at midline): 0 = $\geq 0.7\times$; 1 = $\leq 0.6\times$.
128. T2, laterally with distinct oval velvety patch: 0 = absent; 1 = present (Pasteels & Pasteels 1971: fig. 1). This velvety patch is sometimes present also on T3.
129. T3, deep postgradular groove (Gonzalez *et al.*, 2012: char. 126): 0 = absent; 1 = present.
130. T3, mid portion, deep postgradular groove: 0 = absent, clearly visible only laterally; 1 = present.
131. T3, fasciate marginal zones: 0 = absent; 1 = present.
132. T3, well marked premarginal line: 0 = absent; 1 = present.
133. T6, pygidial plate (Roig-Alsina & Michener, 1993: char. 116): 0 = present; 1 = absent.
134. T6, pubescence, color relative to that of T1–T4: 0 = concolorous (black, pale, or yellowish); 1 = not concolorous (orange, yellowish, or pale).
135. T6, short (\leq OD), appressed setae: 0 = absent; 1 = present.
136. T6, disc in profile, shape: 0 = straight or slightly concave; 1 = strongly convex, without preapical notch; 2 = strongly convex, with preapical notch.
137. T6, erect setae on disc: 0 = present; 1 = absent.
138. T6, clubbed setae on disc: 0 = absent; 1 = present.
139. T6, wide apical hyaline flange (Gonzalez *et al.*, 2012: char. 131): 0 = absent; 1 = present (Gonzalez *et al.*, 2012: fig. 15).
140. Sternal scopa (Roig-Alsina & Michener, 1993: char. 110): 0 = present; 1 = absent.

141. S1, midapical tooth or spine (Gonzalez *et al.*, 2012: char. 137): 0 = absent; 1 = present.
142. S3, apical white fasciae under scopa: 0 = absent; 1 = present.
143. S3, mid portion, apical white fasciae: 0 = absent; 1 = present.
144. S6, length (measured along midline) relative to width (Gonzalez *et al.*, 2012: char. 138): 0 = short, as long as or shorter than; 1 = elongated, $\geq 2.0\times$.
145. S6, shape: 0 = subtriangular or broad basally, not parallel-sided; 1 = somewhat parallel-sided, not subtriangular or broad basally.
146. S6, apodeme, disc between marginal ridge and transapodemal ridge (Gonzalez *et al.*, 2012: char. 139): 0 = present (Gonzalez *et al.*, 2012: fig. 18; Packer, 2004: fig. 6a, d); 1 = reduced or absent (Gonzalez *et al.*, 2012: figs. 19, 20; Packer, 2004: fig. 7f).
147. S6, anterior margin between apodemes, depth and shape: 0 = shallow, without U- or V-shaped concavity; 1 = deep, with U- or V-shaped concavity.
148. S6, anterior margin, deep and narrow medial furrow: 0 = absent; 1 = present (Gonzalez *et al.*, 2012: fig. 19).
149. S6, superior lateral margin just below apodemes, distinct swollen border: 0 = absent; 1 = present.
150. S6, lateral surface near lateral ridge, with a strong recurved border or carina: 0 = absent; 1 = present.
151. S6, pregradular area parallel to lateral margin, with a deep invagination: 0 = absent; 1 = present.
152. S6, pregradular area, degree of sclerotization (modified from Gonzalez *et al.*, 2012: char. 142): 0 = well sclerotized; 1 = entirely membranous or weakly sclerotized, often easily broken during dissection (Gonzalez *et al.*, 2012: fig. 19); 2 = membranous or weakly sclerotized only medially.
153. S6, apex, shape (modified from Gonzalez *et al.*, 2012: char. 144): 0 = truncate to broadly rounded; 1 = V-shaped, pointed.
154. S6, distal margin, shape: 0 = simple, not bilobed; 1 = bilobed.
155. S6, setose area, length of area relative to sternal length, as measured it from base of apodemes to apex of sternum: 0 = covering at most apical fourth; 1 = covering about one-third; 2 = covering at least half.
156. S6, setose area, density of setae: 0 = uniformly covered or nearly so; 1 = bare or nearly so.
157. S6, strong preapical border or carina: 0 = absent; 1 = present.
158. S6, fringe of branched setae on or near apical margin: 0 = absent; 1 = present.
159. S6, smooth, bare rim behind apical fringe of branched setae: 0 = absent; 1 = present.
160. S6, bare rim, thickness and shape: 0 = thin, translucent, posteriorly directed; 1 = thick, rolled or abruptly bent dorsally.
161. Sting apparatus, 7th hemitergite, orientation: 0 = vertical (sting apparatus laterally-compressed); 1 = horizontal (sting apparatus dorso-ventrally compressed).
162. Sting apparatus, apex of gonostylus, setal density and length relative to maximum gonostylar width as seen in lateral view (Gonzalez *et al.*, 2012: char. 147): 0 = nearly asetose to sparsely covered by short setae ($\leq 1.0\times$); 1 = densely covered by long plumose setae ($\geq 1.2\times$).
163. 7th hemitergite, lamina spiracularis, sculpturing: 0 = smooth and shiny, not sculptured; 1 = weakly to markedly sculptured (Packer, 2003: fig. 2e).
164. 7th hemitergite, lamina spiracularis with a strong protrusion near base of lateral process (Gonzalez *et al.*, 2012: char. 150): 0 = absent or reduced; 1 = present (Packer, 2003: fig. 5b).

Male

Head

165. Clypeus, pubescence, density: 0 = sparse throughout, integument visible among setae; 1 = dense throughout, integument not visible among setae (Gonzalez *et al.*, 2018: fig. 5C); 2 = basal half with sparse setae (integument visible) or mostly bare, distal half densely covered by setae (integument not visible) (Gonzalez *et al.*, 2018: fig. 5D).
166. Clypeus, coloration: 0 = dark brown to black; 1 = yellow.
167. Antenna, F1, length relative to length of F2: 0 = 1.5–2.0 \times ; 1 = about as long as; 2 = shorter

than.

168. Antenna, F5–F10, shape: 0 = cylindrical, flattened, or crenulate; 1 = deeply concave on one side.
169. Antenna, F11, shape: 0 = cylindrical; 1 = compressed or flattened (Engel & Baker, 2006: fig. 5).
170. Hypostomal area, with a concavity or protuberance: 0 = absent; 1 = present (Gonzalez *et al.*, 2018: fig. 5E).
171. Gena, with an oblique, low, smooth, and shiny carina bordered with a dense row of white branched setae: 0 = absent; 1 = present.
172. Mandible, tooth count: 0 = two; 1 = three; 2 = four; 3 = distal margin of mandible with basal two-thirds edentate or nearly so, at most, one or two very small teeth as in *Chalicodoma*.
173. Mandible, upper distal margin, shape and size relative to length and width as remaining teeth: 0 = rounded or pointed, similar length and width; 1 = triangular, conspicuously broader and longer than.
174. Mandible, inferior border, with tooth, process, or projection (Gonzalez *et al.*, 2012: char. 156): 0 = absent; 1 = present (Gonzalez *et al.*, 2018: fig. 5F).
175. Mandible, inferior process, shape and orientation: 0 = broad, subtriangular, posteriorly-directed, on basal third of inferior border (Gonzalez *et al.*, 2018: fig. 5E); 1 = slender, posteriorly-directed (Fig. 5A; Praz, 2017: fig. 8); 2 = broad, small or large, anteriorly-directed, on basal two-thirds of inferior border (Fig. 5B); 3 = broad, with a very dense brush of stiff branched setae (Fig. 5C; Gonzalez & Engel, 2012: fig. 42); 4 = with a small angle midapically (Durante & Cabrera, 2009: fig. 6).
176. Mandible, inner surface, degree of concavity: 0 = weak; 1 = strong.

Mesosoma

177. Procoxal spine (Gonzalez *et al.*, 2012: char. 157): 0 = absent; 1 = present (Gonzalez & Engel, 2012: fig. 43).
178. Procoxal spine, shape and length relative to OD: 0 = short ($\leq 1.5\times$), pointed or somewhat parallel-sided; 1 = long ($\geq 2.0\times$), not parallel-sided; 2 = long (≥ 2.0), parallel-sided or nearly so.
179. Procoxal spine, ventral surface, pubescence: 0 = very sparse to nearly aetose, integument clearly visible; 1 = densely covered with branched setae, integument barely visible among setae.
180. Procoxa, disc, pubescence: 0 = uniformly covered with branched setae, integument barely visible among setae; 1 = aetose or nearly so, integument clearly visible.
181. Procoxa, tuft of stiff ferruginous setae: 0 = absent; 1 = present.
182. Protrochanter, inferior margin apically produced: 0 = absent; 1 = present.
183. Profemur, shape and color: 0 = not strongly compressed, same color of femora of remaining legs; 1 = antero-posteriorly strongly compressed, bright yellow or pale, contrasting with color of femora of remaining legs.
184. Protibia, shape and length relative to width: 0 = not enlarged or swollen, $\geq 3.0\times$; 1 = distinctively swollen, enlarged, $\leq 2.8\times$.
185. Protarsi, shape and color (Gonzalez *et al.*, 2012: char. 158): 0 = not enlarged or excavated, without conspicuous dark spots on inner surface; 1 = slightly or distinctly enlarged or excavated, often with conspicuous dark spots on inner surface.
186. Protarsi, degree of excavation and color: 0 = slightly excavated, with dark spots on inner surface, usually of the same color of tarsi of remaining legs (Michener, 2007: fig. 84-19b); 1 = strongly modified, distinctively enlarged or excavated, inner surface with dark spots, bright yellow or pale, contrasting with tarsi of remaining legs (Michener, 2007: fig. 84-19a).
187. Protarsi, basal tarsomere (probasitarsus), shape: 0 = not in the shape of a concave, long, distally directed lobe; 1 = forming a distinctly concave, long, distally directed lobe.
188. Mesocoxa, inner surface, small tooth or protuberance: 0 = absent, 1 = present.
189. Mesotibia, inner surface, tooth or protuberance: 0 = absent, 1 = present.
190. Mesotibial spur: 0 = present; 1 = absent.
191. Mesotibial spur, length relative to apical width of metatibia: 0 = at least as long as; 1 = much

shorter than.

192. Mesotibial spur, articulation with mesotibia: 0 = free, not fused to tibia; 1 = fused to tibia.
 193. Mesobasitarsus, length relative to width: 0 = long, $\geq 2.5\times$; 1 = short, $\leq 2.0\times$.
 194. Metafemur, posterior surface, patch of microtrichia (metafemoral keirottrichia): 0 = absent; 1 = present (Gonzalez *et al.*, 2018: fig. 5I). We coded *M. (Leptorachis) laeta* Smith as having character state 1 even though this structure is very small.
 195. Metatibia, inner spur: 0 = present; 1 = absent.
 196. Metabasitarsus, length relative to width: 0 = long, $\geq 2.3\times$; 1 = short, $\leq 2.0\times$.
 197. Propretarsus, arolium: 0 = present (Baker & Engel, 2006: fig. 5); 1 = reduced or absent.

Metasoma

198. T3, marginal zone, color relative to tergal disc: 0 = concolorous; 1 = not concolorous, semi-translucent to translucent.
 199. T6, transverse preapical carina (Gonzalez *et al.*, 2012: char. 162): 0 = absent; 1 = present.
 200. T6, transverse preapical carina, shape: 0 = strong, medially emarginate, not toothed or denticulate (Fig. 5E); 1 = strong, entire or nearly so (Fig. 5D); 2 = strong, toothed or denticulate, with or without a median emargination (Fig. 5F); 3 = weak, little projected in profile, entire or nearly so (Baker & Engel, 2006: fig. 2).
 201. T6, preapical carina divided in two or more dorsal processes, and a pair of ventral processes: 0 = absent; 1 = present (Michener, 2007: fig. 84-7).
 202. T6, above preapical carina, with strong longitudinal median ridge or protuberance: 0 = absent; 1 = present.
 203. T6, above preapical carina, with distinct median concavity: 0 = absent; 1 = present.
 204. T6, region of preapical carina, shape: 0 = not swollen or bulbous; 1 = swollen or bulbous, except medially.
 205. T6, dorsal surface, density and length of setae relative to OD: 0 = densely covered (integument not visible) by long (2.0–3.0 \times) setae; 1 = bare or sparsely covered (integument visible) by long (2.0–3.0 \times) or short ($\leq 1.0\times$) setae; 2 = densely covered by short ($\leq 1.0\times$), appressed, branched setae.
 206. T6, apical margin, with lateral spine or tooth: 0 = absent (Fig. 5D); 1 = present (Fig. 5F).
 207. T6, apical margin, with submedian spine or tooth: 0 = absent; 1 = present (Fig. 5E).
 208. T6, apical margin, size of lateral spine or tooth: 0 = large; 1 = small (Fig. 5E).
 209. T6, apical margin, submedian spine or tooth, size relative to size of lateral spine or tooth: 0 = similar; 1 = conspicuously longer and broader than.
 210. T7, degree of visibility in dorsal view and orientation (Gonzalez *et al.*, 2012: char. 164): 0 = exposed, posteriorly directed; 1 = hidden, and/or anteriorly or ventrally directed.
 211. T7, strongly carinate gradulus: 0 = absent; 1 = present (Gonzalez *et al.*, 2018: fig. 6B).
 212. T7, transverse carina, shape: 0 = rounded, truncate, or emarginate (Fig. 5G); 1 = long, acute, spiniform (Fig. 5H); 2 = angular (Fig. 5I).
 213. T7, with distinct, strong longitudinal median ridge: 0 = absent; 1 = present.
 214. T7, apical margin, shape: 0 = straight or nearly so, not emarginate or strongly projecting; 1 = with a small median tooth; 2 = deeply and broadly emarginate, forming two prominent teeth (Engel & Baker, 2006: fig. 6); 3 = little projected medially, with small, submedian tooth; 4 = little projected medially, without submedian tooth.
 215. T7, pygidial plate (Roig-Alsina & Michener, 1993: char. 118): 0 = present; 1 = absent.
 216. Sterna, number of fully exposed sclerites (modified from Gonzalez *et al.*, 2012: char. 168): 0 = three; 1 = four; 2 = five or six; 3 = two.
 217. S1, midapical spine: 0 = absent; 1 = present.
 218. S5, width relative to length (Gonzalez *et al.*, 2012: char. 175): 0 = $\leq 2.0\times$; 1 = $\geq 2.1\times$.
 219. S5, gradulus, degree of sclerotization and definition: 0 = weak, barely distinguishable; 1 = strong, indicated by a well-defined transverse line or border.
 220. S5, postgradular area laterally, with setose, sclerotized surface: 0 = absent; 1 = present.
 221. S5, apical margin, shape: 0 = straight or nearly so; 1 = deeply or shallowly concave.

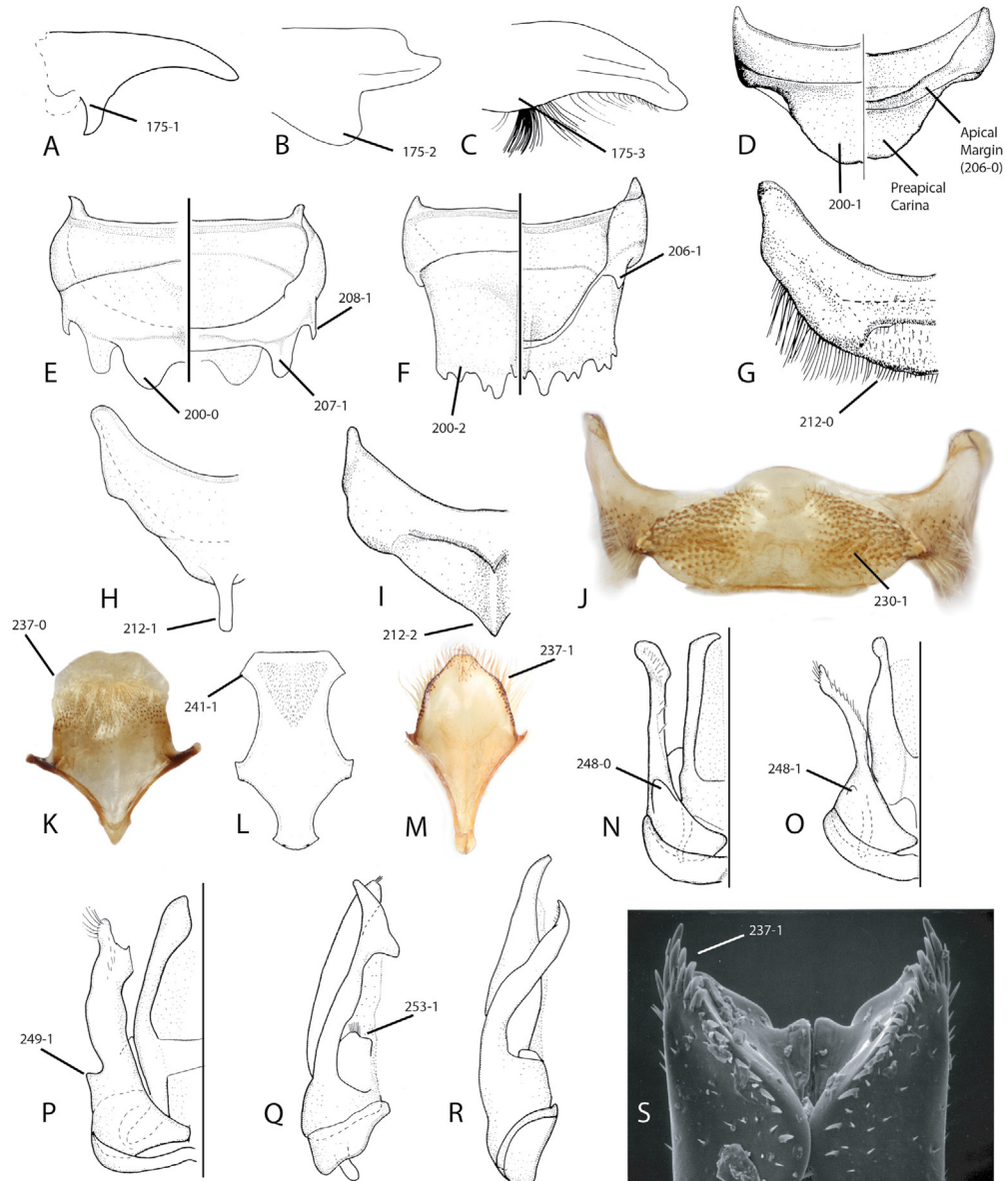


Figure 5. Some male morphological features used in the phylogenetic analysis. **A–C.** Ventral projection of mandible. **D–F.** Dorsal (left half) and ventral (right half) views of sixth tergum. **G–I.** Dorsal view of seventh tergum. **J.** Ventral view of sixth sternum. **K–M.** Ventral view of eighth sternum. **N–P.** Dorsal view of genital capsule. **Q, R.** Profile view of genital capsule. **S.** Apex of penis valves. Taxa: *Megachile (Acentron) albitarsis* Cresson (**A, L**); *M. (Callomegachile) biseta* Vachal (**B**); *M. (Maximegachile) maxillosa* Guérin-Méneville (**C**); *M. (Argyropile) longuistosa* Gonzalez & Griswold (**D, G**); *M. (Grosapis) cockerelli* (**E, H, R**); *M. (Creightonella) cognata* Smith (**F, I**); *M. (Zonomegachile) moderata* Smith (**J, K**); *M. (Largella) donbakeri* Gonzalez & Engel (**M**); *M. (Austromegachile) montezuma* Cresson (**N**); *M. (M.) centuncularis* (Linnaeus) (**O**); *M. (Moureapis) maculata* Smith (**P**); *M. (Chalicodoma) parietina* (Geoffroy) (**Q**); *M. (Chalicodoma) sicula* (Rossi) (**S**).

222. S5, with short, well-sclerotized midapical process: 0 = absent; 1 = present (Mitchell, 1980: fig. 42).
223. S5, postgradular area, size of setose area relative to width of sternum (Gonzalez *et al.*, 2012: char. 177): 0 = large, $\geq 0.6\times$; 1 = small, $\leq 0.5\times$.
224. S5, postgradular area, type of setae (modified from Gonzalez *et al.*, 2012: char. 176): 0 = simple, branched or plumose (Fig. 6A); 1 = lanceolate, ovate-acuminate (Figs. 6B, C); 2 = capitate or spatulate (Figs. 6E, F); 3 = fan-shaped (Fig. 6D). Sometimes we found more than one type of setae, and thus we coded the most abundant type.
225. S5, postgradular area, with broad, aetose, and weakly sclerotized area above pubescence: 0 = absent; 1 = present (Gonzalez *et al.*, 2018: fig. 26D).
226. S5, apicolateral margin, type and length of setae relative to those on postgradular area: 0 = aetose or with short setae of similar length; 1 = with simple or branched longer ($2.0\text{--}3.0\times$) setae.
227. S5, midapical margin, with dense tuft of stiff, thickened, simple setae: 0 = absent; 1 = present.
228. S6, width relative to length (Gonzalez *et al.*, 2012: char. 183): 0 = $\leq 2.0\times$; 1 = $\geq 2.1\times$. Because the midapical margin of S6 is highly variable, we measured the length of S6 on its lateral margin, from the base of the apodeme to the apical margin of the sternum.
229. S6, degree of sclerotization (Gonzalez *et al.*, 2012: char. 182): 0 = well-sclerotized; 1 = weakly sclerotized to membranous.
230. S6, postgradular area, pubescence (Gonzalez *et al.*, 2012: char. 184): 0 = absent or very sparse (integument clearly visible among setae), without forming distinct patches; 1 = dense, forming distinct patches (Fig. 5J). In *Trichothurgus wagenknechti* (Moure), a mediolongitudinal bare area divides the discal pubescence of S3–S6. Thus, the resulting patches of setae on S6 might not be homologous to those found in other megachilinae bees. However, we coded this species as having character-state 1.
231. S6, bare area between setal patches, width relative to one patch width: 0 = wide, $\geq 1.0\times$; 1 = small, $\leq 0.5\times$.
232. S6, postgradular area, type of setae (modified from Gonzalez *et al.*, 2012: char. 185): 0 = unmodified, simple or branched (Fig. 6A); 1 = modified, lanceolate, ovate-acuminate (Figs. 6B, C), capitate, spatulate (Figs. 6E, F), or fan-shaped (Fig. 6D).
233. S7, degree of sclerotization (modified from Gonzalez *et al.*, 2012: char. 186): 0 = entirely well-sclerotized, usually setose; 1 = weakly sclerotized, membranous, frequently aetose.
234. S8, length relative to width: 0 = $\leq 2.5\times$; 1 = $\geq 2.6\times$.
235. S8, spiculum, shape: 0 = pointed or broadly rounded (Michener, 2007: figs. 77-1b, 80-4d); 1 = subrectangular; 2 = as an elongate, narrow process (Michener, 2007: fig. 82-2i); 3 = as a short process with an expanded apex (Gonzalez & Griswold, 2013: fig. 508).
236. S8, lateral apodemes: 0 = absent or weakly sclerotized (Michener, 2007: fig. 80-4d); 1 = distinct (Michener, 2007: fig. 82-2b).
237. S8, lateral margins, setae: 0 = absent (Figs. 5K, L); 1 = present, forming a distinct fringe (Fig. 5M).
238. S8, apex, length relative to sternal length, as measured from lateral apodemes to distal margin: 0 = short, about $\frac{1}{4}$ (Michener, 2007: fig. 80-4d); 1 = long, about half.
239. S8, apex, width relative to width of spiculum: 0 = wider; 1 = about as wide as or narrower than.
240. S8, apex, shape: 0 = broadly or narrowly rounded; 1 = subrectangular (Fig. 5L).
241. S8, apex, shape: 0 = not expanded; 1 = expanded (Fig. 5L).
242. S8, distal margin, shape: 0 = entire, straight, broadly rounded or pointed (Michener, 2007: fig. 84-4b); 1 = entire, with a small midapical projection (Michener, 2007: fig. 77-1b); 2 = bilobed (Michener, 2007: fig. 82-2b).
243. Genital capsule, length relative to width: 0 = short, about as long as; 1 = elongate, longer than. We measured maximum total length from the base of the gonobase to apex of the penis valves or gonostylus and maximum width at the base of the gonobase.
244. Genital foramen, orientation: 0 = anteriorly directed or nearly so (Michener, 2007: fig. 80-4c); 1 = ventrally directed (Michener, 2007: fig. 77-1a).

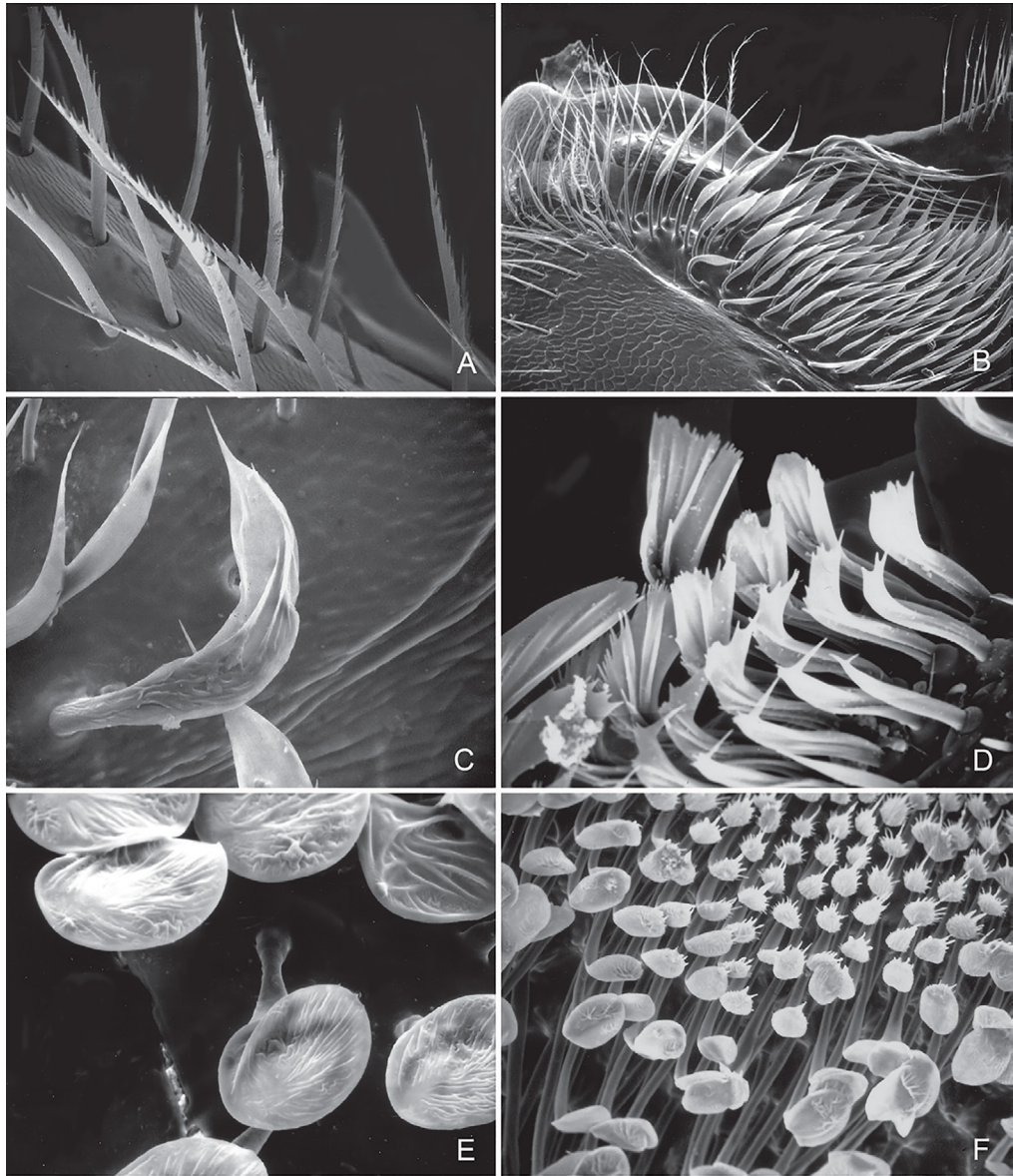


Figure 6. Examples of the types of setae found on the male S4–S6 of *Megachile* Latreille *s.l.* **A.** Branched, unmodified, S4, *Megachile (Acentron) albitarsis* Cresson. **B.** Acuminate, S4, *M. (Megachile) centuncularis* (Linnaeus). **C.** Acuminate, S6, *M. (Chalicodoma) sicula* (Rossi). **D.** Fan-shaped, S6, *M. (Chelostomoides) exilis* Cresson. **E.** Capitately-spatulate, S5, *M. (Chelostomoides) rugifrons* (Smith). **F.** Capitately-spatulate, S5, *M. (Xanthosarus) fortis* Cresson.

245. Gonobase (modified from Roig-Alsina & Michener, 1993: char. 122): 0 = present, distinguishable; 1 = reduced or absent.

246. Articulation between gonostylus and gonocoxite (modified Roig-Alsina & Michener, 1993: char. 125): 0 = distinct, at least ventrally; 1 = fused, thus forming an unsegmented appendage.

247. Gonocoxite, dorsal lobe: 0 = absent; 1 = present (Gonzalez *et al.*, 2018: fig. 6E).

248. Gonocoxite, dorsal lobe, shape: 0 = large, strong, digitiform (Fig. 5N; Engel & Baker, 2006:

- fig. 11); 1 = small, acute (Fig. 5O).
249. Gonocoxite, small sublateral lobe: 0 = absent; 1 = present (Fig. 5P).
250. Volsella (modified from Roig-Alsina & Michener, 1993: char. 126): 0 = absent; 1 = present.
251. Articulation between volsella and gonocoxite: 0 = fused; 1 = articulated, distinguishable as a separated sclerite (Michener, 2007: fig. 77-1a).
252. Volsella, apex, shape: 0 = rounded or pointed; 1 = distinctly notched or bilobed, thus suggesting a medial digitus and a lateral cuspis (Gonzalez & Engel, 2012: fig. 28).
253. Volsella with setae on distal margin: 0 = absent; 1 = present (Fig. 5Q).
254. Gonostylus, length relative to gonocoxite: 0 = equal or shorter than; 1 = $\geq 2.0\times$.
255. Gonostylus, length relative to penis valves in ventral view (modified from Gonzalez *et al.*, 2012: char. 196): 0 = subequal to; 1 = longer than; 2 = shorter than.
256. Gonostylus, shape in lateral view: 0 = curved or arched; 1 = straight or nearly so.
257. Gonostylus, width in lateral view: 0 = not conspicuously narrow, widest at midlength or at apex (Fig. 5Q); 1 = very narrow, about the same width across its entire length (Fig. 5R).
258. Gonostylus, shape in cross section: 0 = not flattened; 1 = flattened.
259. Gonostylus, apex, orientation in dorsal view: 0 = laterally directed; 1 = medially directed; 2 = posteriorly directed.
260. Gonostylus, apex, shape: 0 = not expanded; 1 = clearly expanded.
261. Gonostylus, apical lobes: 0 = absent; 1 = present.
262. Gonostylus, apical lobes, types: 0 = one lateral and one medial (Gonzalez *et al.*, 2018: fig. 6D); 1 = one dorsal and one ventral. The gonostylus of *M. (Xanthosarus) lagopoda* (Linnaeus) has three apical lobes; one on each medial, ventral, and dorsal surfaces. We coded this species as having character states 1 and 2.
263. Gonostylus, medial apical lobe, size: 0 = small, barely indicated; 1 = large and conspicuous (Gonzalez *et al.*, 2018: fig. 6D).
264. Gonostylus, apex with large, deep concavity between dorsal and medial lobes: 0 = absent; 1 = present (Gonzalez *et al.*, 2018: fig. 6D).
265. Gonostylus, medial surface, pubescence: 0 = absent; 1 = present.
266. Gonostylus, medial surface, length of setae relative to maximum apical gonostylar width: 0 = short, $\leq 2.0\times$; 1 = long, $\geq 2.1\times$ (Gonzalez & Engel, 2012: fig. 28).
267. Penis valve, apodemes, length relative to their visibility outside genital capsule: 0 = short, not visible; 1 = long, visible as they project through genital foramen (Michener, 2007: fig. 82-2d).
268. Penis valve, shape in dorsal view: 0 = distinctly curved or arched; 1 = straight or nearly so.
269. Penis valve, basal shape: 0 = not enlarged or protuberant; 1 = distinctly expanded.
270. Penis valve, lateral margin, shape: 0 = not enlarged or protuberant; 1 = distinctly enlarged or protuberant.
271. Penis valve, apical shape in ventral view: 0 = straight or nearly so; 1 = distinctly curved or arched inward; 2 = distinctly curved or arch outward (as in *Aztecantidium* Michener & Orday).
272. Penis valve, apex with row of thick, spine-like setae: 0 = absent; 1 = present (Fig. 5S).

DATA CHARACTERIZATION: We scored characters from all tagmata of the adult body in both sexes (Fig. 7A). However, more characters were scored from the female than from the male (Chi-squared test, $\chi^2_{[1]} = 5.14$, $p = 0.023$, $n = 252$), even after excluding some characters (~10%) that are present in both sexes but were scored only in the female to avoid duplication. We scored more characters from the metasoma than from other tagmata ($\chi^2_{[2]} = 13.07$, $p = 0.001$, $n = 272$). The number of characters within each sex was significantly different among tagmata (♀ : $\chi^2_{[2]} = 10.59$, $p = 0.005$, $n = 164$; ♂ : $\chi^2_{[2]} = 64.5$, $p < 0.001$, $n = 108$). In the female, most characters are from the head and mesosoma whereas for the male most characters are from the metasoma.

PHYLOGENETIC ANALYSES: We analyzed this dataset using maximum parsimony under two weighting schemes. We treated all characters as unordered and nonadditive, and used equal weights (EW) and implied weights (IW) in Tree Analysis Using New

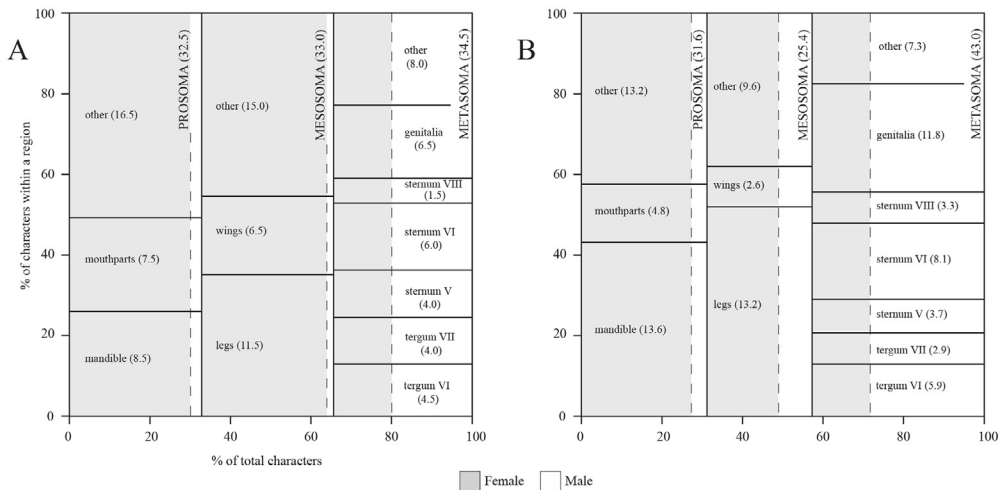


Figure 7. Character distribution maps of the morphological datasets used in the generic-level phylogeny of Megachilini (**A**, $n = 272$ characters) and the tribal-level phylogeny of Megachilidae (**B**, $n = 200$ characters). The x -axis represents the percentage of total characters in each tagma or body region (*e.g.*, prosoma) while the y -axis represents the percentage of characters of selected structures (*e.g.*, mandible) within a tagma. Percentage in parentheses represents contribution to the total number of characters. See Whitlock & Wilson (2013) for further explanation on character distribution maps.

Techology (TNT; Goloboff *et al.*, 2003a). The IW analysis downweights characters according to their degree of homoplasy (*i.e.*, characters with higher homoplasy have lower weights) during the heuristic search for parsimonious hypotheses (Goloboff, 1993). In IW analyses, instead of using random k -values to vary the strength of the weighting function, we explored a range of constant k -values calculated for average character fits (F) of 50, 54, 58, 62, 66, 70, 74, 78, 82, 86, and 90%. We obtained these k -values using the following formula described in Mirande (2009), Reemer (2012), and Reemer & Ståhls (2013): $k = (F \times S) / (1 - F)$. S is a measure of the average homoplasy per character, calculated as the number of observed steps minus the minimum number of steps divided by the number of characters. The number of observed steps is based on the shortest tree found under EW, which for our dataset is 2364. The minimum number of steps is the cumulative number of minimum character state changes for all 272 characters, which amounts to 323. Thus, the value of S is: $(2364 - 323) / 272 = 7.50$, while the k -value for the character fit of 50% is: $(0.5 \times 7.50) / (1 - 0.5) = 7.50$. Resulting k -values are in Appendix 4. We chose to conduct the IW analysis because studies have proven its effectiveness in recovering topologies congruent with those of total evidence phylogenies (*e.g.*, Reemer, 2012), sometimes outperforming other methods (*e.g.*, Goloboff *et al.*, 2018). This weighting approach is also frequently used in the analysis of morphological datasets along with EW (*e.g.*, Kim & Ahn 2016; Marín *et al.*, 2017; Rocha Filho & Packer, 2017).

We searched for trees under both weighting schemes by implementing sectorial searches with tree drifting (TD) and tree fusing (TF), and ratchet runs with TD and TF. We used the following search: keep a maximum of 10,000 random trees, 500 random addition sequences, and 1000 ratchet iterations, including 100 cycles of TD and 100 rounds of TF per iteration. In EW analysis, we estimated branch robustness using standard bootstrap (sample with replacement) and absolute Bremer support in TNT,

and plotted the values on the strict consensus topology obtained from the final TNT parsimony run. We used 10,000 bootstrap replicates under a heuristic tree search that consisted of 10,000 replicates of Wagner trees with random addition sequences, followed by Tree Bisection Reconnection (TBR) branch swapping (saving 10 trees per replicate). Resulting values per node represent frequency differences GC for Group present/Contradicted (Goloboff *et al.*, 2003b). We calculated Bremer support by withholding 10,000 suboptimal trees up to 10 steps longer than the parsimonious trees under a traditional search (10,000 replicates of Wagner trees, followed by TBR, saving 10 trees per replicate).

We assessed the performance of each IW analysis by comparing the number of parsimonious trees, tree length, retention index, and node support. For the latter, we used Jackknife with symmetric resampling expressed as GC frequency-difference values, which Reemer (2012) found useful when determining the reliability of trees under different k -values. We searched trees under each k -value and used 1000 replicates under a heuristic tree search that consisted of 10 replicates of Wagner trees with random addition sequences, followed by Tree Bisection Reconnection (TBR) branch swapping (saving 10 trees per replicate). We calculated average and median GC frequency-difference from the value displayed at each node, which we plotted on the resulting tree or strict consensus tree (if the analysis yielded more than one parsimonious tree). Groups that are more often contradicted than supported displayed values in brackets, which we considered as having a support of zero and excluded them from the calculations. In addition, we calculated in TNT the SPR distance (Goloboff, 2008) between the resulting topology from each IW analysis and the topology obtained from the analysis of this dataset combined with molecular data (*vide infra*).

We visualized cladograms in WinClada, collapsing unsupported nodes and using DELTRAN (slow) for character optimization; when the choice is equally parsimonious, the latter favours repeated origins of characters over reversals. We used the abbreviations MPT, L, CI, and RI for maximum parsimonious tree, tree length, and consistency and retention indices, respectively. In the text, we referred to characters states in the form 21-1, where 21 is the character and 1 the character state.

PHYLOGENETIC SIGNAL OF MORPHOLOGICAL CHARACTERS: The current trend in evolutionary biology is the analysis of large datasets composed of both molecular and morphological data. Thus, to facilitate future comparative cladistics analyses, we assessed the phylogenetic signal of the scored characters and determined the level of homoplasy among character sets. We compared the median value of RI per character set and conducted partitioned phylogenetic analyses. We grouped characters by sex (male and female characters), tagmata (pro-, meso-, and metasoma), and by the following set of characters of taxonomic importance in the diagnosis and recognition of supraspecific groups: female mandible, female terminalia (T6, S6, and sting apparatus), male legs, and male terminalia (T6, T7, S5–S8, and genitalia). We conducted phylogenetic analyses only to the subset of male and female characters using the settings for EW analyses under parsimony as indicated above. For each analysis, we recorded the number of MPT and tree statistics (L, CI, and RI).

Origin of the Interdental Lamina in the Female Mandible

To determine the possible mandibular structure(s) from which interdental laminae originated, we conducted a comparative study of the female mandible across all taxa of Megachilini used in the phylogenetic analyses. We examined specimens with

unworn mandibles and, whenever possible, we removed one of them from the head capsule, washed it with 95% ethanol, and then mounted it on a card point for examination. We made inferences on the origin of the interdental lamina based on topological correspondence, a robust criteria for recognizing primary homologies (e.g., Remane, 1952; Rieppel & Kearney, 2002; Agnarsson & Coddington, 2008).

Evolutionary Origins of the Interdental Lamina

In addition to using the tree topology inferred from the morphological dataset of Megachilini to examine patterns of variation of the interdental lamina, we also conducted preliminary Bayesian total-evidence tip-dating analyses to explore other hypotheses of relationships. We conducted these preliminary analyses because the phylogenetic hypothesis of Trunz *et al.* (2016) based on molecular data differed from ours (*vide* Results, *infra*), and because these authors employed a node-dating approach to estimate the origin of LC bees. Thus, we conducted two sets of analyses aimed at obtaining more accurate divergence time estimates. First, we conducted a phylogenetic analysis of all tribes in the family Megachilidae. Then, we used the divergence time estimates generated from that analysis to inform priors for the phylogenetic analysis of the genera of Megachilini.

For these combined analyses, we used the morphological data matrix of Gonzalez *et al.* (2012) for the tribal-level analysis of Megachilidae. For the generic-level analysis of Megachilini, we used the newly developed morphological dataset documented in this work. The dataset of Gonzalez *et al.* (2012) includes all tribes, representatives of all fossil taxa, and 80% of the extant generic-level diversity of the family (Appendix 2). It consisted of characters scored from all tagmata of the adult body in both sexes (Fig. 7B), particularly from the female (Chi-squared test, $\chi^2_{[1]} = 52.02, p \leq 0.001, n = 200$). The number of characters is similar among tagmata ($\chi^2_{[2]} = 0.13, p = 0.937, n = 200$) but differs between sexes (♀ : $\chi^2_{[2]} = 13.60, p = 0.001, n = 151$; ♂ : $\chi^2_{[2]} = 51.47, p \leq 0.001, n = 49$). In the female, most characters are from the head and mesosoma whereas for the male most characters are from the metasoma.

MOLECULAR DATA: We used molecular sequences available through GenBank from the following five gene regions generated by Litman *et al.* (2011) and Trunz *et al.* (2016): the protein-coding genes elongation factor 1- α (EF1 α), LW-rhodopsin (Opsin), conserved ATPase domain (CAD), sodium potassium adenosine triphosphatase (NAK), and the ribosomal gene 28S (Appendix 5). We aligned gene fragments using MAFFT ver. 7.305 (Katoh & Standley, 2013), with the secondary structure of 28S accounted for using the Q-INS-I method (Katoh & Toh, 2008). The alignments were then cleaned, frame checked, and concatenated in Mesquite ver. 3.40 (Maddison & Maddison, 2018). Because the gene fragments EF1 α , Opsin, and CAD have introns (Trunz *et al.*, 2016), we conducted analyses using two approaches. In one analysis, we retained introns, as originally aligned by MAFFT. In the other one, we removed introns and their surrounding variable regions using Gblocks (Castresana, 2000; Talavera & Castresana, 2007) under the less stringent selection options of 'allow gap positions' and 'allow less strict flanking positions'. We also removed the highly variable regions of 28S using Gblocks under these parameters. To find the partition scheme of the molecular data for phylogenetic analysis, we used PartitionFinder ver. 2.1.1 (Lanfear *et al.*, 2016) on both approaches of the concatenated molecular datasets under the 'greedy' search algorithm (Lanfear *et al.*, 2012), with unlinked branch-lengths, and Akaike information criterion corrected (AICc) model selection.

COMBINED DATA: DNA sequences are available for many of the species used in the morphological analyses. However, they are not available for many others, particularly those species known from the holotype or from a small number of specimens, which in most cases represent the type species of a genus-group name. In those cases, we used available molecular data for closely related species (*i.e.*, same subgenus or species group) to those scored in the morphological analysis. We chose to use these chimeric taxa for pragmatic reasons, in an attempt to increase the taxonomic representation of our analyses. Although we did not assess the differences in the number of character states between the pair of species combined, we are confident that the anatomical overlap is high because closely related taxa tend to share a high number of morphological features. In addition, because our goal was to explore the relationships among tribes and genera, we pursued and scored morphological characters that might reflect those levels of relationships (*i.e.*, morphological features common to a group of genera or subgenera), not characters aimed to reveal relationships among the species within a subgenus. We referred to those chimeric taxa by their generic name, and sometimes subgenus, followed by a combination of the first three letters of both specific epithets in square brackets (Appendix 2). For example, the name for the operational taxonomic unit (OTU) resulting from *Nomada utahensis* Moalif and *N. maculata* Cresson is referred as *Nomada* [uta×mac] in the combined dataset.

For the tribal-level analysis, six taxa with morphological information [*Anthidioma chalicodomoides* Pasteels, *Gnathanthidium prionognathum* (Mavromoustakis), *Indanthidium crenulaticauda* Michener & Griswold, *Osmia* (*Hoplosmia*) *scutellaris* (Morawitz), *Xenoheriades micheneri* Griswold, *Xenostelis polychroma* Baker] did not have closely related species with DNA sequences available and thus we excluded them from the analyses. Six out of the 73 remaining taxa of the original morphological dataset of Gonzalez *et al.* (2012) are Baltic amber fossils and 44 are species with available DNA sequences. Thus, the remaining 23 terminal taxa are chimeric taxa (Appendix 2). The resulting dataset consisted of 73 OTUs, 200 morphological characters, and 5667 aligned nucleotide positions. For the generic-level analysis, the combined dataset consisted of 67 OTUs, 268 morphological characters, and 6981 aligned nucleotide positions. One of the OTUs is a fossil taxon, 34 have available DNA sequences, and the remaining 33 are chimeric taxa. This combined dataset has 45% less the number of taxa used in the morphological analysis because species of many subgenera do not have available molecular data. However, most of these are from a large, well-supported clade (Clade C, see Fig. 8) that includes the LC bees. Thus, reducing the taxonomic representation of this clade does not significantly affect the overall taxonomic coverage of the different lineages of the tribe. After reducing the number of taxa from the original morphological dataset, four characters became inapplicable and thus we excluded them. To explore other hypotheses of generic-level relationships, we also analyzed a combined dataset that had all taxa used in the morphological analysis, even though many of them lacked molecular data. We referred to these datasets as the reduced (67 OTUs) and full datasets (122 OTUs).

PHYLOGENETIC ANALYSES: For the analyses of the molecular datasets and combined molecular and morphological datasets, we used maximum likelihood (ML) and Bayesian inference (BI). We conducted ML analyses using the message passing interface (MPI) version of IQ-Tree 1.5.5 (Nguyen *et al.*, 2015). We used the command ModelFinder (Kalyaanamoorthy *et al.*, 2017) to select the substitution model during the analyses to avoid *a priori* models. To examine the effects of introns on the phylogeny, we first ran ML analyses on the concatenated molecular datasets with and without introns,

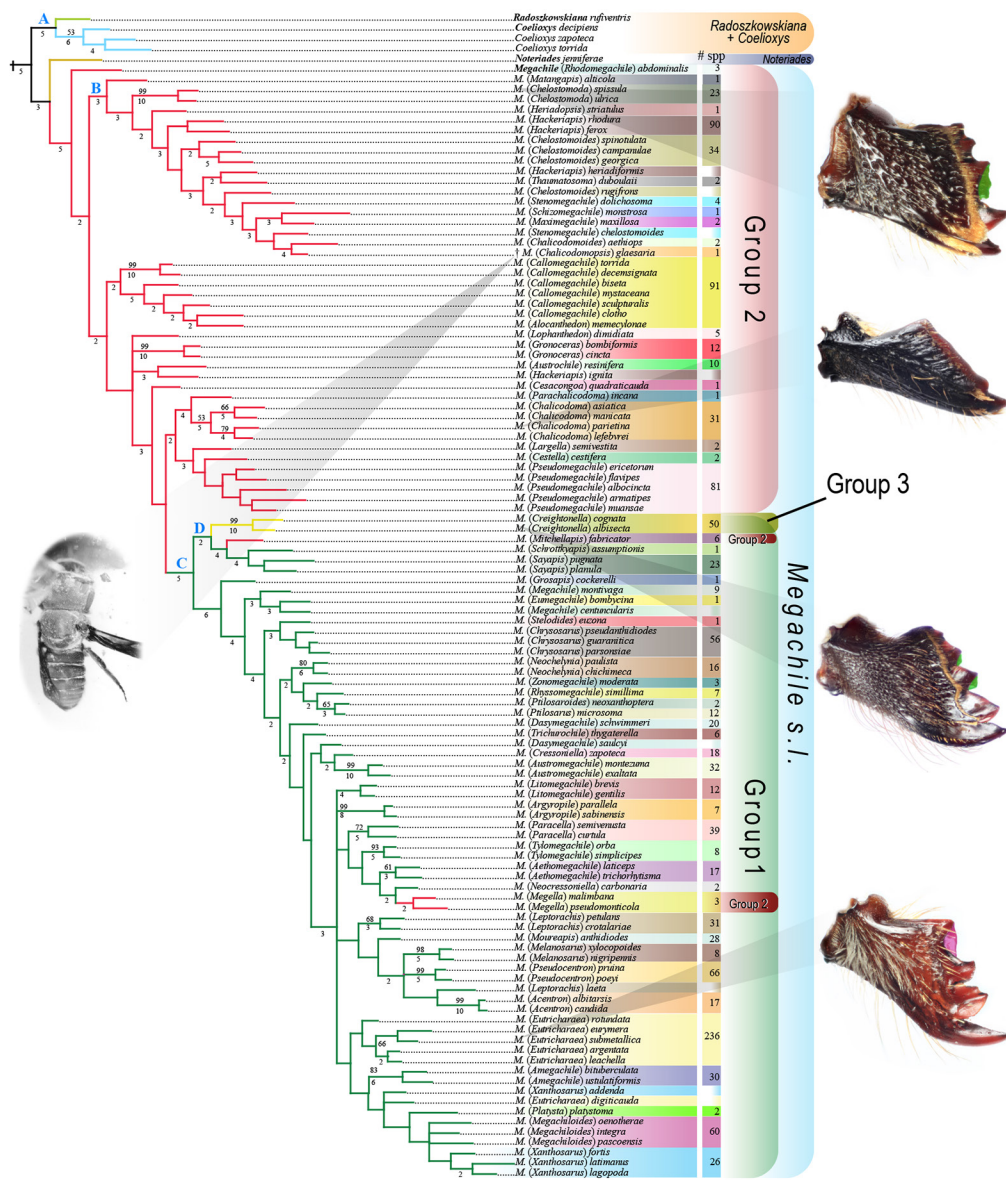


Figure 8. Strict consensus tree of 30 parsimonious trees obtained under equal weighting. Numbers above nodes are standard bootstrap values, numbers below nodes are absolute Bremer values. Branches without numbers indicate bootstrap values below 50% and Bremer values of 1. A capital letter above a node indicates a clade discussed in the text. Species within boxes of the same color correspond to the same subgenus of *Megachile* Latreille s.l. following Michener’s (2007) classification. The colored column after the species names indicates approximate number of species per subgenus. Half-colored boxes without a number correspond to species that did not cluster with the other species of the same subgenus included in the analysis. Species richness taken from Michener (2007), Moure *et al.* (2007), and Ascher & Pickering (2018). Mandibles with interdigital laminae highlighted in green (odontogenic) and pink (ctenogenic).

as described above. While introns had negligible effects on the topology of both the tribal- and generic-level phylogenetic trees, their inclusion resulted in higher support

values in the generic-level analysis. Thus, we used the molecular data without introns in the combined analysis of the tribal-level phylogeny and the dataset with introns in the generic-level study. Then, we conducted ML analyses on these combined datasets, giving the morphological data a separate partition. We estimated branch support using 1,000 replicates of ultrafast bootstrapping (Minh *et al.*, 2013).

We conducted BI analyses using the MPI version of MrBayes 3.2.6 (Ronquist *et al.*, 2012b; Zhang *et al.*, 2016) on the total-evidence datasets described above, with the morphological data given its own partition. We did not select an *a priori* substitution model; instead, we used the reversible-jump Markov chain Monte Carlo (MCMC) method with gamma-distributed rate variation across sites to test the probability of different models *a posteriori* during the analysis (Huelsenbeck *et al.*, 2004; Ronquist *et al.*, 2012b). We conducted two different types of BI analyses, a time-free and a time-calibrated analysis. For the time-free analysis, we did not add further specifications following the input for the reversible-jump MCMC. We set the MCMC generation to run 10 million generations using four chains (three heated, one cold) with the swap number set to one, and a temperature of 0.1 for the heated chains. We monitored MCMC convergence of both time-free and time-calibrated analyses with Trace v.1.6 (Rambaut *et al.*, 2014). We considered a value of ESS ≥ 200 a good indicator of convergence.

We used a tip-dating approach (Pyron, 2011; Ronquist *et al.*, 2012a) for the time-calibrated analyses. First, we estimated the base molecular clock rates as outlined by Ronquist *et al.* (2012a). For the tribal-level analysis, the base clock rate and root age were informed using the age of the oldest crown bee fossil (Engel, 2000, 2001) for the minimum age, and 120 Ma for the mean age based on previous estimates for the age of Megachilidae by Cardinal & Danforth (2013). Then, we used the divergence time estimates generated by the tip-dated tribal-level analysis to inform these priors in the generic-level analysis. We used the fossilized birth-death macroevolutionary model (Heath *et al.*, 2014) following the methods of Zhang *et al.* (2016). The sampling strategy was set to diversity, with sampling probability set to 0.016 in the tribal-level analysis (66 megachilids sampled from the 4,105 known species) and to 0.029 for the generic-level analysis (59 megachilines of the 2,000 known species of the tribe Megachilini). We assigned an uncorrelated relaxed clock model IGR with the prior on rate variation across lineages set to exponential 10. We gave the fossils a uniform calibration prior based on the dated ages of their amber deposits (Engel, 2001).

To aid convergence in the time-free analyses, we applied several constraints on well-supported groups. In the tribal-level analysis, we constrained both melittine taxa, as well as Apidae and Megachilidae, as sister groups. In the generic-level analysis, we applied constraints to unite taxa representing the following groups: Lithurgini, Osmiini, Megachilini, and Osmiini + Megachilini. We also conducted additional analyses constraining the fossil species *M. (Chalicodomopsis) glaesaria* with different taxa of *Megachile s.l.* based on the results of the EW parsimony analysis of the morphological dataset.

The MCMC generation settings for the time-calibrated analyses were initially set identically to the time-free analyses, and we completed the preferred tribal-level tip-dated tree under these settings. However, we experienced considerable difficulty getting both the tribal- and generic-level tip-dated analyses to converge. Convergence of the generic-level analysis was accomplished after providing the time-free total-evidence Bayesian tree as a starting tree, lowering the heated chain temperature to 0.010, and increasing the MCMC generations to 50 million. Thus, we applied a similar approach to the tribal-level analysis, increasing the number of chains and swaps, and

increasing MCMC generation to 200 million, but it still did not attain convergence. Furthermore, allowing the tip-dated tribal-level analysis to run longer resulted in unrealistically old divergence time estimates, placing the root of the tree in the Permian with a median age of 256 Ma. Thus, the resulting preferred tip-dated tribal-level tree did not reach convergence, but the topology is identical to that obtained across the different attempts to reach convergence. It has similar support values, but it differs in the age estimates, which are considerably more realistic and in line with previous estimates using node-calibration approaches (Cardinal & Danforth, 2013; Litman *et al.*, 2011).

PATTERNS OF VARIATION OF THE INTERDENTAL LAMINA: We used Mesquite (Maddison & Maddison, 2018) to trace the evolutionary history of the interdental lamina. We reconstructed ancestral character states using a parsimony model with unordered character states and visualized them on the tree topology obtained from the analysis of the combined full dataset using BI.

To test for character association between the LC behavior and some female cephalic and mandibular features, we used the phylogenetic pairwise comparison implemented in Mesquite. We used the option that searches for pairs of taxa contrasting in the state of two characters, with a maximum number of pairings set to 1,000,000 pairs. To maximize the number of pair comparisons, we used the resulting tree topology from the analysis of the combined full dataset using BI. We tested the following five characters that we considered dependent characters: ocellocipital distance (character #12), mandible length (#28), mandibular apical width (#33), shape of acetabular interspace in the outer surface of mandible (#38), and pubescence on the adductor interspace in the inner surface of mandible (#56). We chose these characters because they appeared to be under the same selective pressure, which is the type of nesting material used (Mitchell, 1980; Williams & Goodell, 2000). The size and shape of the mandible also influences the size and shape of the head, as the latter contains the mandibular musculature. Thus, we used these characters as proxy of the head size and mandibular size and shape. We also included the pubescence on the adductor interspace of the mandible because we observed that setae on this area appears to be absent in many species of LC bees. We tested each of these five characters for association with the presence of interdental laminae, a feature unquestionably indicative of LC behavior. For analysis, we scored each species as having either character state 0 when these laminae are absent, or as having character state 1, when they are present on at least one dental interspace. We did not compare these characters with the presence or absence of LC behavior because the nesting biology of most species in our analysis is unknown. Additionally, some species that lack interdental laminae still cut leaves while others do not (*e.g.*, *M. montivaga*). Thus, assuming an absence of LC behavior in species that lack interdental laminae is not applicable.

RESULTS

Morphological-based Phylogeny of Megachilini

The analysis of the morphological data matrix under EW yielded 30 MPTs ($L = 2364$, $CI = 13$, $RI = 57$); nine nodes collapsed in the consensus tree (Fig. 8) and most branches were weakly supported by homoplastic characters. The clade of cleptoparasitic bees (Clade A) consisting of *Coelioxys* and *Radoszkowskiana* resulted as the sister group of all other Megachilini. *Noteriades* is the sister group to the entire clade con-

taining *Rhodomegachile* Michener (Group 2) and all remaining *Megachile s.l.* Most subgenera of Group 2 clustered in multiple clades along the tree, except for *Mitchellapis* and *Megella*, which were in a large derived clade (Clade C) containing all subgenera of Group 1 and *Creightonella* (Group 3). The fossil taxon, *Chalicodomopsis*, resulted in a clade that included *Matangapis*, *Chelostomoda*, *Hackeriapis* Cockerell, and other hopliform or heriadiform taxa of Group 2 (Clade B).

Implied weighting analyses under the 11 k -values each resulted in a single MPT, except for two analyses (character fits 66 and 70%) that yielded two MPTs. All resulting trees are longer than the MPTs obtained under EW, but have similar CI and RI values. The topologies obtained with character fits 54 and 62 to 70% have the highest SPR values (Appendix 4). However, the median GC frequency-difference value was similar among analyses (Kruskal-Wallis H test, $H = 0.773$, $p = 0.99$) and it was not associated with SPR values (Spearman's correlation, $r_s = 0.146$, $p = 0.667$). Likewise, the number of supported nodes was similar among analyses [Chi-squared goodness-of-fit test, $\chi^2(10, n = 715) = 1.139$, $p = 1.00$].

The resulting topology from the IW analyses was similar to that of the EW analysis, but the position of several taxa significantly changed among k -values (results not shown). For example, *Noteriades* resulted as the sister group of Megachilini in all analyses, except in those with character fits 86 and 90%, in which it appeared as sister of *Megachile s.l.* as in the EW analysis. *Chelostomoda*, a member of Group 2 of subgenera (see Clade B in EW consensus, Fig. 8), clustered with *Creightonella*, *Mitchellapis*, *Sayapis* Titus, and *Schrottkyapis* Mitchell (see Clade D in EW consensus) in analyses with character fits ranging from 50 to 70%. In remaining analyses, *Chelostomoda* clustered within Clade B. *Rhodomegachile* and *Chalicodomopsis* were sister groups, either as part of Clade B (analyses with character fits 50 and 58%), or as the sister group of all other Megachilini (analyses with character fits 62 to 86%) excluding *Noteriades* and Clade A. In the analysis with the highest character fit, both taxa resulted in positions similar to those in the EW consensus topology. Likewise, *Gronoceras* (Group 2) resulted either as the sister group of all other Megachilini, excluding *Noteriades* and Clade A (character fits 50 and 54%), or in the same clade with *Lophanthedon* Gonzalez & Engel (Character fits 58, 70–90%). *Megachile* (*Callomegachile*) *decemsignata* Radoszkowski and *M. (Callomegachile) torrida* Smith, members of Group 2, clustered with *Lophanthedon* in Clade D (character fits 50–58, 66, 70%) or with other members of *Callomegachile* in the remaining analyses. *Matangapis* was the sister group of *Heriadopsis* and clustered within Clade B (character fits 50–58%). However, in analyses with character fits 62–70, and 86%, *Heriadopsis* remained within the same clade but *Matangapis* resulted singly in a branch after the clade consisting of *Rhodomegachile* and *Chalicodomopsis*. In remaining analyses, *Matangapis* was the sister group of all members of Clade B, as in the EW consensus. Clade C was consistently recovered, but the arrangement of internal nodes changed among analyses.

PHYLOGENETIC SIGNAL: The female and male character sets were similar in the median RI value (Mann-Whitney test, $U = 13334$, $p = 0.192$), as well as in the percentage of unambiguous synapomorphic characters (Table 1). However, unlike the analysis of the male characters that resulted in a highly unresolved tree, female characters recovered Megachilini and several major lineages (not shown). For both sexes, we did not find statistically significant differences between the median RI values and percentage of unambiguous synapomorphic characters between character sets (\varnothing , RI value: $U = 1452$, $p = 0.183$; % unambiguous synapomorphic characters: Chi-squared goodness-of-fit test, $\chi^2_{[1]} = 0.67$, $p = 0.414$. σ : $U = 1630$, $p = 0.209$; $\chi^2_{[1]} = 0.014$, $p = 0.907$).

Table 1. Phylogenetic signal of selected character sets used in the morphological phylogeny of Megachilini. Retention index per morphological character set and quantitative descriptors of trees obtained from partitioned analysis using female and male characters. RIc = average retention index of character set followed, in parentheses, by median, standard deviation, and number of characters; % Unambiguous Synapomorphies = Percentage of unambiguous synapomorphic characters in the analysis of the full data matrix; MPT = number of parsimonious trees; Collapsed nodes = number of nodes that collapsed in the consensus strict tree; L = tree length; CI = consistency index; RI_t = retention index of MPTs. Non-applicables are indicated by an em dash symbol (—).

Character set	RIc	% Unambiguous Synapomorphies	MPT	Collapsed nodes	L	CI	RI _t
Female	54.33 (50.0, ± 29.87, n = 156)	13.9	310	74	1146	16	64
Mandible	54.63 (59.0, ± 32.19, n = 32)	9.4	—	—	—	—	—
Terminalia	54.33 (58.0, ± 35.88, n = 24)	16.7	—	—	—	—	—
Male	50.17 (50.0, ± 27.23, n = 107)	13.8	340	104	1079	12	55
Legs	54.10 (53.0, ± 25.63, n = 29)	15.8	—	—	—	—	—
Terminalia	48.93 (42.0, ± 28.07, n = 71)	14.5	—	—	—	—	—

Origin and Evolution of the Interdental Lamina

COMBINED PHYLOGENIES: In the preferred Bayesian analysis for the family Megachilidae (Fig. 9), Pararhophitinae resulted as the sister group of Lithurginae, both taxa sister to Megachilinae. Within the latter subfamily, Dioxyini were the sister group of Glyptapini while Aspidosmiini rendered Ctenoplectrellini paraphyletic. Megachilini also rendered Osmiini paraphyletic, as they clustered with the osmiine genera *Afroheriades* Peters and *Pseudoheriades* Peters. The remaining osmiines are together in another clade (Fig. 9). The origin of crown Megachilidae was estimated at a median age of 111.3 Ma (95% highest posterior density 80.94–127.56 Ma) with crown Megachilini at 42.0 Ma (24.75–49.55 Ma). A similar topology resulted from the ML analysis of the combined dataset with extant taxa only. However, Pararhophitinae were the sister group of Lithurginae + Megachilinae, Aspidosmiini and Dioxyini clustered in the same clade, and the osmiine genus *Ochreriades* Mavromoustakis resulted as the sister group of a clade that contained Megachilini and the remaining Osmiini.

In the generic study of Megachilini, the fossil *M. glaesaria* resulted as the sister group of all other Megachilini using the reduced dataset of Megachilini, Clade A was the sister of some members of Group 2 of subgenera, Clade B was segregated in several clades, and *Chelostomoda* was sister to Clade C (Fig. 10). The origin of Clade C was estimated at a median age of 14.92 Ma (95% highest posterior density 11.83–19.42 Ma) and that of *Chelostomoda* + Clade C at a median age of 15.61 Ma (12.80–19.16 Ma). Constraining the position of *M. glaesaria* to the clade that includes *Thaumatosoma*, as in the EW topology, yielded older estimates for the origin of Clade C (23.63 Ma, 18.96–28.93 Ma) and for that of *Chelostomoda* + Clade C (24.82 Ma, 20.25–30.24 Ma). Likewise,

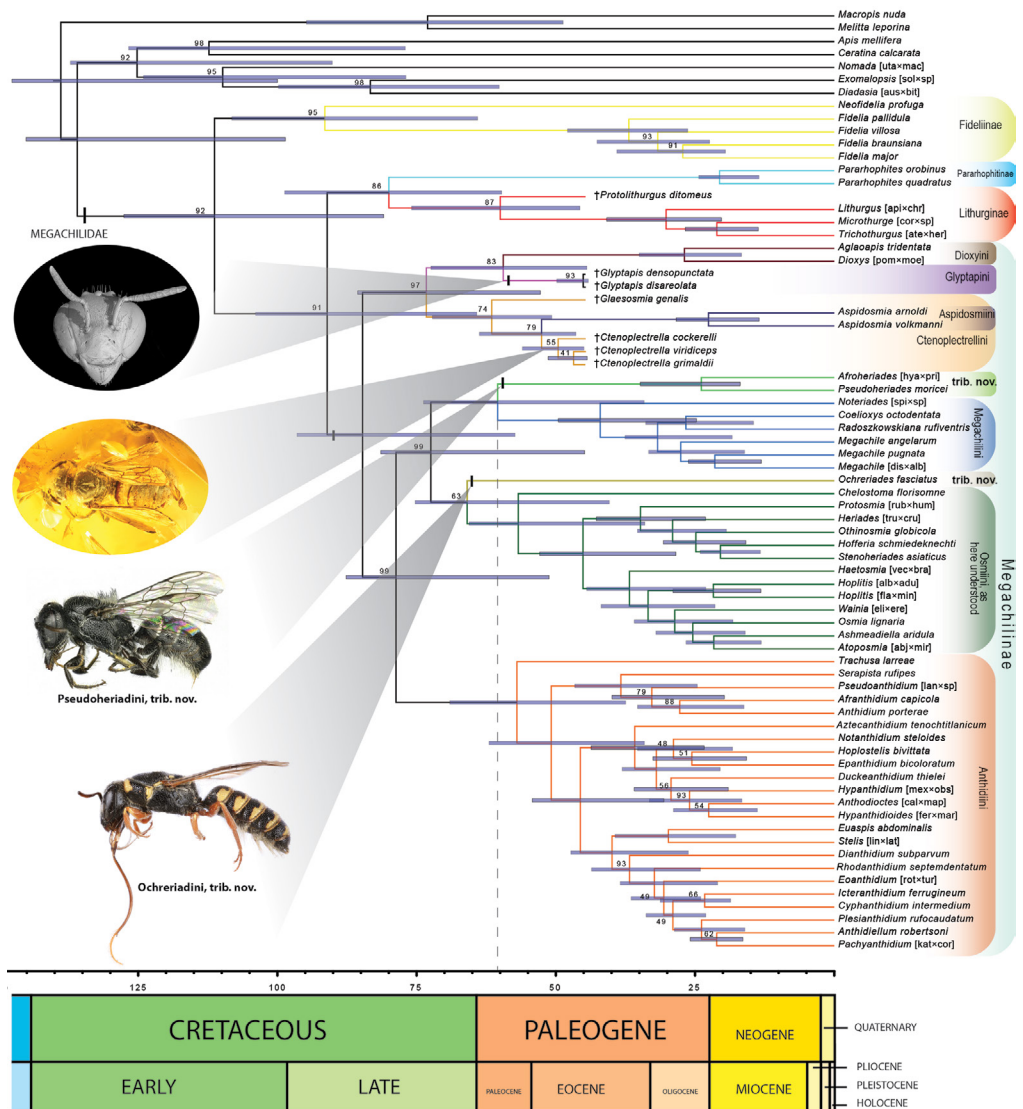


Figure 9. Preferred total evidence dated phylogeny of Megachilidae. Majority-rule consensus tree from Bayesian analysis using fossils as terminals under the FBD tree prior. Blue bar at each node represents the 95% highest posterior density age range. Posterior probability below 100 indicated above each node.

constraining the position of *M. glaesaria* to the clade that includes *Matangapis* yielded older estimates for the origin of Clade C (22.42 Ma, 19.11–26.98 Ma) and for that of *Chelostomoda* + Clade C (23.58 Ma, 20.27–28.24 Ma). We obtained the same topology when we analyzed the full dataset (Fig. 11). However, estimated median ages were older for Clade C (17.6 Ma, 15.22–21.80 Ma) as well as for that of *Chelostomoda* + Clade C (18.6 Ma, 16.12–23.35 Ma). A similar topology resulted from the ML analysis of the reduced dataset, except that *Noteriades* was the sister group of all Megachilini, and *Matangapis* and *Heriadopsis* clustered with members of Clade C.

TYPES OF INTERDENTAL LAMINA: We found two types of interdental laminae that

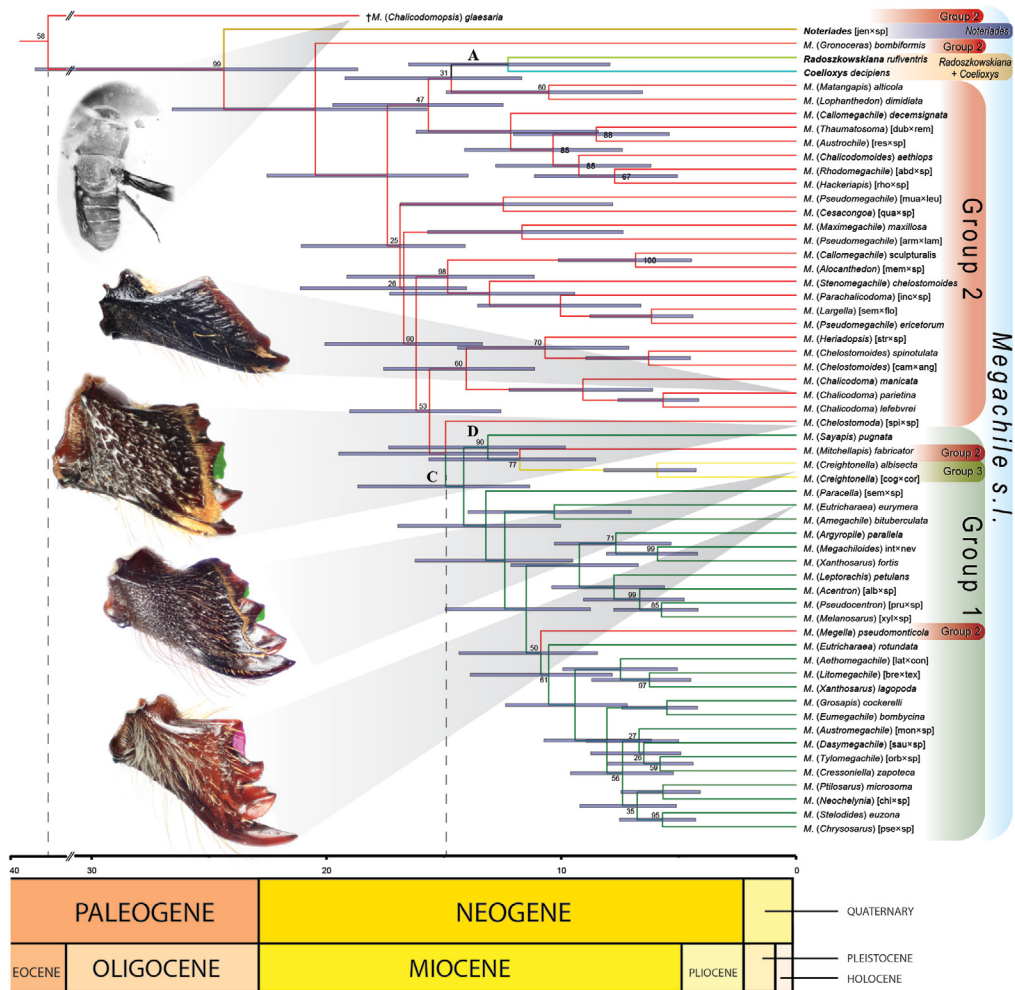


Figure 10. Preferred total evidence dated phylogeny of Megachilini from the analysis of the reduced morphological data matrix (67 OTUs). Majority-rule consensus tree from Bayesian analysis using fossils as terminals under the FBD tree prior. Blue bar at each node represents the 95% highest posterior density age range. Posterior probability below 100 indicated above each node. A capital letter above a node indicates a clade discussed in the text. Mandibles with interdentary laminae highlighted in green (odontogenic) and pink (ctenogenic).

likely develop from different structures in the mandible. The first type is clearly a ventral extension of the corono-radicular ridge (CR), a strong ridge that runs basally from the apex or cusp of the inner surface of each tooth (Fig. 3B). This CR ridge is usually strongest on Mt_1 , sometimes continuing dorsally into the adductor interspace or curving ventrally, thus running parallel to or towards the adductor ridge (Figs. 3C, D). Gonzalez *et al.* (2012) recognized the portion of this ridge running parallel to or towards the adductor ridge as the adductor apical ridge (AP). Interdentary laminae originating from teeth, hence called *odontogenic laminae*, often partially fill the dental interspaces (*i.e.*, incomplete). Even in species of *Schrottkyapis* and *Stelodides* Moure, which have secondarily lost interdentary laminae, there still is a hidden small projection from the CR ridge of Mt_3 suggestive of a lamina.

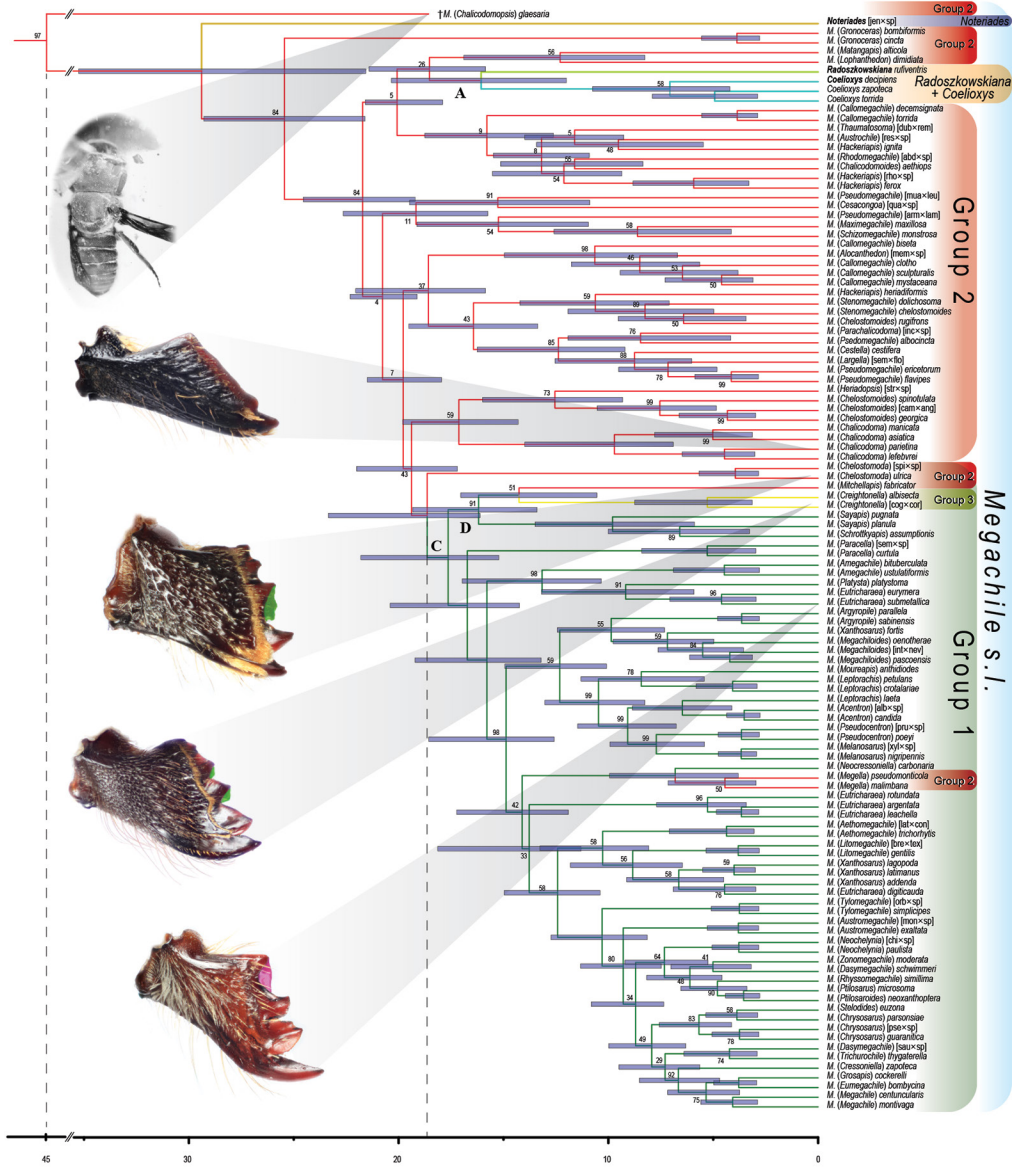


Figure 11. Total evidence dated phylogeny of Megachilini from the analysis of the full morphological data matrix (122 taxa). Majority-rule consensus tree from Bayesian analysis using fossils as terminals under the FBD tree prior. Blue bar at each node represents the 95% highest posterior density age range. Posterior probability below 100 indicated above each node. A capital letter above a node indicates a clade discussed in the text. Mandibles with interdentary laminae highlighted in green (odontogenic) and pink (ctenogenic).

The second type of interdentary lamina is usually complete and is likely an extension from a transverse ridge at the base of the teeth, which runs parallel to the inner fimbria on the inner surface of the mandible. When this transverse ridge is laminate and apically extended so that it can be seen from the outside of the mandible in between the teeth, it becomes an interdentary lamina. In megachiline bees that never developed interdentary laminae, this ridge runs from the upper carina to the base of Mt₂,

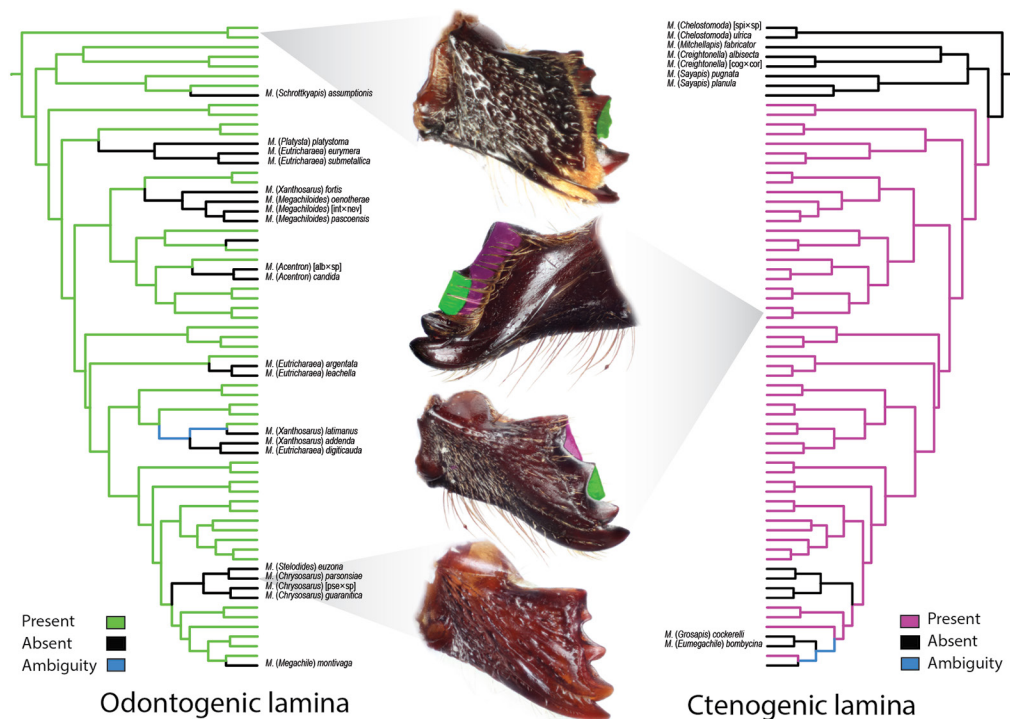


Figure 12. Parsimony reconstruction of the two types of interdentary laminae of the leaf-cutter bee mandible. We used the tree topology obtained from the total-evidence analysis of the full data set (122 taxa) to visualize character states on the clade of leaf-cutter bees. All photographs are outer views of the mandibles, except for the second from top to bottom, which is an inner view of the mandible below. Odontogenic lamina highlighted in green and ctenogenic lamina in pink.

merging with the CR of that tooth, and forming a rather concave surface, which sometimes is divided by the CR of the other teeth (Fig. 3B). In *Chelostomoda*, *Creightonella*, and *Sayapis*, such a transverse ridge is laminate or nearly so, but it does not extend enough apically to form an interdentary lamina (Fig. 3C–E). In species that have secondarily lost interdentary laminae, this transverse ridge is conspicuous and distinctly elevated compared to that of most species of Group 2 that never developed interdentary laminae. Michener & Fraser (1978) recognized that the transverse ridge was associated with the inner fimbria and thus named it the *fimbrial ridge* or *fimbrial carina*. Consequently, we referred to the lamina that develops from this fimbrial ridge as either the *fimbrial lamina* or *ctenogenic lamina* (from the Greek κτερίς, *kteis*, meaning “comb”).

EVOLUTION OF THE INTERDENTARY LAMINA: Odontogenic laminae evolved first and have secondarily been lost or modified multiple times. In contrast, ctenogenic laminae developed once in more derived clades of LC bees and have been lost or modified comparatively fewer times than odontogenic laminae (Fig. 12). Odontogenic laminae are often restricted to Mt_3 and thus visible in the second interdentary space only (Figs. 2E–H), except in *Creightonella* where they are also present on Mt_{4-5} (Fig. 3G).

Mandibles of species that only have odontogenic laminae tend to have a thick distal margin with the acetabular interspace of the outer surface gently curving towards the base of the mandible, thus resembling the mandible of species of Group 2 that never developed interdentary laminae (Fig. 2C). In contrast, mandibles that have both

Table 2. Phylogenetic pairwise comparisons between the presence of interdental laminae in the female mandible (independent character) and some female cephalic and mandibular characters (dependent characters). See materials and methods for description of each character. # Pairs = number of pairs contrasting in the state of two characters; Relationship = number of pairs with a positive (+) or negative (-) relationship. In a positive relationship, one of the paired species has a character state 1 for both characters and the other species character state 0 for both characters. In a negative relationship, one of the paired species has a character state 1 for one character and a 0 for the other character while the other species has the opposite. P-value: significance value for the number of pairs contrasting in the state of two characters; Range of P-values: range of significance values for all optimal set of pairs of pairwise comparisons.

Compared character #	# Pairs	Relationship	P-value	Range of P-values
12-ocelloccipital distance	4	1+, 3-	0.313	0.313–0.688
28-mandible length	3	2+, 1-	0.5	0.5–0.5
33-mandibular apical width	3	2+, 1-	0.5	0.5–0.5
38-acetabular interspace	4	3+, 1-	0.313	0.313–0.313
56-pubesence on adductor interspace	4	3+, 1-	0.313	0.063–0.313

odontogenic and ctenogenic laminae exhibit a distinct basal, lateral surface and a distal, anterior surface because the acetabular interspace is clearly flattened or depressed (Fig. 2E–J). The mandible is also much broader apically, with the distal margin flattened, and with both types of laminae often at different levels from the mandibular margin and from each other. However, in some species whose mandible is flattened at the apex, both laminae are thin and nearly at the same level with the interspace margin, sometimes fused and indistinguishable. The CR ridges are usually absent in apically flattened mandibles, except for that of *Mt*₁. In some species with thicker mandibular apex, the ctenogenic interdental laminae are narrow (not reaching apex of teeth), well behind or deeper to the interspace margin, and often hidden by it (Fig. 2D). A mandible of this kind would appear to lack laminae when seen in it from the outside.

According to the phylogenetic pairwise comparisons, the presence of interdental laminae is not associated with characters #12, 28, 33, 38, or 56 (ocelloccipital distance, mandible length, mandibular apical width, shape of acetabular interspace, and pubescence on the adductor interspace, respectively), which we used as proxy of head size and mandible size and shape (Table 2).

DISCUSSION

Phylogenetic Relationships within Megachilini

The morphological phylogeny presented here provides an additional hypothesis that allowed us to place the fossil species as well as some rare megachiline taxa for which DNA is not yet available. Neither our morphological analysis nor the preliminary total-evidence phylogeny supports the proposal of Trunz *et al.* (2016) of recognizing *Heriadopsis* and *Matangapis* at the generic level, while simultaneously retaining other Group 2 taxa within *Megachile*. In our analyses, *Heriadopsis* always clustered near *Chelostomoides*, but the position of *Matangapis* changed from being part of the same clade with *Heriadopsis* to sister of *Lophanthedon* in the combined analysis. Thus,

separating these taxa alone at the generic rank, as Trunz *et al.* (2016) proposed, creates a large paraphyletic *Megachile s.l.*

Although sharing the presence of arolia with both *Heriadopsis* and *Matangapis*, *Noteriades* never clustered with any of these taxa. It resulted either as the sister group of *Megachile s.l.* (EW analysis of morphological data, Fig. 8) or as sister of Megachilini (IW analyses of morphological data and combined analyses, Figs. 10, 11). Thus, our study further supports the placement of *Noteriades* within Megachilini, as well as its recognition at the generic rank.

Michener (2007) suggested that *Coelioxys* might render *Megachile s.l.* paraphyletic because of its shared morphological features, particularly with *Chelostomoides*. He also suggested that cleptoparasitism might have evolved independently in *Radoszkowskiana* and *Coelioxys*. Morphologically, *Radoszkowskiana* differs from *Coelioxys* in the short axilla, bare compound eyes, and the blunt metasoma of the male, which has a low transverse apical carina on T6 that is not divided into dorsal and ventral processes as in most *Coelioxys* (but is similar to that of males in *Chelostomoides*). Some species of *Coelioxys* combine features of both genera. For example, *Coelioxys (Boreocoelioxys) funeraria* Smith and *C. (Liothyrapis) decipiens* Spinola have short axillae and bare compound eyes; also, the S6 of the female of *C. (Torridapis) torrida* Smith is broad and rounded, and entirely sclerotized as in *Radoszkowskiana* whereas it is elongate and pointed with a distinct median weakly sclerotized area in most *Coelioxys*. Furthermore, the mode of cleptoparasitism in *Radoszkowskiana* seems to fall within the known repertoire of parasitism of *Coelioxys* (Rozen & Kamel, 2007). Thus, *Radoszkowskiana* seems to be a close relative of *Coelioxys* despite the distinctive male characters. Our analyses consistently placed *Radoszkowskiana* as the sister group to *Coelioxys* (Clade A), a relationship also recovered in the phylogenetic analyses of Rocha Filho & Packer (2017) and Trunz *et al.* (2016). However, the position of this clade of cleptoparasitic bees varied among our analyses.

In the morphological analysis under EW, the clade *Radoszkowskiana* + *Coelioxys* resulted as the sister group of *Noteriades* + *Megachile s.l.* (Fig. 8), but it rendered the latter genus paraphyletic when we analyzed the morphological data under IW. Our preliminary total-evidence phylogeny does not resolve the position of this clade either, as the posterior probabilities values were very low (Figs. 10, 11). Furthermore, our analyses do not support Michener's (2007) view of two independent origins of cleptoparasitism. Behavioral, morphological, and molecular data strongly indicate that cleptoparasitism evolved only once in Megachilini.

Most subgenera of *Megachile s.l.* fell into morphological groups previously associated with differences in nesting behavior. Basal branches included those subgenera of Group 2 that use mud or resins as nesting materials. These subgenera grouped in different clades whose taxonomic composition changed among analyses, except in a few cases (*e.g.*, *Maximegachile* Guigla & Pasteels and *Schizomegachile* Michener always resulted as sister groups). Michener (2007: p. 553) discussed some of these relationships, which we mostly recovered in the morphological analysis under EW, but not under IW nor in the combined phylogeny. Thus, our analyses support the suspicion of Michener (2007) that Group 2 [*Chalicodoma sensu* Michener (1962) and Mitchell (1980)] is nonmonophyletic but it does not support the majority of his divisions or phylogenetic lines.

Taxa that exhibit LC behavior clustered in a large, more derived clade containing all subgenera of Group 1, and included *Megella*, *Mitchellapis* (Group 2), and *Creightonella* (Group 3). These taxa combine some features that are typical of Group 1 and 2 and thus, they have been difficult to place with confidence in any group based on a few

morphological features. The basal position *Creightonella* and *Mitchellapis* within the LC clade is in agreement with the fact that they retained some of the Group 2 features (e.g., chalicodiform body, male S8 with marginal setae) whereas the more derived position of *Megella* indicates the recurrence of some features of Group 2. Because the cost of a character gain might be much higher than its loss, the reacquisition of characters makes some taxa, such as *Megella*, difficult to place in a given taxonomic category. However, studies have documented the recurrence of complex structures, such as eyes and wings (e.g., West-Eberhard, 2003; Whiting *et al.*, 2003). This is likely the result of turning off controlling genes while retaining the underlying genetic architecture, such that even though a complex trait may not be expressed in a given taxon it can be expressed again later in the evolution of the lineage by reactivating the necessary controlling elements. Thus, the gain of less complex structures, such as the marginal setae of S8 and arolia, seems even more plausible in Megachilini.

Chelostomoda is another group that combines features of Groups 1 and 2 of *Megachile s.l.* In the EW analysis of the morphological data, this subgenus was near *Chelostomoides* in Clade B (Fig. 8), but it resulted as the sister group of LC bees when we analyzed this dataset under IW and in combination with molecular data (Figs. 10, 11). The IW scheme shows that the characteristics of Group 2 (e.g., elongate body, terga with strong postgradular grooves, and S8 with marginal setae) exhibited by *Chelostomoda* are homoplastic features. The nesting biology of *Chelostomoda*, *Creightonella*, and *Megella*, which make extensive use of leaf pieces (e.g., Katayama, 2004; Maeta, 2005; Michener, 2007), also supports their placement in Group 1; the biology of *Mitchellapis* is unknown.

Our results also recovered some major phylogenetic lines or groups of subgenera within the LC clade previously discussed by Michener (1965, 2007) and Mitchell (1980). Some of them, such as the *Creightonella* and *Pseudocentron* groups, are distinct and easily recognizable by one or two morphological features; others lack distinct features. We briefly discussed some of them here.

Chrysosarus group: Mitchell (1980) included in this lineage the subgenera *Chrysosarus*, *Dactylomegachile* Mitchell, *Stelodides*, and *Zonomegachile* Mitchell. Based on the description (Raw, 2006) and photographs of the types, *Austrosarus* seems to belong here. Both type of interdental laminae are secondarily lost in this group, except in *Zonomegachile* (Gonzalez *et al.*, 2018). Gonzalez (2013) considered these taxa within a single subgenus, *Chrysosarus*, but our analyses indicate that *Zonomegachile* does not belong to this group.

Creightonella group: This lineage includes the subgenera *Creightonella*, *Mitchellapis*, *Sayapis*, and *Schrottkyapis*. The members of this group have a chalicodomiform body shape and odontogenic interdental laminae only. A remarkable feature of this lineage is the S6 of the female; at least in the species we examined for this study, it is elongate and with a membranous or weakly sclerotized pregradular area (visible only after dissection). Mitchell (1980) recognized this lineage under the generic name of *Eumegachile* Friese; however, he also included the subgenera *Eumegachile* and *Grosapis* Mitchell but separated *Creightonella* generically (Appendix 1).

Megachiloides group: Mitchell (1980) included *Megachiloides* Mitchell, *Argyropile* Mitchell, and three other names that Michener (2000, 2007) synonymized under *Megachiloides* or *Xanthosarus* Robertson. Unlike most species of LC bees, members of this group appear to dig their own nest in the ground (Eickwort *et al.*, 1981).

Pseudocentron group: All members of this group of subgenera are primarily Neotropical in distribution; *Acentron* Mitchell, *Leptorachis* Mitchell, *Melanosarus*, *Moureapis*

Table 3. Monotypic, monophyletic, and non-monophyletic subgenera of *Megachile* Latreille *s.l.* *sensu* Michener (2007). * = subgenera represented by a single species in this study but they are likely monophyletic given their morphological uniformity; † = fossil taxa.

Monotypic	Monophyletic	Likely Monophyletic*	Non-monophyletic
<i>Cesacongoa</i>	<i>Acentron</i>	<i>Alocanthedon</i>	<i>Callomegachile</i>
† <i>Chalicodomopsis</i>	<i>Aethomegachile</i>	<i>Austrochile</i>	<i>Chelostomoides</i>
<i>Eumegachile</i>	<i>Amegachile</i>	<i>Cestella</i>	<i>Chrysosarus</i>
<i>Grosapis</i>	<i>Argyropile</i>	<i>Chalicodomoides</i>	<i>Dasymegachile</i>
<i>Heriadopsis</i>	<i>Austromegachile</i>	<i>Cressoniella</i>	<i>Eutricharaea</i>
<i>Matangapis</i>	<i>Chalicodoma</i>	<i>Largella</i>	<i>Hackeriapis</i>
<i>Parachalicodoma</i>	<i>Chelostomoda</i>	<i>Lophanthedon</i>	<i>Leptorachis</i>
<i>Parachizomegachile</i>	<i>Creightonella</i>	<i>Maximegachile</i>	<i>Pseudomegachile</i>
<i>Schrottkyapis</i>	<i>Gronoceras</i>	<i>Mitchellapis</i>	<i>Sayapis</i>
<i>Stelodides</i>	<i>Litomegachile</i>	<i>Moureapis</i>	<i>Stenomegachile</i>
	<i>Megachile</i>	<i>Neocressoniella</i>	<i>Xanthosarus</i>
	<i>Megachiloides</i>	<i>Platysta</i>	
	<i>Megella</i>	<i>Ptilosaroides</i>	
	<i>Melanosarus</i>	<i>Ptilosarus</i>	
	<i>Neochelynia</i>	<i>Rhyssomegachile</i>	
	<i>Paracella</i>	<i>Rhodomegachile</i>	
	<i>Pseudocentron</i>	<i>Thaumatosoma</i>	
	<i>Tylomegachile</i>	<i>Trichurochile</i>	
		<i>Zonomegachile</i>	

Raw, and *Pseudocentron* Mitchell are included here. Mitchell (1980) recognized this lineage and placed them in the genus *Pseudocentron* (Appendix 1). The most distinctive character is the S6 of the female. It has at least the posterior half bare or nearly so, except for a subapical row of short setae, behind which there is a bare, smooth rim directed posteriorly.

Mitchell (1980) grouped the remaining subgenera of LC bees in two genera, *Megachile* and *Cressoniella* Mitchell (Appendix 1). In our analyses, these subgenera resulted in multiple clades but some taxa clustered as suggested by Mitchell. For example, he placed *Ptilosarus* Mitchell, *Ptilosaroides* Mitchell, *Rhyssomegachile* Mitchell, and *Neochelynia* Schrottky in *Cressoniella*. We recovered these subgenera in the same clade but apart from the other subgenera included by Mitchell (1980) in his genus *Cressoniella*.

Unlike the fossil tribes Ctenoplectrellini and Glyptapini, whose phylogenetic positions were consistent among analyses (Fig. 9), that of the Dominican fossil *M. glaesaria* varied from being near *Chelostomoides* (Fig. 8) to be the sister group of all Megachilini (Figs. 10, 11). Interestingly, Engel (1999) discussed the possibility of both phylogenetic positions. Such instability might be the result of the low number of characters that we were able to score from this fossil (75 of 272).

MONOPHYLY OF SUBGENERA OF MEGACHILE S.L.: Ten of the 57 subgenera of *Megachile* *s.l.* included in this study are monotypic (Table 3). The 19 subgenera containing more than one species but represented in our analyses by a single species are also putatively monophyletic because each is morphologically uniform (*e.g.*, *Maximegachile*, *Ptilosarus*). The monophyly of 18 subgenera was either strongly supported (*e.g.*, *Pseudocentron*) or weakly supported but consistently recovered among analyses. Our analyses support the non-monophyly of several subgenera, which previous authors had already suspected or suggested (Michener, 2007; Trunz *et al.*, 2016). Among the subgenera of Group 2, *M. biseta* Vachal, *M. decemsignata*, *M. memecyloniae* (Engel), and *M. torrida*

rendered *Callomegachile* paraphyletic; *M. ignita* Smith and *M. heriadiformis* Smith rendered *Hackeriapis* polyphyletic; *M. muansae* Friese, *M. cestifera* Benoist, and *M. incana* Friese rendered *Pseudomegachile* Friese paraphyletic; *M. dolichosoma* Benoist rendered *Stenomegachile* Pasteels polyphyletic; and *M. rugifrons* (Smith) rendered *Chelostomoides* paraphyletic. Among the clade of LC bees, *M. assumptionis* rendered *Sayapis* paraphyletic; *M. platystoma* Pasteels, *M. eurymera* Smith, *M. submetallica* Benoist, and *M. digiticauda* Cockerell rendered *Eutricharaea* Thomson polyphyletic; *M. fortis* Cresson and *M. addenda* Cresson rendered *Xanthosarus* polyphyletic; *M. laeta* rendered *Leptorachis* polyphyletic; *M. schwimmeri* Engel (a replacement name for *M. mitchelli* Raw: *vide* Engel, 2017) rendered *Dasymegachile* Mitchell polyphyletic; and *M. euzona* rendered *Chrysosarus* paraphyletic.

In some cases, the recognition of highly derived species at the subgeneric level rendered some taxa paraphyletic. For example, as Michener (2007) suspected, the monotypic subgenus *Schrottkyapis* renders *Sayapis* paraphyletic. A single putative synapomorphy supports such a relationship: S6 of the female with a nearly membranous pregradular area and a distinct invagination parallel to the lateral margin of the sternum (visible only after dissection). In other cases, such as in *Eutricharaea*, *Hackeriapis*, and *Callomegachile*, current taxon concepts are broad and Michener (2007) proposed them as practical solutions to show relationships among diverse, poorly known groups. For example, when Michener (2007) synonymized various groups under *Eutricharaea*, as he did for many other bees, he acknowledged the arbitrariness of his decision. He also highlighted morphological features that supported their relationships, which turned out to be homoplastic characters in our analyses (e.g., apical fasciae under scopa, T6 preapical carina toothed or denticulate and medially emarginate). Thus, in several instances breaking up Michener's (2007) heterogeneous circumscriptions into multiple subgenera (e.g., resurrecting *Eumegachilana* Michener and others among *Callomegachile*) aids the recognition of natural groups as well as stimulates revisionary studies which can be undertaken on more manageable units.

PHYLOGENETIC SIGNAL OF MORPHOLOGICAL CHARACTERS: The morphological character sets used in the phylogeny of Megachilini showed different levels of homoplasy (Table 1), as per RI value and percentage of unambiguous synapomorphic characters, but such differences were not statistically significant. Thus, these character sets were equally informative for the phylogeny. However, the analysis of female characters alone, which also excluded those present in the male but coded only for the female to avoid duplication, recovered Megachilini and several major lineages, unlike the analysis of male characters that resulted in a large polytomy. This does not mean that male characters were useless, but rather that our dataset was female-biased (Fig. 7A).

Several authors have recognized important morphological features of taxonomic value in the male (e.g., Mitchell, 1980; Michener, 2007; Engel & Gonzalez, 2011; Gonzalez & Engel, 2012; Gonzalez *et al.*, 2018), which appear to show high rates of evolution, as they are sometimes highly variable within and among distinct phylogenetic lineages. For example, secondary sexual features such as the preapical carina of T6, mandibular projection, coxal spine, and modifications of front legs, are associated with particular strategies of mating system (Wittmann & Blochtein, 1995). The morphology of these structures are largely unexplored and, depending on the level of study and finer levels of character conceptualization, they might prove phylogenetically informative as in other group of bees (e.g., *Xylocopa* Latreille; Minckley, 1998). Equally unexplored is the female mandible. We conceptualized a number of characters for our study, but the mandible has a plethora of anatomical features with potential phyloge-

netic and taxonomic values at other levels of study. Michener & Fraser (1978) established terminology and homologies for the various structures of the bee mandible, but they only considered the body, not the apex. Among these ignored structures in the mandibular apex were the interdental laminae, which as we have shown, are relevant for understanding the biology, taxonomy, and phylogeny of Megachilini.

Origin and Patterns of Variation of the Interdental Lamina

We demonstrate for the first time that interdental laminae, the most distinctive and taxonomically significant feature of LC bees, likely developed from two different structures in the female mandible. We also show that odontogenic laminae evolved once and prior to the development of ctenogenic laminae, which developed from the fimbrial ridge and appeared in more derived LC taxa (Fig. 12). These findings have major implications for our understanding of the connection between character evolution and diversification. The most obvious is that interdental laminae represent two characters that evolved in a sequence of evolutionary events, not a single character that evolved once as current dogma surmises (Michener, 2007; Trunz *et al.*, 2016).

Our analyses also suggest that the presence of odontogenic laminae is a putative synapomorphy for all LC bees, which exhibits more phenotypic plasticity than ctenogenic laminae. The multiple modifications and secondary losses observed across the phylogeny are more likely in this type of lamina perhaps because of its small size and less involved structural modifications relative to ctenogenic laminae. However, losses in ctenogenic laminae occurred independently in two clades, the *Chryzosarus* and *Megachile s.str.* groups of subgenera, sometimes also with the loss of odontogenic laminae (Fig. 12). While retaining the use of leaves, these groups have incorporated other nesting materials, such as mud or petals (*e.g.*, Laroca *et al.*, 1992; Banaszak & Romasenko, 1998; Zillikens & Steiner, 2004; Michener, 2007). At least one species, *M. (M.) montivaga*, makes nests entirely of petals (*e.g.*, Mitchell, 1935b; Michener, 2007; Orr *et al.*, 2015). The environmental factors that favor the use of mud or petals in LC bees are unknown. As far as we know, species with secondarily lost interdental laminae co-occur in the same habitats with LC bees, and sometimes even occupy a wide range of habitats (*e.g.*, *M. montivaga*).

Although the mandible of LC bees appears to be shorter, apically wider, and with rather two distinct outer surfaces than that of dauber bees, pairwise tests for trait correlation revealed no significant associations between each of them and the presence of interdental laminae. Pairwise comparisons also suggest similar independence of trait evolution between a short ocelloccipital distance and the absence of setae on the adductor interspace in the inner surface of the mandible (Table 2). Parsimony reconstructions suggest that these are ancestral character states (not shown). They are also present in some dauber bees in the genus *Megachile s.l.*, as well as in some outgroups. Thus, these cephalic and mandibular features, rather than being associated with leaf cutting, are likely the result of a shift in processing and handling foraging materials (leaves, plant hairs, pebbles, resins, &c.) as an alternative to using glandular secretions to waterproof cells in the soil (Michener & Fraser, 1978; Eickwort *et al.*, 1981).

Origin of Leaf-cutting Behavior

Our preliminary total-evidence tip-dated analyses aimed to provide additional hypotheses of relationships and to assess the temporal discrepancy between the recent

age (20–25 Ma) estimated from molecular analyses using a node-dating approach (Litman *et al.*, 2011; Trunz *et al.*, 2016) and the much older age (60 Ma) suggested by fossil traces (Michez *et al.*, 2012). A tip-dating approach allows the incorporation of all available fossils into phylogenetic analyses, which not only expands the taxonomic coverage and ancestral character states, but also provides more accurate fossil information to the analysis than *ad hoc* node age constraints (*e.g.*, Pyron, 2011; Ronquist *et al.*, 2012a; Slater & Harmon, 2013; Arcila *et al.*, 2015). However, tip-dating analyses tend to estimate much older divergence times when compared to the node-dating approach, sometimes unrealistically (*e.g.*, O'Reilly *et al.*, 2015; O'Reilly & Donoghue, 2016). In our case, the tip-dated analyses suggested a similar recent divergence time (15–25 Ma) to those obtained from molecular analyses using a node-dating approach (Figs. 10, 11). The position of the fossil *M. glaesaria* as the sister group to all other Megachilini, which differed from that obtained in the morphological analysis (Fig. 8), influenced the divergence time estimates. Constraining the position of this fossil near *Thaumatostoma*, as in the morphological analysis, yielded older estimates for the origin of LC bees, yet these values were never greater than 30 Ma.

Our analyses support the idea that Eocene trace fossils might not be the result of LC bees, but we should interpret these results with caution. First, we used a low number of fossils in our analyses, particularly in the generic-level phylogeny, and studies have shown that including more fossil taxa across different clades increases the precision of tip-dating estimates (Pyron, 2011; Ronquist *et al.*, 2012a; Dos Reis & Yang, 2013). Second, if age estimates are correct, they are indicating the origin of taxa within *Megachile s.l.* with interdental laminae, not the origin of the LC behavior itself.

Although the presence of interdental laminae is associated with leaf cutting, these structures are not required to express this behavior. For example, LC bees that secondarily lost these laminae are still able to cut leaves (*e.g.*, Laroca *et al.*, 1992; Zillikens & Steiner 2004; Torretta *et al.*, 2014). Leaf-cutter ants, which never developed interdental laminae (Fig. 13A–C), are also able to cut leaves, petals, and grasses efficiently. Shifts in behavior might act as drivers of evolutionary diversification and phenotypic change (*e.g.*, Duckworth, 2009; Lapedra *et al.*, 2013). Thus, it is likely that interdental laminae might have evolved after the LC behavior was already in place. This idea is supported by the use of chewed leaf pulp, large petal pieces, and irregular leaf pieces in some *Osmiini* and in some *Callomegachile* that lack interdental laminae (Michener, 2007; Rozen *et al.*, 2010). Lower costs in handling and processing large leaf pieces when compared with masticated plant material, and a greater access to more readily available vegetative plant resources (flowers are not often continuously available), might have facilitated a transition to leaf cutting.

The development of interdental laminae might have either allowed a more efficient way to cut and process leaves, or allowed access to more leaf types and plants. Bee species with odontogenic laminae only or without it, cut irregularly margined leaf pieces [*e.g.*, Soh, 2014: *M. (Creightonella) atrata* Smith]. In species with both types of laminae, the margins of the leaf pieces are smooth (Michener, 2007). The study of MacIvor (2016) supports the second adaptive hypothesis. For example, *M. (Sayapis) pugnata* Say, a species with odontogenic lamina only, significantly uses less plant species than *M. (Megachile) centuncularis* and *M. (E.) rotundata*, species from lineages that developed both types of laminae. However, leaf choice might not only depend on the ability to cut certain types of leaves, but also on the local availability as well as on their chemical, mechanical, and antimicrobial properties.

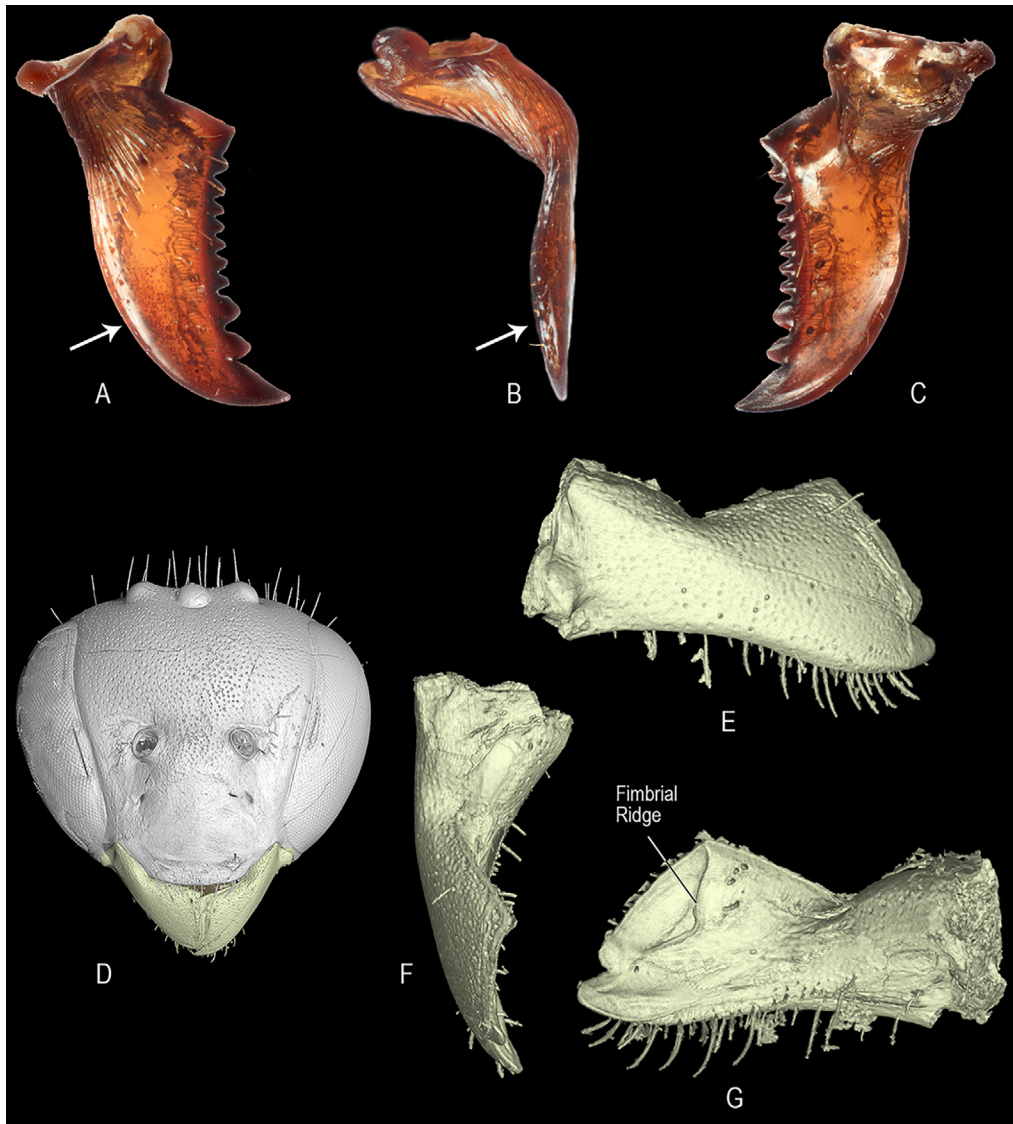


Figure 13. Female mandible of leaf-cutter ants and extinct Baltic amber megachilids. **A–C.** Right mandible of leaf-cutter ant (Formicidae: Attini: *Atta* sp.) in frontal, lateral, and inner views, respectively. Arrow points to the lower margin. **D–G.** Synchrotron-radiation μ CT scan of *Glyptapis* sp. (Glyptapini) from Eocene Baltic amber; facial view of the head and right mandible in outer, superior, and inner views, respectively [note that the scan resolution could not resolve the finest setae, such as those of the compound eyes which are present in this specimen as in all species of *Glyptapis* Cockerell (Engel, 2001)].

If the derived clade of LC bees evolved recently, and interdental laminae are not required for and likely evolved after the LC behavior, which insects are then responsible for the Eocene fossil leaf excisions? There are few insects capable of leaving similar cuts on leaf margins (for a discussion see Wedmann *et al.*, 2009) and one of them are LC ants. However, LC ants are restricted to the Neotropics and they evolved even more recently (8–12 Ma) than LC bees (Schultz & Brady, 2008). Larval sawflies, larval lepi-

dopterans, and adult and larval beetles also produce arcuate excisions on leaf margins, but these are quite different from megachilids, as they are uniformly cusped, sharp, and entire (Labandeira, 2002: fig. 6m, n). Another possibility is that extinct lineages of megachilid bees from the Eocene (e.g., Ctenoplectrellini and Glyptapini) also cut leaves, or even extinct lineages within Osmiini or stem-group Megachilini.

An examination of the mandibular structure of fossils from Ctenoplectrellini and Glyptapini, both using light microscopy and CT scans, showed two different types of mandibles. In Glyptapini, the lateral surface of the mandible gently curves towards the apex; its distal margin has a single apical tooth and a long, edentate upper margin (trimmal expansion); and the inner surface of the mandible possesses a distinct fimbrial ridge apically, which is long and parallel to the edentate upper margin (Figs. 13D–G). Thus, the mandible of Glyptapini resembles that of some species of Anthidiini that use resins, as well as that of some species of Group 2 of *Megachile s.l.* Unlike Glyptapini, the female mandible of Ctenoplectrellini is tridentate (males are bidentate) and has two distinct outer surfaces that merge rather abruptly with each other, one lateral basally and one anterior distally (Engel, 2001). Thus, the mandible of Ctenoplectrellini is somewhat similar to that of some species of *Osmia* Panzer. Finally, interdental laminae and fimbrial carinae are completely absent in both tribes.

Based on the mandibular structure, it is therefore unlikely that these particular extinct taxa might have cut leaves, principally Glyptapini. However, it is likely that Ctenoplectrellini might have used plant resources as nesting materials because *Aspidosmia*, its extant closest relative, uses masticated leaf pulp to build their nests (Brauns, 1926). Thus, the identity of the Eocene LC insects remains elusive, and may or may not have included extinct Megachilinae or stem-group Osmiini or Megachilini. Alternatively, the estimated dates of divergence may be grossly underestimated. For now, the only direct evidence from the Eocene and other deposits demonstrates that some taxon, either a LC bee or LC bee-like relative, was present and capable of producing cuts indistinguishable from those of modern LC bees and different from those other insects that cut or chew leaves.

Classificatory Implications

FAMILY MEGACHILIDAE: The phylogenetic relationships obtained from our preliminary total-evidence analyses were generally congruent with previous phylogenetic hypotheses (Litman *et al.*, 2011; Gonzalez *et al.*, 2012). However, they revealed new relationships that might help to resolve phylogenetic positions of problematic taxa and adjust current classificatory proposals. For example, our analysis suggests that both Dioxyini and Aspidosmiini are extant relatives of the extinct tribes Ctenoplectrellini and Glyptapini. Previous authors placed all these tribes within either Anthiidini or Osmiini (e.g., Engel, 2001; Michener, 2007), but our analyses clearly show them in a well-supported clade, sister to the remaining Megachilinae. The relationship of Dioxyini with these fossil taxa is a new phylogenetic hypothesis for this distinctive taxon. All four of these tribes have aroliae, cleft pretarsal claws, and the crossvein 2m-cu basal to 2rs-m, but these features are also present in other Megachilinae. Aspidosmiini rendered Ctenoplectrellini paraphyletic in our analysis, and in that case, it would be appropriate to synonymize the former under the latter tribe. Gonzalez *et al.* (2012) discussed this option but ultimately decided to recognize it in its own tribe because of the limited number of scored characters for these fossils, which could have biased the results. Thus, we suggest recognizing Aspidosmiini until further analyses test these relationships using a larger number of characters for the fossil taxa.

Table 4. Hierarchical suprageneric classification of Megachilidae including two new tribes described in the text (*vide infra*). Classification follows Engel (2005) and Gonzalez *et al.* (2012). † = fossil taxa.

Subfamily Fideliinae Cockerell
Tribe Neofideliini Engel
Tribe Fideliini Cockerell
Subfamily Pararhophitinae Popov
Subfamily Lithurginae Newman
Tribe †Protolithurgini Engel
Tribe Lithurgini Newman
Subfamily Megachilinae Latreille
Tribe †Glyptapini Cockerell
Tribe Dioxyini Cockerell
Tribe †Ctenoplectrellini Engel
Tribe Aspidosmiini Gonzalez & al.
Tribe Pseudoheriadini Gonzalez & Engel, new tribe
Tribe Megachilini Latreille
Tribe Ochreriadini Gonzalez & Engel, new tribe
Tribe Osmiini Newman
Subtribe Chelostomina Kirby
Subtribe Heriagina Michener
Subtribe Osmiina Newman
Tribe Anthidiini Ashmead
Subtribe Trachusina Robertson
Subtribe Anthidiina Ashmead

The osmiines *Afroheriades* and *Pseudoheriades* are sister genera that form a well-supported clade. The morphological analysis of Gonzalez *et al.* (2012) placed them among the *Heriades*-group of genera of Osmiini whereas the molecular analysis of Praz *et al.* (2008) placed them either as sister of either Anthidiini or Megachilini. Griswold (1985) also suggested a relationship with Megachilini based on the modified setae on the fifth sternum of the male. Our analyses consistently placed these two genera and Megachilini in a well-supported clade (Fig. 9). All other Osmiini clustered in another clade. Thus, in order to recognize a monophyletic Osmiini, we would need to either transfer them to Megachilini or distinguish them in their own tribe. Transferring them to Megachilini weakens the recognition and diagnosis of this tribe because a morphological synapomorphy unambiguously present in that clade is unknown. In contrast, recognizing *Afroheriades* and *Pseudoheriades* in their own tribe might highlight their distinctiveness while maintaining the current taxon concept for Megachilini. The tribe Osmiini will thus contain those taxa clustered in the other clade, which is sister to Megachilini + (*Afroheriades* + *Pseudoheriades*), except for *Ochreriades*.

The phylogenetic position of *Ochreriades* has varied among morphological (Gonzalez *et al.*, 2012), molecular (Praz *et al.*, 2008), and our combined analyses. For example, it resulted among the *Heriades*-group of genera, as sister to all of Megachilinae, or as sister to Megachilini and Osmiini. In our Bayesian analysis, *Ochreriades* clustered with the majority of osmiines (excluding *Afroheriades* + *Pseudoheriades*) in a clade with low support. *Ochreriades* is morphologically distinctive among megachilids. It has yellow integumental markings as in the Anthidiini, a very long body with an elevated pronotum that surrounds the mesoscutum anteriorly, and long mouthparts that reach the tip of the metasoma. Thus, *Ochreriades* is a taxon with distinctive features whose separation from Osmiini might be desirable. Based on these results, we propose to

recognize two new tribes (Pseudoheriadini and Ochreeradini, *vide infra*), thus, narrowing and strengthening the taxon concept of Osmiini. Our preliminary analyses also support the recognition of three subtribes or genus groups within Osmiini and two within Anthidiini (Table 4).

TRIBE MEGACHILINI: Our morphological phylogeny suggests that recognizing *Gronoceras*, *Heriadopsis*, and *Matangapis* as genera distinct from *Megachile s.l.*, but not other Group 2 subgenera, renders that latter genus paraphyletic. Our preliminary total-evidence analyses also support this idea, although branch support is low. We discuss three possible phylogeny-based solutions, but advocate for one that maximizes information storage and retrieval, memorability, and congruence with modern classification in other bee taxa.

The first classificatory proposal is to recognize only two extant genera in Megachilini, *Noteriades* and *Megachile*. The cleptoparasitic genera *Coelioxys* and *Radoszkowskiana*, would be subgenera of *Megachile*. The fossil subgenus *Chalicodomopsis* could be treated either as a subgenus of *Megachile* given its position in the morphological analysis under EW or as a genus, as suggested in the IW and combined analyses.

The second proposal recognizes some of the subgenera of Group 2 at the generic rank, namely those taxa that clustered in a large clade with *Coelioxys* and *Radoszkowskiana*. All of these taxa are Old World in distribution and the majority of them are hoplitiform or heriadiform in body shape (e.g., *Thaumatoma*, *Rhodomegachile*, *Hackerriapis*). Thus, this proposal would recognize about 15 genera alongside *Megachile*, the latter including a mixture of Groups 1, 2, and 3.

The third proposal differs from the second in that *Megachile* would be restricted to the derived, well-supported clade that includes the LC bees only (Clade C in Figs. 8, 10, 11). This proposal would treat the remaining taxa at the generic level, thus recognizing about 28 genera total (Table 5, Fig. 14). Therefore, our proposals are somewhat similar to those discussed by Trunz *et al.* (2016), but differ in the number and identity of the taxa recognized at the generic level due to differences in the clade composition with our total-evidence phylogeny.

All three proposals imply new combinations of names and each proposal has practical advantages and disadvantages. An obvious advantage of retaining a large genus *Megachile s.l.*, as in the first proposal, is that even with further knowledge of its phylogeny, the combinations of names created by the second and third proposals would not have to be accepted and perhaps, later, altered again. Phylogenies are always subject to change with the discovery of new taxa or the analysis of new morphological, behavioral, and molecular data. For example, features of immature stages might provide additional informative characters, but available information suggests little morphological variation in the major lineages of *Megachile s.l.* (Rozen *et al.*, 2016). However, the first proposal also requires the inclusion of *Coelioxys* and *Radoszkowskiana* in *Megachile*, which would create more than 470 combinations of names and perhaps many new homonyms. *Megachile* would be an enormous genus with nearly 2000 species, more than 75 subgenera, and a wide range of biologies and morphologies. Such a retrograde classification is therefore highly undesirable.

Adopting the second or third proposal would not create as many new combinations of names as in the first proposal. As previously outlined in the introduction, several authors initially described some taxa of Group 2 at the generic rank (e.g., *Chelostomoides*, *Gronoceras*, *Heriadopsis*, *Thaumatoma*), which others subsequently treated first as subgenera of *Chalicodoma* and then of *Megachile*. Furthermore, because of the economic importance and worldwide distribution of Group 1, most published work

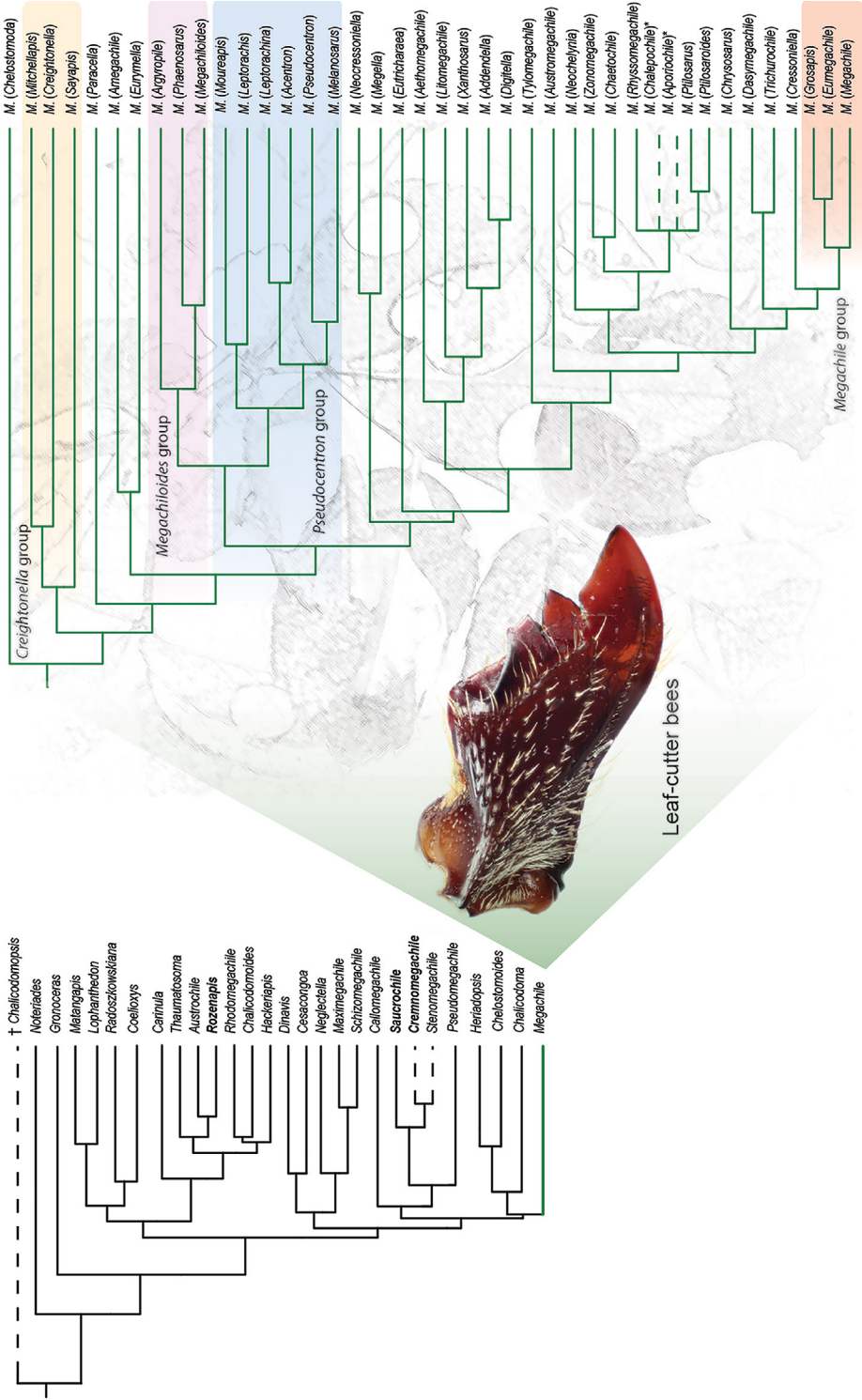


Figure 14. Summary of the proposed classification for Megachilini (Table 5 and Appendices 6, 7). Broken lines indicate uncertain positions. New taxa described herein are bold faced. Gonzalez et al. (2018) recognized and described two new subgenera of Megachile after this work was completed (indicated with an asterisk) and were not included in the analyses. Groups of subgenera of Megachile highlighted in color are discussed in the text.

Table 5. New classification of Megachilini following Proposal #3 (see text). The list follows the order of taxa according to the phylogeny represented in figure 11. It does not include the subgenera of *Coelioxys* Latreille. † = fossil taxa; * = new status.

Genus † <i>Chalicodomopsis</i> Engel*	Genus <i>Megachile</i> Latreille
Genus <i>Noteriades</i> Cockerell	Subgenus <i>Chelostomoda</i> Michener
Genus <i>Gronoceras</i> Cockerell	Subgenus <i>Mitchellapis</i> Michener
Genus <i>Matangapis</i> Baker & Engel	Subgenus <i>Creightonella</i> Cockerell
Genus <i>Lophanthedon</i> Gonzalez & Engel*	Subgenus <i>Sayapis</i> Titus
Genus <i>Coelioxys</i> Latreille	Subgenus <i>Paracella</i> Michener
Genus <i>Radoszkowskiana</i> Popov	Subgenus <i>Amegachile</i> Friese
Genus <i>Carinula</i> Michener & al.*	Subgenus <i>Eurymella</i> Pasteels
Genus <i>Thaumatoma</i> Smith	Subgenus <i>Argyropile</i> Mitchell
Genus <i>Austrochile</i> Michener*	Subgenus <i>Phaenosarus</i> Mitchell
Genus <i>Rozenapis</i> Gonzalez & Engel, n. gen.	Subgenus <i>Megachiloides</i> Mitchell
Genus <i>Rhodomegachile</i> Michener*	Subgenus <i>Mourepis</i> Raw
Genus <i>Chalicodomoides</i> Michener*	Subgenus <i>Leptorachis</i> Mitchell
Genus <i>Hackeriapis</i> Cockerell*	Subgenus <i>Leptorachina</i> Mitchell
Genus <i>Dinavis</i> Pasteels*	Subgenus <i>Acentron</i> Mitchell
Genus <i>Cesacongoa</i> Koçak & Kemal*	Subgenus <i>Pseudocentron</i> Mitchell
Genus <i>Neglectella</i> Pasteels*	Subgenus <i>Melanosarus</i> Mitchell
Genus <i>Maximegachile</i> Guiglia & Pasteels*	Subgenus <i>Neocressoniella</i> Gupta
Genus <i>Schizomegachile</i> Michener*	Subgenus <i>Megella</i> Pasteels
Genus <i>Callomegachile</i> Michener*	Subgenus <i>Eutricharaea</i> Thomson
Subgenus <i>Alocanthedon</i> Engel & Gonzalez	Subgenus <i>Aethomegachile</i> Engel & Baker
Subgenus <i>Callomegachile</i> Michener	Subgenus <i>Litomegachile</i> Mitchell
Subgenus <i>Eumegachilana</i> Michener	Subgenus <i>Xanthosarus</i> Robertson
Subgenus <i>Morphella</i> Pasteels	Subgenus <i>Addendella</i> Mitchell
Genus <i>Saucrochile</i> Gonzalez & Engel, n. gen.	Subgenus <i>Digitella</i> Pasteels
Genus <i>Cremnochile</i> Gonzalez & Engel, n. gen.	Subgenus <i>Tylomegachile</i> Moure
Genus <i>Stenomegachile</i> Pasteels*	Subgenus <i>Austromegachile</i> Mitchell
Genus <i>Pseudomegachile</i> Friese*	Subgenus <i>Neochelynia</i> Schrottky
Subgenus <i>Archimegachile</i> Alfken	Subgenus <i>Zonomegachile</i> Mitchell
Subgenus <i>Cestella</i> Pasteels	Subgenus <i>Chaetochile</i> Mitchell
Subgenus <i>Largella</i> Pasteels	Subgenus <i>Rhyssomegachile</i> Mitchell
Subgenus <i>Parachalicodoma</i> Pasteels	Subgenus <i>Chalepochile</i> Gonzalez & Engel
Subgenus <i>Pseudomegachile</i> Friese	Subgenus <i>Aporiochile</i> Gonzalez & Engel
Subgenus <i>Xenomegachile</i> Rebmann	Subgenus <i>Ptilosarus</i> Mitchell
Genus <i>Heriadopsis</i> Cockerell	Subgenus <i>Ptilosaroides</i> Mitchell
Genus <i>Chelostomoides</i> Robertson*	Subgenus <i>Chrysosarus</i> Mitchell
Subgenus <i>Chelostomoides</i> Robertson	Subgenus <i>Dasymegachile</i> Mitchell
Subgenus <i>Chelostomoidella</i> Snelling	Subgenus <i>Trichurochile</i> Mitchell
Genus <i>Chalicodoma</i> Lepeletier de Saint Fargeau	Subgenus <i>Cressionella</i> Mitchell
	Subgenus <i>Grosapis</i> Mitchell
<i>Incertae sedis</i>	Subgenus <i>Eumegachile</i> Friese
Genus <i>Stellenigris</i> Meunier	Subgenus <i>Megachile</i> Latreille

has been done on members of this group rather than on Group 2 or 3. Thus, the new combinations of names resulting from treating the subgenera of Group 2 at the generic level would not have a major effect in the literature.

Recognizing some subgenera of Group 2 at the generic rank while others as subgenera of *Megachile*, as in the second proposal, would still make *Megachile* highly heterogeneous morphologically and biologically, rendering the genus difficult to diag-

nose as well as differentiate from remaining Megachilini. However, the third proposal allows a more efficient retrieval of information and significantly improves the recognition and diagnosability of *Megachile* when the genus only consists of groups that cut leaves and developed interdental laminae. For example, recognizing *Megachile* in a narrower sense than in the second proposal would highlight the differences in nesting behavior and morphology among groups. This division may also encourage faster taxonomic revisions and comparative biological studies that would in turn increase our understanding of Megachilini.

The multigeneric classification of the third proposal might seem like an extreme change, but upon inspection, is not. First, authors have previously recognized several subgenera within Group 2 at the genus rank, and the need for a multigeneric classification in Megachilini has repeatedly been voiced (e.g., Mitchell, 1980; Engel & Baker, 2006; Michener, 2007; Trunz *et al.*, 2016). The problem at the time had been in choosing the best approach to picking which taxa to recognize at the genus rank in the absence of phylogenetic hypotheses. Second, the morphological differences among the subgenera of Group 2 are comparable or even greater than that among other genera of bees, including other megachilid tribes. For example, the morphological differences between the stingless bee genera *Trigona* Jurine and *Partamona* Schwarz (Apidae: Meliponini), or between the wool carder bee genera *Anthidium* Fabricius and *Afranthidium* Michener (Megachilidae: Anthidiini), seem trivial when we compare that between *Hackeriapis* and *Chalicodoma*. Such a difference in the breadth of generic concepts among bee groups might be a reflection of the levels of taxonomic, phylogenetic, and morphological knowledge within each group. Third, many bee taxa now widely accepted as genera today, were treated in the past as subgenera of much larger genera, just like in the case of *Megachile s.l.* For example, Michener (1944) and Schwarz (1948) treated the more than 20 genera of Meliponini recognized today as subgenera of *Trigona*. Fourth, other authors (e.g., Almeida, 2008; Almeida & Danforth, 2009) have recently proposed to elevate at the genus rank numerous subgenera of other similarly diverse bee genera, such as *Leioproctus* Smith *s.l.* (Colletidae) *sensu* Michener (2007). For these reasons, we advocate the third proposal given its practical advantages, its hierarchical arrangement, and congruence with modern generic concepts of bees.

In addition to elevating the status of subgenera of Group 2 to the genus level following the third proposal (Table 5), one might need to create some new genera for species that rendered some taxa paraphyletic, as well as new synonymies and taxonomic arrangements (*vide infra*). For example, if one wishes to recognize *Callomegachile* Michener at the generic level, several genus-group names are available and could be treated as subgenera (e.g., *Alocanthesdon* Engel & Gonzalez). The five species placed in *Carinula* Michener *et al.* are more related to *Hackeriapis* than *Callomegachile*. The presence of translucent distal margins in the male terga reinforces their affinity to *Hackeriapis*. The species placed in *Parachalicodoma* Pasteels, *Largella* Pasteels, and *Cestella* Pasteels showed a close relationship with *Pseudomegachile*, rendering the latter paraphyletic in some analyses. They could be regarded as species groups or subgenera of *Pseudomegachile* (Table 5). *Dinavis* Pasteels and *Negletella* Pasteels did not cluster with *Pseudomegachile* and thus they could be treated as separate genera. *Megachile* (*Chelostomoides*) *rugifrons* rendered *Chelostomoides* paraphyletic in all analyses, clustering closer to groups such as *Schizomegachile*. However, the morphology of both sexes is highly variable among the species of this group and we were not able to find a single morphological feature that consistently separated *M. rugifrons* from the remaining *Chelostomoi-*

des. Thus, we suggest retaining this species in *Chelostomoides* despite its position in the analyses until a finer analysis can be undertaken on this clade.

In the genus *Megachile*, according to the third proposal, we would recommend resurrecting the following subgenera: *Eurymella* Pasteels and *Digitella* Pasteels from *Eutricharaea* Thomson; *Phaenosarus* Mitchell and *Addendella* Mitchell from *Xanthosarus*; *Leptorachina* Mitchell from *Leptorachis*; and *Chaetochile* Mitchell from *Dasymegachile*. We also newly synonymize *Schrottkyapis* under *Sayapis* (new synonymy), while *Stelodides* was previously placed under *Chrysosarus* and our results corroborate such a synonymy (Gonzalez, 2013) (Appendices 6, 7). While Trunz *et al.* (2016) already established some of the changes indicated above (e.g., *Parachalicodoma* as a synonym of *Pseudomegachile*), some other authors (e.g., Durante & Abrahamovich, 2006; Moure *et al.*, 2007) never adopted Michener's (2007) classification and still recognize some of the subgenera (e.g., *Leptorachina*, *Chaetochile*) that we recovered as independent lineages in our analyses.

Finally, Trunz *et al.* (2016) proposed to synonymize *Grosapis* and *Eumegachile* under *Megachile s.str.*, and *Paracella* Michener under *Anodonteutricharaea* Tkalců, the order of the latter synonym corrected by Praz (2017). Such taxonomic changes might be correct but we do not recommend following these changes at this time because *Eumegachile* only rendered *Megachile s.str.* in the morphological analysis under EW, and both groups resulted as the sister group to *Megachile s.str.* in the combined analysis. *Grosapis* and *Eumegachile* are each morphologically distinctive and, although we included a few species of *Megachile s.str.* in our analyses, synonymizing these taxa under *Megachile s.str.* would make it difficult to diagnose and recognize. Trunz *et al.* (2016) suggested the synonymy of *Paracella* under *Anodonteutricharaea* (*vide etiam* Praz, 2017) based on the phylogenetic position of *M. villipes* Morawitz, a species assigned to *Anodonteutricharaea*, a subgenus already synonymized under *Eutricharaea* by Michener (2007). However, neither these authors nor we were able to include the type species of *Anodonteutricharaea*, *M. lanigera* Alfken, in the analyses, and thus the phylogenetic position of this species remains uncertain along with such a synonymy. It cannot be presumed at this time that *M. lanigera* would fall into the same phylogenetic position as *M. villipes*.

Conclusions and Future Directions

Interdental laminae, the most distinctive and taxonomically significant feature of LC bees, developed from two different structures in the female mandible (Figs. 3B–H). One type of lamina developed from the tooth (odontogenic laminae) while the other from the fimbrial ridge (ctenogenic laminae). Odontogenic laminae, a putative synapomorphy for all LC bees, evolved first and exhibited more phenotypic plasticity than ctenogenic laminae (Fig. 12).

Our preliminary total-evidence tip dating analyses favor the hypothesis of a recent origin (15–25 Ma) for LC bees with interdental lamina (Figs. 8, 10, 11). Based on this estimate, Eocene trace fossil excissions would not likely to be the result of the activity of bees within this particular clade (Clade C in Figs. 8, 10, 11). Our observations on the mandibular morphology of Glyptapini and Ctenoplectrellini, extinct lineages from the Eocene, also indicate these taxa were unlikely to cut leaves (Figs. 13E–G). Thus, the identity of the Eocene LC insects remains elusive. However, considering that interdental laminae are not necessary for cutting leaves and the behavior certainly predated the origin of cutting structures, these traces may represent the activity of as-of-yet un-

identified stem-group Megachilini or Osmiini. A greater number of fossils are needed to more accurately and finely calibrate future phylogenetic studies of Megachilidae.

Citing Labandeira (2002: p. 50) as evidence, Trunz *et al.* (2016: p. 255) indicated that Eocene leaf trace fossils are hypothetical because many other herbivore insects produce similar cuts. However, reading Labandeira's (2002) paper, it is clear that he never doubted that megachilids were responsible for the Eocene leaf traces he examined, except for those of an unidentified fern that were clearly different (Labandeira, 2002: fig. 6m-n). Furthermore, the study of Sarzetti *et al.* (2008) supports the idea that many Eocene trace fossils are the product of megachilid bees based on analyses of the ellipse eccentricity of the excisions and leaf discs of brood cells from living bees.

Our preliminary total evidence analyses support the proposal of Gonzalez *et al.* (2012) in recognizing four subfamilies within Megachilidae, each with several tribes. It also provides insights on long-standing issues in the systematics of Megachilidae, namely the non-monophyly of Osmiini, phylogenetic position of Dioxyini, and the internal relationships of Megachilini. The IW analyses of the morphological dataset of Megachilini, using a range of constant k -values calculated for average character fits (Appendix 4), support the effectiveness of this weighting scheme in recovering topologies congruent with total evidence phylogenies. As in Reemer (2012), we found that tree topologies obtained with k -values calculated for character fits near 70% are highly congruent with the preliminary total-evidence phylogeny.

Finally, our study provides a framework to formulate and address novel and interesting evolutionary questions regarding the LC behavior in bees. For example, is there a phylogenetic pattern between the type of interdental laminae and the plants used by LC bees? Do mandibular shape and interdental laminae correlate with any leaf feature (*e.g.*, toughness) or any particular cutting and handling process? Are interdental laminae stronger and more resistant to abrasion when compared with each other as well as with teeth? Do interdental laminae contain heavy metals and halogens to increase hardness as in the mandible of other insects? Certainly, plants vary in leaf traits and the variable morphology of the mandible of LC bees suggest mechanical solutions to some functional problems. In LC ants, for example, the mandible and the LC behavior of species that cut dicot leaves are different from those that cut grasses (*e.g.*, Camargo *et al.*, 2015). In addition, the mandibular teeth of LC ants have heavy metals (*e.g.*, Schofield *et al.*, 2002), which increase their hardness and influence their ability to cut leaves. These aspects are unknown for LC bees, although there seems to be great variation within and among species in the degree and manner of leaf use. For example, a few records indicate that some species of *Litomegachile* Mitchell, *Megachiloides*, *Megachile s.str.*, and *Xanthosarus* use small circular pieces of leaves to make the bottom of a brood cell (Williams *et al.*, 1986; Krombein & Norden, 1995). In other subgenera, such as *Eutricharaea*, bees make the bottom of the cell by bending the leaf pieces from the cell cup (Medler, 1965; Kim, 1992). However, the nesting biology of the vast majority of species of *Megachile s.l.* remains unknown.

Limitations of the Study

Our work has several limitations. First, we were not able to code all morphological characters for all species because some taxa are accessible only from the type specimen or a small number of specimens, and thus we could not dissect them. In other cases, only one of the sexes was available to us. Second, a large number of the taxa we coded for morphology do not have available DNA sequences or when available, they

are incomplete. For example, sequence data from a single gene (28S) are only available for *Matangapis* and *Heriadopsis*. For practical purposes, we included chimeric taxa to increase the taxonomic representation in our analysis. Although we are confident that the anatomical overlap is high between the pair of chosen species given that the morphological characters we pursued and scored reflect higher levels of relationships, this approach is not ideal. Some of the taxa with available information in GenBank are from specimens identified only to species groups within a subgenus or tentatively assigned to a subgenus (see supplemental Table S1 of Trunz *et al.*, 2016). Thus, our total-evidence analyses are preliminary in nature. The support of many clades is weak and the monophyly of several groups need to be tested using more taxa. Further studies should attempt to score morphological data from the hologenophore (Astrin *et al.*, 2013), as well as to employ non-destructive extraction of DNA from museum specimens, such as Ultraconserved Elements (UCEs) (*e.g.*, Blaimer *et al.*, 2016).

Descriptions of New Taxa

Family Megachilidae Latreille
Subfamily Megachilinae Latreille

Key to Extant Tribes of Megachilinae (modified from Michener, 2007)

1. Metanotum with median spine or tubercle (except in *Allodioxys* Popov and *Ensliniana* Alfken); mandible of female slender apically, bidentate, similar to that of male; pronotum (except in *Prodioxys* Friese) with prominent obtuse or right-angular dorsolateral angle, below which a vertical ridge extends downward; sting and associated structures greatly reduced (scopa absent) Dioxyini
- Metanotum without median spine or tubercle; mandible of female usually wider apically, with three or more teeth, except rarely bidentate when mandible is greatly enlarged and porrect and clypeus is also modified; pronotum with dorsolateral angle weak or absent (or produced to a tooth in some *Chelostoma* Latreille but without vertical ridge below it); sting and associated structures well developed 2
- 2(1). Pterostigma less than twice as long as broad, inner margin basal to r-rs usually little if any longer than width, rarely about 1.5× width; pretarsal claws of female cleft or with an inner tooth (except in *Trachusoides* Michener & Griswold); body commonly with yellow or ivory integumental marks 3
- Pterostigma over twice as long as broad, inner margin basal to r-rs longer than width; pretarsal claws of female simple (except in *Osmia* subgenus *Metalinella* Tkalců, Palearctic); body without yellow or white integumental marks, except in Ochreariadini 4
- 3(2). Outer surface of metatibia with long setae forming a distinct scopa; prestigma much more than twice as long as broad; preaxilla, below posterolateral angle of mesoscutum, sloping and with small patch of setae, these as long as those of adjacent sclerites Aspidosmiini
- Outer surface of metatibia usually with abundant simple bristles, not forming a distinct scopa; prestigma commonly short, usually less than twice as long as broad; preaxilla vertical, smooth and shining, usually without setae Anthidiini

- 4(2). Body distinctly elongate with enlarged pronotum surrounding mesoscutum anteriorly, thus practically eliminating omaular surface of mesepisternum and anterior surface of mesoscutum; body with yellow or ivory integumental markings at least on metasoma Ochrieriadini, n. trib.
- Body not as elongate and slender as above, pronotum not enlarged nor surrounding mesoscutum anteriorly, mesepisternum with distinct omaular surface; body without yellow or white integumental marks 5
- 5(4). Outer surfaces of pro- and mesotibiae apically with an acute angle (usually produced into a spine) and distinct notch anteriorly; male T6 with preapical carina often present; arolia normally absent, except in a few tropical Old World taxa (*Noteriades*, *Matangapis*, and *Heriadopsis*); body nonmetallic or nearly so Megachilini
- Outer surfaces of pro- and mesotibiae apically without an acute angle or spine and lacking distinct notch anteriorly; male T6 without preapical carina; arolia present; body sometimes metallic green, blue, or brassy 6
- 6(5). Maxillary palpus with two palpomeres; propodeum with basal area not marked posteriorly by a strong carina, if present, it does not extend laterally behind propodeal spiracle; male T7 large, exposed, quadrately surrounded by T6; male S5 with modified discal setae (female: T6 with wide apical hyaline rim, S1 with slender, erect spine, posterolateral angle of mesoscutum with marginal ridge rounded or carinate, if rounded, with dense patch of long setae laterally) Pseudoheriadini, n. trib.
- Maxillary palpus with at least with three palpomeres; propodeum with basal area not marked posteriorly by carina, or if present, then extending laterally behind propodeal spiracle; male T7 small, usually hidden, not quadrately surrounded by T6; male S5 with branched or simple discal setae Osmiini

Pseudoheriadini Gonzalez & Engel, new tribe

ZooBank: urn:lsid:zoobank.org:act:DEC53F0B-8A55-418B-B72D-840B9F388F09

(Fig. 15)

TYPE GENUS: *Pseudoheriades* Peters, 1970.

DIAGNOSIS: This tribe can be readily separated from all other tribes of Megachilinae by the following combination of features: small body size (4.0–8.5 mm in length); heriadiform (Fig. 15A); maxillary palpus dimerous (two palpomeres); propodeum with basal area not marked posteriorly by a strong carina, but if present, it does not extend laterally behind propodeal spiracle; outer surfaces of pro- and mesotibiae without a distinct notch on distal margin; arolia present; female T6 with wide apical hyaline rim; male T7 large, exposed, quadrately surrounded by T6 (Fig. 15B); male S3 with gradulus projecting into thin, basal hyaline lamella; male S5 with capitate discal setae.

DESCRIPTION: ♀: Preoccipital carina present (laterally in *Pseudoheriades*, dorsally in *Afroheriades*); clypeus little to not overhanging labral base; labrum not elongate, margin without fringe or apical tuft of setae; maxillary palpi dimerous (two palpomeres); mesoscutellum flat or slightly convex, not overhanging metanotum; metepisternum with dorsal carina or lamella (weakly present in *Afroheriades*); T6 with wide apical hyaline rim; S6 without lateral or apical projection.

♂: Metasoma with two or three sterna visible; T7 large, exposed, quadrately surrounded by T6; S3 with gradulus projecting into thin, basal hyaline lamella; S5 with capitate discal setae.

COMMENTS: This tribe contains at least 15 species (Griswold & Gonzalez, 2011; Ascher & Pickering, 2018) grouped in two Eastern Hemisphere genera, *Afroheriades* and *Pseudoheriades*. The first genus is restricted to the Cape Province of South Africa whereas the second is more widespread, occurring across Africa, the Middle East, and India. Griswold (1985) provided detailed descriptions and diagnostic features of both genera, some of which Griswold & Gonzalez (2011) illustrated.

Ochreriadini Gonzalez & Engel, new tribe

ZooBank: urn:lsid:zoobank.org:act:D70C4AF0-CE03-4A89-9881-AA8ABAE29225

(Fig. 15)

TYPE GENUS: *Ochreriades* Mavromoustakis, 1956.

DIAGNOSIS: This tribe is readily separated from all other tribes of Megachilinae by the following combination of features: body elongate and with yellow or ivory integumental markings; pronotum distinctly elevated and surrounding mesoscutum anteriorly; mouthparts elongate, reaching tip of metasoma.

DESCRIPTION: ♀: Clypeus not overhanging labral base; labrum not elongate, margin without fringe or apical tuft of setae; maxillary palpus trimerous (three palpomeres); metepisternum with dorsal carina or lamella; pronotum enlarged and surrounding mesoscutum anteriorly, practically eliminating omaular surface of mesepisternum and anterior surface of mesoscutum; mesoscutellum flat, on same plane with metanotum and propodeal base, as seen in profile; T6 without wide apical hyaline rim; S6 without lateral or apical projection.

♂: Metasoma with six sterna visible; S2 and S3, each with disc swollen; S4 with dense pubescence on disc; S5 not emarginate, with branched or simple discal setae; T7 exposed, inferiorly directed.

COMMENTS: This tribe contains a single genus, *Ochreriades*, which consists of two species. *Ochreriades fasciatus* (Friese) occurs in the Middle East whereas *O. rozeni* Griswold occurs in Namibia, Africa (Griswold, 1994; Ascher & Pickering, 2018).

Tribe Megachilini Latreille

Cremnomegachile Gonzalez & Engel, new genus

ZooBank: urn:lsid:zoobank.org:act:9B13591A-A7C6-4781-AF42-4B131460E1B5

(Fig. 16)

TYPE SPECIES: *Megachile dolichosoma* Benoist, 1962.

DIAGNOSIS: This genus resembles *Stenomegachile* in the elongate, shiny female mandible (Fig. 16A), female hypostomal area toothed, and male preapical carina of T6 bilobed (Fig. 16E). It can easily be separated by the shape of the mesoscutum, which is midanteriorly projected and truncate, thus forming an anterior-facing area (Fig. 16B).

DESCRIPTION: Small to moderate sized-bees (10.0–12.0 mm in body length). Integument shiny, with punctures coarse and spaced. Preoccipital border strongly carinate on gena; ocellocipital distance distinctly greater than ocellocular distance.

♀: Mandible without interdental laminae, elongate, outer surface shiny, with apex about as broad as base, four-toothed, Mt₄ on upper margin and clearly separated from Mt₁₋₃ which are on distal margin; clypeus not covering base of labrum; labrum elongate, triangular, with distinct preapical protuberance bearing long, stiff tuft of setae; hypostomal carina with posterior portion ending in a tooth. Pronotal lobe with trans-

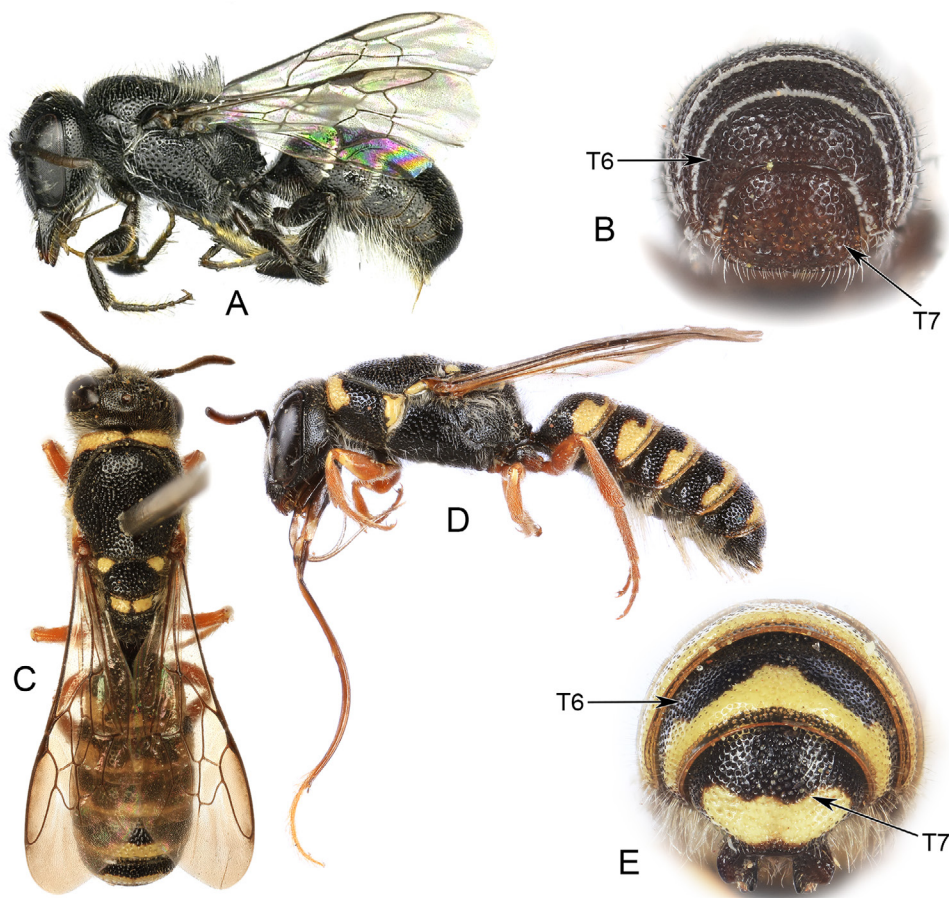


Figure 15. Tribes Pseudoheriadini and Ochriadini. **A.** Female of *Afroheriades hyalinus* Griswold & Gonzalez in lateral view. **B.** Male terminal terga of *Pseudoheriades moricei* (Friese). **C, D.** Female of *Ochriades fasciatus* (Friese) in dorsal and lateral views. **E.** Male terminal terga of *O. fasciatus*.

verse lamella; mesoscutum flat on disc, midanteriorly projected and truncate, thus forming an anterior-facing area; mesoscutellum flat, not overhanging metanotum in dorsal view (Fig. 4C). Metasoma narrow, parallel-sided, with white apical fasciae and distinct postgradular grooves on T2–T4; sterna without apical fasciae beneath scopa; T6 straight (vertical) in profile.

♂: Antennal flagellum unmodified, F1 shorter than F2; mandible tridentate, without basal projection or tooth on lower margin; hypostomal carina unmodified, area behind mandible unmodified, without a projection or concavity; procoxa aspinose; pro- and mesotibiae and tarsi unmodified; metabasitarsus elongate, about 4.0× longer than broad; mesotibial spur present, articulated to mesotibia, about as long as apical width of mesotibia. T6 vertical in profile, with deep concavity above broad, medially emarginate preapical carina, distal margin without a distinct tooth or projection; T7 with preapical carina broadly rounded; S4 exposed, with punctation and vestiture similar to those of preceding sterna; S8 with marginal setae. Genital capsule elongate, 1.9× longer than wide; gonostylus straight or nearly so in ventral view, apically simple

(not bifid), much narrower than base in lateral view, with long setae along its medial margin; volsella present, apically truncate.

ETYMOLOGY: The new genus-group name is a combination of of the Greek word, *kremnos*, meaning “overhanging wall”, in reference to the projected and anterior-facing surface of the mesoscutum, and the generic name *Megachile*. The gender of the name is feminine [as noted by Gonzalez *et al.* (2018: p. 19), although *Megachile* is a neuter plural and should be nomenclaturally considered masculine, precedence is to consider names based on *chile* (χείλος), meaning, “lip” or “rim”, to be feminine].

COMMENTS: The genus is known from the type species only, which occurs in southern Madagascar (Pauly *et al.*, 2001). This results in the **new combination**, *Cremnomegachile dolichosoma* (Benoist).

In addition to the features indicated in the diagnosis, the male of *Stenomegachile* differs from that of *Cremnomegachile* in the four-toothed mandible (tridentate in *Cremnomegachile*); the hypostomal area, behind the mandible, which is strongly projected into a tooth (unmodified in *Cremnomegachile*); and the pro- and mesotarsi that are expanded (normal in *Cremnomegachile*). The genital morphology is quite different, particularly in the shape of the volsella, which is narrow and apically notched (*vide* Pasteels, 1965: p. 513). In the female of *Stenomegachile* the mandible is more elongate and apically curved, and the labrum is long but parallel-sided. The hypostomal projection of *Stenomegachile* might not be homologous to the hypostomal tooth of *Cremnomegachile* because it is not part of the posterior portion of the hypostomal carina as in the latter genus.

Rozenapis Gonzalez & Engel, new genus

ZooBank: urn:lsid:zoobank.org:act:6CD5BAC1-311E-4476-8F26-755312E57364

TYPE SPECIES: *Megachile ignita* Smith, 1853.

DIAGNOSIS: This genus superficially resembles some robust species of *Hackeriapis* with the terminal terga reddish and thus contrasting with the preceding black terga. The female shares with *Austrochile* a large, conspicuous midapical spine on S1 (absent in *Hackeriapis*), but it differs in the mandible. In *Austrochile* the transverse ridge is strong and extends basally to merge with the acetabular carina, whereas in *Rozenapis* such a ridge is entirely absent. The male differs from *Austrochile* in the absence of the midapical spine of S1 and the shape of T6, which has four equally distant teeth on its distal margin and a preapical carina that extends almost across the entire width of the tergum. In *Austrochile* the spine of S1 is present, the preapical carina of T6 is restricted to the median third, and the median projections of the distal margin are closer than the distance from one of them to a lateral tooth. The male of *Rozenapis* differs from *Hackeriapis* (*sensu* King, 1994) in the impunctate distal margins of T2–T4, which are narrow and nearly concolorous with the discal areas (broad, distinctive, and hyaline in *Hackeriapis*). It also differs in the pretarsal claws, which lack a basal tooth (present in *Hackeriapis*).

DESCRIPTION: Moderate-sized bees (12.0–15.0 mm in body length). Integument shiny, with punctures coarse and nearly contiguous. Preoccipital border rounded, not carinate; ocellocipital distance slightly longer than ocellocular distance in female, much longer in male.

♀: Mandible without interdental laminae, short, outer surface dulled without transverse ridge, with apex about as broad as base, four-toothed; clypeus barely covering base of labrum; labrum rectangular. Pronotal lobe with transverse carina; me-

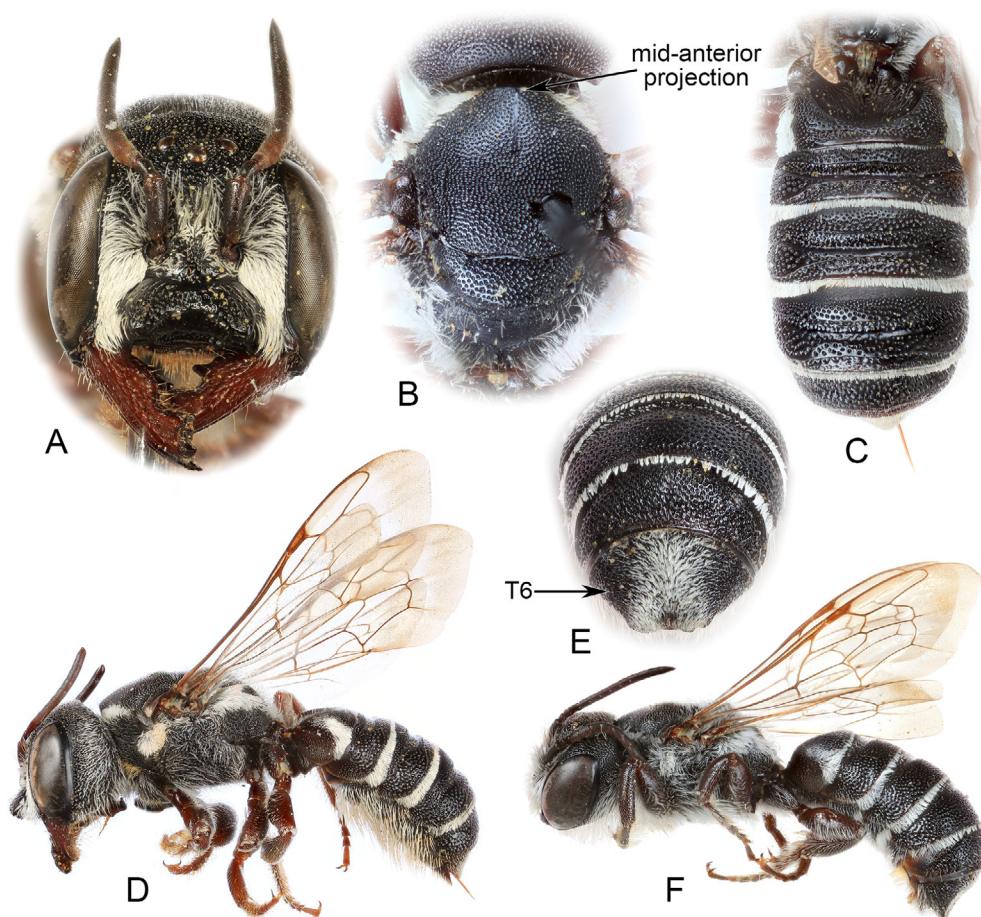


Figure 16. *Cremnomegachile dolichosoma* (Benoist), new combination. **A.** Facial view of female. **B.** Detail of female mesoscutum. **C.** Female metasoma in dorsal view. **D.** Lateral view of female. **E.** Male terminal terga. **F.** Lateral view of male.

soscutellum not overhanging metanotum in dorsal view. Metasoma robust, parallel-sided, with white apical fasciae laterally only and weak postgradular grooves on basal terga; S1 with long, distinct midapical projection; sterna without apical fasciae beneath scopa; T6 gently convex in profile, slightly concave preapically.

♂: Antennal flagellum unmodified, F1 shorter than F2; mandible tridentate, without basal projection or tooth on lower margin; hypostomal area behind mandible unmodified, without a projection or concavity; procoxal spine small; pro- and mesotibiae and tarsi slightly expanded; metabasitarsus elongate, about 4.0× longer than broad; mesotibial spur present, articulated to mesotibia, about as long as apical width of mesotibia. T6 vertical in profile, with deep concavity above broad, medially emarginate preapical carina, distal margin with four small, equidistant teeth or projections; T7 with preapical carina slightly projecting medially; S4 apically exposed, with punctuation and vestiture similar to those of preceding sterna; S8 with marginal setae. Genital capsule elongate, 1.4× longer than wide; gonostylus straight or nearly so in ventral view, apically simple, truncate, much broader than base in lateral view, with short setae along its medial margin; volsella present, apically notched.

ETYMOLOGY: The new genus-group name is a patronymic honoring Dr. Jerome G. Rozen, Jr., of the American Museum of Natural History, for his significant contributions to the biology and systematics of bees, and his many years of dear friendship and mentorship to M.S.E. The name is a combination of his surname and *Apis* Linnaeus (Latin, meaning, "bee"). The gender of the name is feminine.

COMMENTS: This genus resulted as the sister group of *Austrochile* in our analyses. Only the type species from western Australia is known, which Michener (1965) listed in *Hackeriapis* as a member of species group 'A'. This results in the **new combination**, *Rozenapis ignita* (Smith).

Saucrochile Gonzalez & Engel, new genus

ZooBank: urn:lsid:zoobank.org:act:395871FD-1354-4660-ACDD-1DF694882441

TYPE SPECIES: *Megachile heriadiformis* Smith, 1853.

DIAGNOSIS: This genus is most similar to *Hackeriapis* (*sensu* King, 1994). It differs in the pretarsal claws, which lack of a basal tooth, and in the distal margins of male T2–T4, which are punctate and concolorous with the discal areas. In *Hackeriapis*, the pretarsal claws have a distinct basal tooth and the distal margins of male T2–T4 are impunctate, broad, and hyaline. In addition, the pronotal lobe is distinctly carinate or lamellate, at least dorsally, in *Hackeriapis*, while the pronotal lobe is completely rounded in *Saucrochile*.

DESCRIPTION: Small sized-bees (8.0–11.0 mm in body length). Integument shiny, with punctures coarse and spaced. Preoccipital border rounded, not carinate; ocellocipital distance much longer than ocellocular distance.

♀: Mandible without interdental laminae, elongate, outer surface shiny, with sparse punctures, outer ridge weak, extending basally to acetabular carina, three teeth on distal margin; clypeus not covering base of labrum; labrum elongate, parallel-sided, without preapical protuberance. Pronotal lobe without transverse carina or lamella; mesoscutellum flat, not overhanging metanotum in dorsal view. Metasoma elongate, parallel-sided, with white apical fasciae and strong postgradular grooves on basal terga; sterna without apical fasciae beneath scopa; T6 gently convex in profile.

♂: Antennal flagellum unmodified, F1 shorter than F2; mandible tridentate, without basal projection or tooth on lower margin; hypostomal area behind mandible unmodified, without a projection or concavity; procoxal spine small; pro- and mesotibiae and tarsi unmodified; metabasitarsus elongate, about 4.0× longer than broad; mesotibial spur present, articulated to mesotibia, about as long as apical width of mesotibia. T6 vertical in profile, with weak concavity above narrow, medially emarginate preapical carina, distal margin with four small, equidistant teeth or projections; T7 with preapical carina slightly projecting medially; S4 hidden, with punctation and vestiture different to those of preceding sterna; S8 with marginal setae. Genital capsule elongate, about 2.0× longer than wide; gonostylus straight or nearly so in ventral view, slightly narrower basally in lateral view, apically simple, with short setae along its medial margin; volsella present, apically notched.

ETYMOLOGY: The new genus-group name is a combination of of the Greek words, *saukros*, meaning "graceful", in reference to the general elegant aspect of this group, and *chile*, meaning "lip" or "rim". The gender of the name is feminine (*vide* Etymology for *Cremnomegachile*, *supra*).

COMMENT: Only the type species from the southern half of Australia is known, which Michener (1965) listed in *Hackeriapis* as a member of species group 'A'. This results in the **new combination**, *Saucrochile heriadiformis* (Smith).

ACKNOWLEDGEMENTS

We thank the late Charles D. Michener for his many years of advice, encouragement, and comments on early drafts of this manuscript. Amy R. Comfort, Mabel Alvarado, Laura C.V. Breitreuz, Christopher Praz, and two anonymous reviewers provided helpful comments and suggestions that improved this work. We also thank the curators, collection managers, and staff of the collections we visited or from which we borrowed specimens, and particularly Zachary H. Falin and Jennifer C. Thomas for their constant help throughout the project. The participation of V.H.G. was partially supported by National Science Foundation's REU program (DBI-1560389), while that of G.T.G by a NIH IRACDA postdoctoral fellowship (5K12GM064651), and M.S.E. at various stages by NSF DBI-0096905 and DBI-1057366. This is a contribution of the Division of Entomology, University of Kansas Natural History Museum.

REFERENCES

- Agnarsson, I., & J.A. Coddington. 2008. Quantitative tests of primary homology. *Cladistics* 24(1): 51–61.
- Almeida, E.A.B. 2008. Revised species checklist of the Paracolletinae (Hymenoptera, Colletidae) of the Australian Region, with the description of new taxa. *Zootaxa* 1891: 1–24.
- Almeida, E.A.B., & B.N. Danforth. 2009. Phylogeny of colletid bees (Hymenoptera: Colletidae) inferred from four nuclear genes. *Molecular Phylogenetics and Evolution* 50(2): 290–309.
- Arcila, D., R.A. Pyron, J.C. Tyler, G. Ortí, & R. Betancur-R. 2015. An evaluation of fossil tip-dating versus node-age calibration in tetraodontiform fishes (Teleostei: Percomorphaceae). *Molecular Phylogenetics and Evolution* 82(A): 131–145.
- Ascher, J.S., & J. Pickering. 2018. Discover Life bee species guide and world checklist (Hymenoptera: Apoidea: Anthophila). [http://www.discoverlife.org/mp/20q?guide=Apoidea_species; last accessed 31 March 2018].
- Astrin, J.J., X. Zhou, & B. Misof. 2013. The importance of biobanking in molecular taxonomy, with proposed definitions for vouchers in a molecular context. *ZooKeys* 365: 67–70.
- Baker, D.B., & M.S. Engel. 2006. A new subgenus of *Megachile* from Borneo with arolia (Hymenoptera: Megachilidae). *American Museum Novitates* 3505: 1–12.
- Banaszak, J., & L. Romasenko. 1998. *Megachilid Bees of Europe (Hymenoptera, Apoidea, Megachilidae)*. Pedagogical University of Bydgoszcz; Bydgoszcz, Poland; 239 pp.
- Benoist, R. 1962. Nouvelles espèces d'Apides malgaches [Hym.]. *Bulletin de la Société Entomologique de France* 67: 214–223.
- Blaimer, B.B., M.W. Lloyd, W.X. Guillory, & S.G. Brady. 2016. Sequence capture and phylogenetic utility of genomic ultraconserved elements obtained from pinned insect specimens. *PLoS ONE* 11(8): [1–20] e0161531.
- Brauns, H. 1926. V. Nachtrag zu "Friese, Bienen Afrikas". *Zoologische Jahrbücher, Abteilung für Systematik, Geographie und Biologie der Tiere* 52: 187–230, +pl. 5.
- Camargo, R.S., I.N. Hastenreiter, L.C. Forti, & J.F.S. Lopes. 2015. Relationship between mandible morphology and leaf preference in leaf-cutting ants (Hymenoptera: Formicidae). *Revista Colombiana de Entomología* 41(2): 241–244.
- Cane, J.H. 2004. Exotic nonsocial bees (Hymenoptera: Apiformes) in North America: Ecological implications. In: Strickler, K.L., & J.H. Cane (Eds.), *For Non-native Crops, Whence Pollinators of the Future?*: 113–116. Thomas Say Publications in Entomology, Entomological Society of America; Lanham, MD; 204 pp.

- Cardinal, S., & B.N. Danforth. 2013. Bees diversified in the age of eudicots. *Proceedings of the Royal Society B (Biological Sciences)* 280(1755): [1–9] 20122686.
- Castresana, J. 2000. Selection of conserved blocks from multiple alignments for their use in phylogenetic analysis. *Molecular Biology and Evolution* 17(4): 540–552.
- Cockerell, T.D.A. 1907. Descriptions and records of bees—XV. *Annals and Magazine of Natural History, Series 7* 20(115): 59–68.
- Cockerell, T.D.A. 1922. Descriptions and records of bees—XCV. *Annals and Magazine of Natural History, Series 9* 10(57): 265–269.
- Dalla Torre, C.G., de [K.W., von]. 1896. *Catalogus Hymenopterorum Hucusque Descriptorum Systematicus et Synonymicus. Vol. 10: Apidae (Anthophila)*. Engelmann; Lipsiae [Leipzig], Germany; viii+643 pp.
- Dos Reis, M., & Z. Yang. 2013. The unbearable uncertainty of Bayesian divergence time estimation. *Journal of Systematics and Evolution* 51(1): 30–43.
- Duckworth, R.A. 2009. The role of behavior in evolution: A search for mechanism. *Evolutionary Ecology* 23(4): 513–531.
- Durante, S., & N. Cabrera. 2009. Cladistic analysis of *Megachile* (*Chryosarus*) Mitchell and revalidation of *Megachile* (*Dactylomegachile*) Mitchell (Hymenoptera, Megachilidae). *Zootaxa* 2284: 48–62.
- Durante, S.P., & A.H. Abrahamovich. 2006. Redescription of *Chaetochile* as subgenus of *Megachile* (Hymenoptera, Megachilidae). *Transactions of the American Entomological Society* 132(1): 103–109.
- Eardley, C. 2012. A taxonomic revision of the southern African species of dauber bees in the genus *Megachile* Latreille (Apoidea: Megachilidae). *Zootaxa* 3460: 1–139.
- Eardley, C. 2013. A taxonomic revision of the southern African leaf-cutter bees, *Megachile* Latreille *sensu stricto* and *Heriadopsis* Cockerell (Hymenoptera: Apoidea: Megachilidae). *Zootaxa* 3601(1): 1–133.
- Eickwort, G.C., R.W. Matthews, & J. Carpenter. 1981. Observations on the nesting behavior of *Megachile rubi* and *M. texana* with a discussion of the significance of soil nesting in the evolution of megachilid bees (Hymenoptera: Megachilidae). *Journal of the Kansas Entomological Society* 54(3): 557–570.
- Engel, M.S. 1999. *Megachile glaesaria*, the first megachilid bee fossil from amber (Hymenoptera: Megachilidae). *American Museum Novitates* 3276: 1–13.
- Engel, M.S. 2000. A new interpretation of the oldest fossil bee (Hymenoptera: Apidae). *American Museum Novitates* 3296: 1–11.
- Engel, M.S. 2001. A monograph of the Baltic amber bees and evolution of the Apoidea (Hymenoptera). *Bulletin of the American Museum of Natural History* 259: 1–192.
- Engel, M.S. 2005. Family-group names for bees (Hymenoptera: Apoidea). *American Museum Novitates* 3476: 1–33.
- Engel, M.S. 2007. Ferdinand Meunier and the destruction of his Hymenoptera collections. *Entomologist's Gazette* 58(3): 183–184.
- Engel, M.S. 2017. Replacement names for bees in the tribe Megachilini (Hymenoptera: Megachilidae). *Journal of Melittology* 70: 1–5.
- Engel, M.S., & D.B. Baker. 2006. A remarkable new leaf-cutter bee from Thailand (Hymenoptera: Megachilidae). *Beiträge zur Entomologie* 56(1): 69–74.
- Engel, M.S., & V.H. Gonzalez. 2011. *Alocanthodon*, a new subgenus of *Chalicodoma* from Southeast Asia (Hymenoptera, Megachilidae). *ZooKeys* 101: 51–80.
- Engel, M.S., & E.E. Perkovsky. 2006. An Eocene bee in Rovno amber, Ukraine (Hymenoptera: Megachilidae). *American Museum Novitates* 3506: 1–12.
- Friese, H. 1898. Species aliquot novæ vel minus cognitæ generis *Megachile* Latr. (et *Chalicodoma* Lep.). *Természetrzajzi Füzetek* 21(1–2): 198–202.
- Friese, H. 1899. *Die Bienen Europa's (Apidae europaeae) nach ihren Gattungen, Arten und Varietäten auf vergleichend morphologisch-biologischer Grundlage. Teil V: Solitäre Apiden: Genus Lithurgus, Genus Megachile (Chalicodoma)*. C. Lampe; Innsbruck, Austria; 228 pp.
- Friese, H. 1909. Die Bienen Afrikas nach dem Stande unserer heutigen Kenntnis. In: Schultze,

- L. (Ed.), *Zoologische und anthropologische Ergebnisse einer Forschungsreise im westlichen und zentralen Südafrika ausgeführt in den Jahren 1903–1905 mit Unterstützung der Kgl. [Königlichen] Preussischen Akademie der Wissenschaften zu Berlin [Band 2, Lieferung 1, X Insecta (3^{te} Serie): Jenaische Denkschriften 14]: 83–476, pls. ix–x. Gustav Fischer; Jena, Germany.*
- Friese, H. 1911a. Apidae I. Megachilinae. In: Schulze, F.E. (Ed.), *Das Tierreich: Eine Zusammenstellung und Kennzeichnung der rezenten Tierformen. Lieferung 28: Hymenoptera: v–xxvi+1–440*. Friedländer und Sohn; Berlin, Germany; xxvi+440 pp.
- Friese, H. 1911b. Nachtrag zu “Bienen Afrikas”. *Zoologische Jahrbücher, Abteilung für Systematik, Geographie und Biologie der Tiere* 30(6): 651–670.
- Gerstaecker, A. 1869. Beiträge zur näheren Kenntniss einiger Bienen-Gattungen. *Entomologische Zeitung* 30(4–6): 315–367.
- Goloboff, P.A. 1993. Estimating character weights during tree search. *Cladistics* 9(1): 83–91.
- Goloboff, P.A. 2008. Calculating SPR distances between trees. *Cladistics* 24(4): 591–597.
- Goloboff, P.A., J.S. Farris, & K. Nixon. 2003a. T.N.T.: Tree analysis using new technology. Program and documentation. [<http://www.lillo.org.ar/phylogeny/tnt/>; last accessed 1 December 2018].
- Goloboff, P.A., J.S. Farris, M. Källersjö, B. Oxelman, M.J. Ramírez, & C.A. Szumik. 2003b. Improvements to resampling measures of group support. *Cladistics* 19(4): 324–332.
- Goloboff, P.A., A. Torres, & J.S. Arias. 2018. Weighted parsimony outperforms other methods of phylogenetic inference under models appropriate for morphology. *Cladistics* 34(4): 407–437.
- Gonzalez, V.H. 2008. *Phylogeny and classification of the bee tribe Megachilini (Hymenoptera: Apoidea, Megachilidae), with emphasis on the genus Megachile*. Doctoral dissertation, University of Kansas; Lawrence, KS; 274 pp.
- Gonzalez, V.H. 2013. Taxonomic comments on *Megachile* subgenus *Chrysosarus* (Hymenoptera: Megachilidae). *Journal of Melittology* 5: 1–6.
- Gonzalez, V.H., & M.S. Engel. 2012. African and Southeast Asian *Chalicodoma* (Hymenoptera: Megachilidae): New subgenus, new species, and notes on the composition of *Pseudomegachile* and *Largella*. *Annales Zoologici* 62(4): 599–617.
- Gonzalez, V.H., & T. Griswold. 2013. Wool carder bees of the genus *Anthidium* in the Western Hemisphere (Hymenoptera: Megachilidae): Diversity, host plant associations, phylogeny, and biogeography. *Zoological Journal of the Linnean Society* 168(2): 221–425.
- Gonzalez, V.H., M.S. Engel, & I.A. Hinojosa-Díaz. 2010. A new species of *Megachile* from Pakistan, with taxonomic notes on the subgenus *Eutricharaea* (Hymenoptera: Megachilidae). *Journal of the Kansas Entomological Society* 83(1): 58–67.
- Gonzalez, V.H., T. Griswold, C.J. Praz, & B.N. Danforth. 2012. Phylogeny of the bee family Megachilidae (Hymenoptera: Apoidea) based on adult morphology. *Systematic Entomology* 37(2): 261–286.
- Gonzalez, V.H., T. Griswold, & M.S. Engel. 2013. Obtaining a better taxonomic understanding of native bees: Where do we start? *Systematic Entomology* 38(4): 645–653.
- Gonzalez, V.H., T.L. Griswold, & M.S. Engel. 2018. South American leaf-cutter bees (genus *Megachile*) of the subgenera *Rhyssomegachile* and *Zonomegachile*, with two new subgenera (Hymenoptera: Megachilidae). *Bulletin of the American Museum of Natural History* 425: 1–73.
- Griswold, T.L. 1985. *A generic and subgeneric revision of the Heriades genus-group (Hymenoptera: Megachilidae)*. Doctoral dissertation, Utah State University; Logan, UT; xii+165 pp.
- Griswold, T.L. 1994. A review of *Ochreeriades* (Hymenoptera: Megachilidae: Osmiini). *Pan-Pacific Entomologist* 70(4): 318–321.
- Griswold, T., & V.H. Gonzalez. 2011. New species of the Eastern Hemisphere genera *Afroheriades* and *Noteriades* (Hymenoptera, Megachilidae), with keys to species of the former. *ZooKeys* 159: 65–80.
- Heath, T.A., J.P. Huelsenbeck, & T. Stadler. 2014. The fossilized birth-death process for coherent calibration of divergence-time estimates. *Proceedings of the National Academy of Sciences, U.S.A.* 111(29): E2957–E2966.
- Horne, M. 1995. Leaf area and toughness: Effects on nesting material preference of *Megachile rotundata* (Hymenoptera: Megachilidae). *Annals of the Entomological Society of America*

- 88(6): 868–875.
- Huelsenbeck, J.P., B. Larget, & M.E. Alfaro. 2004. Bayesian phylogenetic model selection using reversible jump Markov chain Monte Carlo. *Molecular Biology and Evolution* 21(6): 1123–1133.
- Kalyaanamoorthy, S., B.Q. Minh, T.K.F. Wong, A. von Haeseler, & L.S. Jermin. 2017. ModelFinder: Fast model selection for accurate phylogenetic estimates. *Nature Methods* 14(6): 587–589.
- Kambli, S.S., M.S. Aiswarya, K. Manoj, S. Varma, G. Asha, T.P. Rajesh, & P.A. Sinu. 2017. Leaf foraging sources of leafcutter bees in a tropical environment: Implications for conservation. *Apidologie* 48(4): 473–482.
- Katayama, E. 2004. Nesting biology of *Megachile pseudomonticola* Hedick, with special reference to the manipulation and adhesion of leaf pieces used for cell construction. *Japanese Journal of Entomology* 7(1): 1–10. [In Japanese].
- Katoh, K., & H. Toh. 2008. Improved accuracy of multiple ncRNA alignment by incorporating structural information into a MAFFT-based framework. *BMC Bioinformatics* 9: [1–13] 212.
- Katoh, K., & D.M. Standley. 2013. MAFFT Multiple Sequence Alignment Software Version 7: Improvements in performance and usability. *Molecular Biology and Evolution* 30(4): 772–780.
- Kim, J. 1992. Nest dimensions of two leaf-cutter bees (Hymenoptera: Megachilidae). *Annals of the Entomological Society of America* 85(1): 85–90.
- Kim, Y.-H., & K.-J. Ahn. 2016. Phylogeny of the Homalotina (Coleoptera: Staphylinidae: Aleocharinae) based on morphology. *Systematic Entomology* 41(2): 323–338.
- King, J. 1994. The bee family Megachilidae (Hymenoptera: Apoidea) in Australia. I. Morphology of the genus *Chalicodoma* Lepeletier, and a revision of the subgenus *Hackeriapis* Cockerell. *Invertebrate Taxonomy* 8(6): 1373–1419.
- Krombein, K.V., & B.B. Norden. 1995. Notes on the behavior and taxonomy of *Megachile (Xeromegachile) brimleyi* Mitchell and its probable cleptoparasite, *Coelioxys (Xerocoelioxys) galactiae* Mitchell (Hymenoptera: Megachilidae). *Proceedings of the Entomological Society of Washington* 97(1): 86–89.
- Labandeira, C.C. 2002. Paleobiology of middle Eocene plant-insect associations from the Pacific Northwest: A preliminary report. *Rocky Mountain Geology* 37(1): 31–59.
- Lanfear, R., B. Calcott, S.Y. Ho, & S. Guindon. 2012. PartitionFinder: Combined selection of partitioning schemes and substitution models for phylogenetic analysis. *Molecular Biology and Evolution* 29(6): 1695–1701.
- Lanfear, R., P.B. Frandsen, A.M. Wright, T. Senfeld, & B. Calcott. 2016. PartitionFinder 2: New methods for selecting partitioned models of evolution for molecular and morphological phylogenetic analyses. *Molecular Biology and Evolution* 34(3): 772–773.
- Lapiedra, O., D. Sol, S. Carranza, & J.M. Beaulieu. 2013. Behavioural changes and the adaptive diversification of pigeons and doves. *Proceedings of the Royal Society B (Biological Sciences)* 280(1755): [1–9] 20122893.
- Laroca, S., Corbella, E., Varela, G. 1992. Biología de *Dactylomegachile affabilis* (Hymenoptera, Apoidea): I. Descripción do ninho. *Acta Biológica Paranaense* 21(1–5): 23–29.
- Latreille, P.A. 1802. *Histoire naturelle des fourmis, et recueil de memoires et d'observations sur les abeilles, les araignées, les faucheurs, et autres insectes*. Crapelet; Paris, France; xvi+445 pp.
- Lepeletier de Saint Fargeau, A.L.M. 1841. *Histoire Naturelle des Insectes—Hyménoptères. Tome Second*. Roret; Paris, France; 680 pp.
- Litman, J.R., B.N. Danforth, C.D. Eardley, & C.J. Praz. 2011. Why do leafcutter bees cut leaves? New insights into the early evolution of bees. *Proceedings of the Royal Society B (Biological Sciences)* 278(1724): 3593–3600.
- MacIvor, J.S. 2016. DNA barcoding to identify leaf preference of leafcutting bees. *Royal Society Open Science* 3(3): [1–13] 150623.
- Maddison, W.P., & D.R. Maddison. 2018. Mesquite: A modular system for evolutionary analysis. Version 3.40. [http://mesquiteproject.org; last accessed on 1 March 2018]
- Maeta, Y. 2005. Substitutional use of the two species of indigenous megachilids bees for seed production of alfalfa (Hymenoptera, Megachilidae). *Chugoku Kontyu* 19: 27–36. [In Japanese].

- Marín, M.A., C. Peña, S.I. Uribe, & A.V.L. Freitas. 2017. Morphology agrees with molecular data: Phylogenetic affinities of Euptychiina butterflies (Nymphalidae: Satyrinae). *Systematic Entomology* 42(4): 768–785.
- Mavromoustakis, G.A. 1956. On the bees (Hymenoptera, Apoidea) of Siria [sic], Part I. *Eos* 32: 215–229.
- Medler, J.T. 1965. A note on *Megachile mendica* Cresson in trap-nests in Wisconsin (Hymenoptera: Megachilidae). *Proceedings of the Entomological Society of Washington* 67(2): 113–116.
- Meunier, F. 1888. Megachilidae [sic]. *Naturalista Siciliano: Organo della Società Siciliana di Scienze Naturali* 7(6): 152.
- Michener, C.D. 1944. Comparative external morphology, phylogeny, and a classification of the bees (Hymenoptera). *Bulletin of the American Museum of Natural History* 82(6): 153–326.
- Michener, C.D. 1953. The biology of a leafcutter bee (*Megachile brevis*) and its associates. *University of Kansas Science Bulletin* 35(16): 1659–1748.
- Michener, C.D. 1962. Observations on the classification of the bees commonly placed in the genus *Megachile* (Hymenoptera: Apoidea). *Journal of the New York Entomological Society* 70(1): 17–29.
- Michener, C.D. 1965. A classification of the bees of the Australian and South Pacific regions. *Bulletin of the American Museum of Natural History* 130: 1–362.
- Michener, C.D. 1983. The classification of the Lithurginae (Hymenoptera: Megachilidae). *Pan-Pacific Entomologist* 59(1–4): 176–187.
- Michener, C.D. 1996. The first South American dioxyine bee and a generic review of the tribe Dioxyini (Hymenoptera, Megachilidae). *Memoirs of the Entomological Society of Washington* 17: 142–152.
- Michener, C.D. 2000. *The Bees of the World*. Johns Hopkins University Press; Baltimore, MD; xiv+[i]+913 pp., +16 pls.
- Michener, C.D. 2007. *The Bees of the World* [2nd Edition]. Johns Hopkins University Press; Baltimore, MD; xvi+[i]+953 pp., +20 pls.
- Michener, C.D., & A. Fraser. 1978. A comparative anatomical study of mandibular structure in bees. *University of Kansas Science Bulletin* 51(14): 463–482.
- Michez, D., M. Vanderplanck, & M.S. Engel. 2012. Fossil bees and their plant associates. In: Patiny, S. (Ed.), *Evolution of Plant-Pollinator Relationships*: 103–164. Cambridge University Press; Cambridge, UK; xv+477+[6] pp.
- Minckley, R.L. 1998. A cladistic analysis and classification of the subgenera and genera of the large carpenter bees, tribe Xylocopini (Hymenoptera: Apidae). *Scientific Papers, Natural History Museum, University of Kansas* 9: 1–47.
- Minh, B.Q., M.A.T. Nguyen, & A. von Haeseler. 2013. Ultrafast approximation for phylogenetic bootstrap. *Molecular Biology and Evolution* 30(5): 1188–1195.
- Mirande, J.M. 2009. Weighted parsimony phylogeny of the family Characidae (Teleostei: Characiformes). *Cladistics* 25(6): 574–613.
- Mitchell, T.B. 1924. New megachilid bees. *Journal of the Elisha Mitchell Scientific Society* 40(3–4): 154–165.
- Mitchell, T.B. 1933 [1934]. A revision of the genus *Megachile* in the Nearctic region. Part I. Classification and descriptions of new species (Hymenoptera: Megachilidae). *Transactions of the American Entomological Society* 59(4): 295–361, +2 pls. [pls. xx–xxi].
- Mitchell, T.B. 1935a. A revision of the genus *Megachile* in the Nearctic region. Part II. Morphology of the male sternites and genital armature and the taxonomy of the subgenera *Litomegachile*, *Neomegachile* and *Cressoniella* (Hymenoptera: Megachilidae). *Transactions of the American Entomological Society* 61(1): 1–44, +1 pl. [pl. i].
- Mitchell, T.B. 1935b. A revision of the genus *Megachile* in the Nearctic region. Part III. Taxonomy of subgenera *Anthemois* and *Delomegachile* (Hymenoptera: Megachilidae). *Transactions of the American Entomological Society* 61(3): 155–205, +2 pls. [pls. viii–ix].
- Mitchell, T.B. 1936a. A revision of the genus *Megachile* in the Nearctic region. Part IV. Taxonomy of subgenera *Xanthosarus*, *Phaenosarus*, *Megachiloides* and *Derotropis* (Hymenoptera: Megachilidae). *Transactions of the American Entomological Society* 62(2): 117–166, +4 pls. [pls. viii–xi].

- Mitchell, T.B. 1936b [1937]. A revision of the genus *Megachile* in the Nearctic Region. Part V. Taxonomy of subgenus *Xeromegachile* (Hymenoptera: Megachilidae). *Transactions of the American Entomological Society* 62(4): 323–382, +5 pls. [pls. xxii–xxvi].
- Mitchell, T.B. 1937a. A revision of the genus *Megachile* in the Nearctic Region. Part VI. Taxonomy of subgenera *Argyropile*, *Leptorachis*, *Pseudocentron*, *Acentron* and *Melanosarus* (Hymenoptera: Megachilidae). *Transactions of the American Entomological Society* 63(1): 45–83, +2 pls. [pls. v–vi].
- Mitchell, T.B. 1937b. A revision of the genus *Megachile* in the Nearctic Region. Part VII. Taxonomy of the subgenus *Sayapis* (Hymenoptera: Megachilidae). *Transactions of the American Entomological Society* 63(2): 175–206, +2 pls. [pls. xii–xiii].
- Mitchell, T.B. 1937c. A revision of the genus *Megachile* in the Nearctic region. Part VIII. Taxonomy of the subgenus *Chelostomoides*, addenda and index (Hymenoptera: Megachilidae). *Transactions of the American Entomological Society* 63(4): 381–425, +4 pls. [pls. xxvi–xxix].
- Mitchell, T.B. 1943. On the classification of neotropical *Megachile* (Hymenoptera: Megachilidae). *Annals of the Entomological Society of America* 36(4): 656–671.
- Mitchell, T.B. 1980. *A Generic Revision of the Megachilinae Bees of the Western Hemisphere*. North Carolina State University; Raleigh, NC; [ii]+95 pp.
- Moure, J.S., G.A.R. Melo, & A. DalMolin. 2007. Megachilini Latreille, 1802. In: Moure, J.S., D. Urban, & G.A.R. Melo (Eds.), *Catalogue of Bees (Hymenoptera, Apoidea) in the Neotropical Region: 917–1001*. Sociedade Brasileira de Entomologia; Curitiba, Brazil; xiv+1058 pp.
- Nguyen, L.-T., H.A. Schmidt, A. von Haeseler, & B.Q. Minh. 2015. IQ-TREE: A fast and effective stochastic algorithm for estimating maximum-likelihood phylogenies. *Molecular Biology and Evolution* 32(1): 268–274.
- Nixon, K.C. 1999. WINCLADA, version 0.9.99tuc.13, beta. Cornell University; Ithaca, NY.
- O'Reilly, J.E., & P.C.J. Donoghue. 2016. Tips and nodes are complementary not competing approaches to the calibration of molecular clocks. *Biology Letters* 12(4): 637–650.
- O'Reilly, J.E., M. dos Reis, & P.C.J. Donoghue. 2015. Dating tips for divergence-time estimation. *Trends in Genetics* 31(11): 637–650.
- Ormosa, C., F.J. Ortiz-Sánchez, & F. Torres. 2007. Catálogo de los Megachilidae del Mediterráneo occidental (Hymenoptera, Apoidea). II. Lithurgini y Megachilini. *Graellsia* 63(1): 111–134.
- Orr, M.C., Z.M. Portman, & T. Griswold. 2015. *Megachile (Megachile) montivaga* (Hymenoptera: Megachilidae) nesting in live thistle (Asteraceae: *Cirsium*). *Journal of Melittology* 48: 1–6.
- Packer, L. 2003. Comparative morphology of the skeletal parts of the sting apparatus of bees (Hymenoptera: Apoidea). *Zoological Journal of the Linnean Society* 138(1): 1–38.
- Packer, L. 2004. Morphological variation in the gastral sterna of female Apoidea (Insecta: Hymenoptera). *Canadian Journal of Zoology* 82(1): 130–152.
- Pasteels, J.J. 1965. Revision des Megachilidae (Hymenoptera Apoidea) de l'Afrique Noire. I. Les genres *Creightoniella* [sic], *Chalicodoma* et *Megachile* (s. str.). *Koninklijk Museum voor Midden-Afrika, Tervuren, België, Annalen, Reeks In-8°, Zoologische Wetenschappen* 137: ix+1–579.
- Pasteels, J.J., & J.M. Pasteels. 1971. Etude au microscope électronique à balayage des plages glandulaires tergaux chez des espèces du genre *Megachile* (Hymenoptera, Apoidea, Megachilidae). *Comptes Rendus de l'Académie des Sciences, Série D (Sciences Naturelles)* 273: 1481–1483.
- Pauly, A., R.W. Brooks, A. Nilsson, Y.A. Pesenko, C.D. Eardley, M. Terzo, T. Griswold, M. Schwarz, S. Patiny, J. Munzinger, & Y. Barbier. 2001. Hymenoptera Apoidea de Madagascar et des îles voisines. *Koninklijk Museum voor Midden-Afrika, Tervuren, België, Annalen Zoologische Wetenschappen* 286: 1–390, +16 pls.
- Peters, D.S. 1970. *Pseudoheriades* n. gen., *Afroheriades* n. subgen., *Pseudoheriades primus* n. sp., neue Formen aus der Familie Megachilidae (Hymenoptera: Apoidea). *Entomologische Zeitschrift* 80(16): 153–160.
- Pitts-Singer, T.L., & J.H. Cane. 2011. The alfalfa leafcutting bee, *Megachile rotundata*: The world's most intensively managed solitary bee. *Annual Review of Entomology* 56: 221–237.
- Praz, C.J. 2017. Subgeneric classification and biology of leafcutter and dauber bees (genus *Megachile* Latreille) of the western Palearctic (Hymenoptera, Apoidea, Megachilidae). *Journal of Hymenoptera Research* 55: 1–54.

- Praz, C.J., A. Müller, B.N. Danforth, T. Griswold, A. Widmer, & S. Dorn. 2008. Phylogeny and biogeography of bees of the tribe Osmiini (Hymenoptera: Megachilidae). *Molecular Phylogenetics and Evolution* 49(1): 185–197.
- Provancher, L. 1882. Faune Canadienne. Les Insectes—Hyménoptères. *Naturaliste Canadien* 13(152): 225–242.
- Pyron, R.A. 2011. Divergence time estimation using fossils as terminal taxa and the origins of Lissamphibia. *Systematic Biology* 60(4): 446–481.
- Radoszkowsky, O.B. 1874. Supplément indispensable à l'article publié par M. Gerstaecker en 1869, sur quelques genres d'Hyménoptères (Suite). *Bulletin de la Société Impériale des Naturalistes de Moscou* 46(3): 133-151, +1 pl.
- Rambaut, A., M. Suchard, D. Xie, & A.J. Drummon. 2014. Tracer v1.6 [<http://tree.bio.ed.ac.uk/software/tracer/>; last accessed on 1 March 2018].
- Rasmussen, C., A.L. Carrion, R. Castro-Urgal, S. Chamorro, V.H. Gonzalez, T.L. Griswold, H.W. Herrera, C.K. McMullen, J.M. Olesen, & A. Traveset. 2012. *Megachile timberlakei* Cockerell (Hymenoptera: Megachilidae): Yet another adventive bee species to the Galápagos Archipelago. *Pan-Pacific Entomologist* 88(1): 98–102.
- Raw, A. 2006. A new subgenus and three new species of leafcutter bees, *Megachile* (*Austrosarus*) (Hymenoptera, Megachilidae) from central Brazil. *Zootaxa* 1228(1): 25–34.
- Reemer, M. 2012. *Unravelling a hotchpotch: Phylogeny and classification of the Microdontinae (Diptera: Syrphidae)*. Doctoral dissertation, Leiden University; Leiden, The Netherlands; 384 pp.
- Reemer, M., & G. Ståhls. 2013. Phylogenetic relationships of Microdontinae (Diptera: Syrphidae) based on molecular and morphological characters. *Systematic Entomology* 38(4): 661–688.
- Remane, A. 1952. *Die Grundlagen des natürlichen Systems, der vergleichenden Anatomie und der Phylogenetik*. Geest and Portig; Leipzig, Germany; vi+400 pp.
- Rieppel, O., & M. Kearney. 2002. Similarity. *Biological Journal of the Linnean Society* 75(1): 59–82.
- Robertson, C. 1901. Some new or little known bees. *Canadian Entomologist* 33(8): 229–231.
- Robertson, C. 1903. Synopsis of Megachilidae and Bombinae. *Transactions of the American Entomological Society* 29(2): 163–178.
- Rocha Filho, L.C.D., & L. Packer. 2017. Phylogeny of the cleptoparasitic Megachilini genera *Coelioxys* and *Radoszkowskiana*, with the description of six new subgenera in *Coelioxys* (Hymenoptera: Megachilidae). *Zoological Journal of the Linnean Society* 180(2): 354–413.
- Roig-Alsina, A., & C.D. Michener. 1993. Studies of the phylogeny and classification of long-tongued bees (Hymenoptera: Apoidea). *University of Kansas Science Bulletin* 55(4): 123–162.
- Ronquist, F., S. Klopfstein, L. Vilhelmsen, S. Schulmeister, D.L. Murray, & A.P. Rasnitsyn. 2012a. A total-evidence approach to dating with fossils, applied to the early radiation of Hymenoptera. *Systematic Biology* 61(6): 973–999.
- Ronquist, F., M. Teslenko, P. van der Mark, D.L. Ayres, A. Darling, S. Höhna, B. Larget, L. Liu, M.A. Suchard, & J.P. Huelsenbeck. 2012b. MrBayes version 3.2: Efficient Bayesian phylogenetic inference and model choice, across a large model space. *Systematic Biology* 61(3): 539–542.
- Rozen, J.G., Jr., & S.M. Kamel. 2007. Investigations on the biologies and immature stages of the cleptoparasitic bee genera *Radoszkowskiana* and *Coelioxys* and their *Megachile* host (Hymenoptera: Apoidea: Megachilidae: Megachilini). *American Museum Novitates* 3573: 1–43.
- Rozen, J.G., Jr., H. Özbek, J.S. Ascher, C. Sedivy, C. Praz, A. Monfared, & A. Müller. 2010. Nest, petal usage, floral preferences, and immatures of *Osmia* (*Ozbekosmia*) *avosetta* (Megachilidae: Megachilinae: Osmiini), including biological comparisons with other osmiine bees. *American Museum Novitates* 3680: 1–22.
- Rozen, J.G., Jr., J.S. Ascher, S.M. Kamel, & K.M. Mohamed. 2016. Larval diversity in the bee genus *Megachile* (Hymenoptera: Apoidea: Megachilidae). *American Museum Novitates* 3863: 1–16.
- Sarzetti, L.C., C.C. Labandeira, & J.F. Genise. 2008. A leafcutter bee trace fossil from the middle Eocene of Patagonia, Argentina, and a review of megachilid (Hymenoptera) ichnology. *Palaeontology* 51(4): 933–941.

- Schofield, R.M.S., M.H. Nesson, & K.A. Richardson. 2002. Tooth hardness increases with zinc-content in mandibles of young adult leaf-cutter ants. *Naturwissenschaften* 89(12): 579–583.
- Schultz, T.R., & S.G. Brady. 2008. Major evolutionary transitions in ant agriculture. *Proceedings of the National Academy of Science, U.S.A.* 105(14): 5435–5440.
- Schwarz, H.F. 1948. Stingless bees (Meliponidae) of the Western Hemisphere: *Lestrimelitta* and the following subgenera of *Trigona*: *Trigona*, *Paratrigona*, *Schwarziana*, *Parapartamona*, *Cephalotrigona*, *Oxytrigona*, *Scaura*, and *Mourella*. *Bulletin of the American Museum of Natural History* 90: i–xvii, 1–546, +8 pls.
- Sereno, P.C. 2007. Logical basis for morphological characters in phylogenetics. *Cladistics* 23(6): 565–587.
- Sheffield, C.S., & S.M. Westby. 2007. The male of *Megachile nivalis* Friese, with an updated key to members of the subgenus *Megachile s.str.* (Hymenoptera: Megachilidae) in North America. *Journal of Hymenoptera Research* 16(1): 178–191.
- Silveira, F.A., G.A.R. Melo, & E.A.B. Almeida. 2002. *Abelhas Brasileiras: Sistemática e Identificação*. Editora IDMAR; Belo Horizonte, Brazil; 253 pp.
- Sinu, P.A., & J.L. Bronstein. 2018. Foraging preferences of leafcutter bees in three contrasting geographical zones. *Diversity and Distributions* 24(5): 621–628.
- Slater, G.J., & L.J. Harmon. 2013. Unifying fossils and phylogenies for comparative analyses of diversification and trait evolution. *Methods in Ecology and Evolution* 4(8): 699–702.
- Smith, F. 1853. *Catalogue of the Hymenopterous Insects in the Collection of the British Museum. Part 1. Andrenidae and Apidae*. British Museum; London, UK; [i]+198 pp., +pls. i–vi.
- Smith, F. 1865. Descriptions of some new species of hymenopterous insects belonging to the families Thynnidae, Masaridae and Apidae. *Transactions of the Entomological Society of London, Series 3* 2(5): 389–399, +pl. xxi.
- Soh, E.J.Y. 2014. *Diversity and trap-nesting studies of Singaporean Megachile bees to inform monitoring and management of tropical pollinators*. Honours thesis, National University of Singapore; Singapore, Singapore; iv+68+[36] pp.
- Talavera, G., & J. Castresana. 2007. Improvement of phylogenies after removing divergent and ambiguously aligned blocks from protein sequence alignments. *Systematic Biology* 56(4): 564–577.
- Taschenberg, E. 1883. Die Gattungen der Bienen (Anthophila). *Berliner Entomologische Zeitschrift* 27(1): 37–100.
- Thomson, C.G. 1872. *Skandinaviens Hymenoptera. 2:a Delen, Innehållande Slägtet Apis Lin.* Berlingska Boktryckeriet; Lund, Sweden; 286 pp.
- Torretta, J.P., S.P. Durante, & A.M. Basilio. 2014. Nesting ecology of *Megachile (Chrysosarus) catar-marcensis* Schrottky (Hymenoptera: Megachilidae), a *Prosopis*-specialist bee. *Journal of Apicultural Research* 53(5): 590–598.
- Trunz, V., L. Packer, J. Vieu, N. Arrigo, & C.J. Praz. 2016. Comprehensive phylogeny, biogeography and new classification of the diverse bee tribe Megachilini: Can we use DNA barcodes in phylogenies of large genera? *Molecular Phylogenetics and Evolution* 103: 245–259.
- Wedmann, S., T. Wappler, & M.S. Engel. 2009. Direct and indirect fossil records of megachilid bees from the Paleogene of central Europe (Hymenoptera: Megachilidae). *Naturwissenschaften* 96(6): 703–712.
- West-Eberhard, M.J. 2003. *Developmental Plasticity and Evolution*. Oxford University Press; Oxford, UK; xx+794 pp.
- Whiting, M.F., S. Bradler, & T. Maxwell. 2003. Loss and recovery of wings in stick insects. *Nature* 421(6920): 264–267.
- Whitlock, J.A., & J.A. Wilson. 2013. Character distribution maps: A visualization method for comparative cladistics. *Acta Zoologica* 94(4): 490–499.
- Williams, H.J., M.R. Strand, G.W. Elzen, S.B. Vinson, & J.S. Merritt. 1986. Nesting behavior, nest architecture, and use of Dufour's gland lipids in nest provisioning by *Megachile integra* and *M. mendica mendica* (Hymenoptera: Megachilidae). *Journal of the Kansas Entomological Society* 59(4): 588–597.

- Williams, N.M., & K. Goodell. 2000. Association of mandible shape and nesting material in *Osmia* Panzer (Hymenoptera: Megachilidae): A morphometric analysis. *Annals of the Entomological Society of America* 93(2): 318–325.
- Winston, M.L. 1979. The proboscis of the long-tongued bees: A comparative study. *University of Kansas Science Bulletin* 51(22): 631–667.
- Wittmann, D., & B. Blochtein. 1995. Why males of leafcutter bees hold the females' antennae with their front legs during mating. *Apidologie* 26(3): 181–196.
- Zhang, C., T. Stadler, S. Klopstein, T.A. Heath, & F. Ronquist. 2016. Total-evidence dating under the fossilized birth-death process. *Systematic Biology* 65(2): 228–249.
- Zillikens, A., & J. Steiner. 2004. Nest architecture, life cycle and cleptoparasite of the Neotropical leaf-cutting bee *Megachile (Chrysosarus) pseudanthidioides* Moure (Hymenoptera: Megachilidae). *Journal of the Kansas Entomological Society* 77(3): 193–202.

ZooBank: urn:lsid:zoobank.org:pub:46F71985-5AF2-4AF8-AD53-1E9070547021

Appendix 1. Summary of major proposals in the classification of the genus *Megachile* s.l., as discussed in the text (*vide supra*). Original names of subgenera are under each genus. Green shaded cells include the leaf-cutter taxa. * = A few recently described taxa are included within this classificatory scheme. † = Extinct taxa. § = *Cesconigoa* Koçak & Kemal is a replacement name for *Cuspidella* Pasteels.

Michener (1965) & Pasteels (1965)	Mitchell (1980)	Michener (2000, 2007)*
<p>Genus <i>Chalicodoma</i>: <i>Archimegachile</i>, <i>Austrochile</i>, <i>Callomegachile</i>, <i>Carinella</i>, <i>Cestella</i>, <i>Chalicodoma</i>, <i>Chalicodomoides</i>, <i>Chelostomoda</i>, <i>Chelostomoides</i>, <i>Cuspidella</i>, <i>Digronoceras</i>, <i>Dinatris</i>, <i>Eumegachilana</i>, <i>Gronoceras</i>, <i>Hackeriapis</i>, <i>Largella</i>, <i>Maximegachile</i>, <i>Morphella</i>, <i>Neglectella</i>, <i>Pseudomegachile</i>, <i>Rhodomegachile</i>, <i>Schizomegachile</i>, <i>Stelodides</i>, <i>Stenomegachile</i>, <i>Thaumatosoma</i></p>	<p>Genus <i>Chalicodoma</i>: <i>Archimegachile</i>, <i>Austrochile</i>, <i>Callomegachile</i>, <i>Carinella</i>, <i>Cestella</i>, <i>Chalicodoma</i>, <i>Chalicodomoides</i>, <i>Chelostomoda</i>, <i>Chelostomoides</i>, <i>Cuspidella</i>, <i>Digronoceras</i>, <i>Dinatris</i>, <i>Eumegachilana</i>, <i>Gronoceras</i>, <i>Hackeriapis</i>, <i>Largella</i>, <i>Maximegachile</i>, <i>Morphella</i>, <i>Neglectella</i>, <i>Pseudomegachile</i>, <i>Rhodomegachile</i>, <i>Schizomegachile</i>, <i>Stelodides</i>, <i>Stenomegachile</i>, <i>Thaumatosoma</i></p>	<p>Genus <i>Megachile</i>: Group 2: <i>Alocanthodon</i>, <i>Austrochile</i>, <i>Callomegachile</i>, <i>SCesconigoa</i>, <i>Cestella</i>, <i>Chalicodoma</i>, <i>Chalicodomoides</i>, †<i>Chalicodomopsis</i>, <i>Chelostomoda</i>, <i>Chelostomoides</i>, <i>Gronoceras</i>, <i>Hackeriapis</i>, <i>Heriadopsis</i>, <i>Largella</i>, <i>Lophanthodon</i>, <i>Matangapis</i>, <i>Maximegachile</i>, <i>Megella</i>, <i>Mitchellapis</i>, <i>Neochalicodoma</i>, <i>Parachalicodoma</i>, <i>Pseudomegachile</i>, <i>Rhodomegachile</i>, <i>Schizomegachile</i>, <i>Stellenigris</i>, <i>Stenomegachile</i>, <i>Thaumatosoma</i></p>
<p>Genus <i>Creightonella</i> Genus <i>Megachile</i>: <i>Acentron</i>, <i>Amegachile</i>, <i>Argyropile</i>, <i>Austromegachile</i>, <i>Callochile</i>, <i>Chrysosarus</i>, <i>Cressoniella</i>, <i>Dactylomegachile</i>, <i>Dasymegachile</i>, <i>Delomegachile</i>, <i>Derotropis</i>, <i>Digitella</i>, <i>Eumegachile</i>, <i>Eury-mella</i>, <i>Eutricharaea</i>, <i>Holcomegachile</i>, <i>Leptorachis</i>, <i>Litomegachile</i>, <i>Megachile</i>, <i>Megachiloides</i>, <i>Megella</i>, <i>Melanosarus</i>, <i>Mitchellapis</i>, <i>Neomegachile</i>, <i>Paracella</i>, <i>Phaenoserus</i>, <i>Platysta</i>, <i>Pseudocentron</i>, <i>Ptilosarus</i>, <i>Sayapis</i>, <i>Tylomegachile</i>, <i>Xanthosarus</i>, <i>Xeromegachile</i></p>	<p>Genus <i>Creightonella</i> Genus <i>Chrysosarus</i>: <i>Chrysosarus</i>, <i>Dactylomegachile</i>, <i>Stelodides</i>, <i>Zonomegachile</i></p>	<p>Group 3: <i>Creightonella</i> Group 1: <i>Acentron</i>, <i>Aethomegachile</i>, <i>Amegachile</i>, <i>Aporiochile</i>, <i>Argyropile</i>, <i>Austrosarus</i>, <i>Austromegachile</i>, <i>Chalepochile</i>, <i>Chrysosarus</i>, <i>Cressoniella</i>, <i>Dasymegachile</i>, <i>Eumegachile</i>, <i>Eutricharaea</i>, <i>Grosapis</i>, <i>Leptorachis</i>, <i>Litomegachile</i>, <i>Megachile</i>, <i>Megachiloides</i>, <i>Melanosarus</i>, <i>Moureapis</i>, <i>Neochelynia</i>, <i>Neocressoniella</i>, <i>Paracella</i>, <i>Platysta</i>, <i>Pseudocentron</i>, <i>Ptilosaroides</i>, <i>Ptilosarus</i>, <i>Rhyssomegachile</i>, <i>Sayapis</i>, <i>Schrottkyapis</i>, <i>Stelodides</i>, <i>Trichurochile</i>, <i>Tylomegachile</i>, <i>Xanthosarus</i>, <i>Zonomegachile</i></p>
<p>Genus <i>Cressoniella</i>: <i>Austromegachile</i>, <i>Chaetochile</i>, <i>Cressoniella</i>, <i>Dasymegachile</i>, <i>Holcomegachile</i>, <i>Neomegachile</i>, <i>Ptilosaroides</i>, <i>Ptilosarus</i>, <i>Rhyssomegachile</i>, <i>Trichurochile</i>, <i>Tylomegachile</i></p>		

Appendix 1. Continued.

Michener (1965) & Pasteels (1965)	Mitchell (1980)	Michener (2000, 2007)*
	<p>Genus <i>Eumegachile</i>: <i>Eumegachile</i>, <i>Grosapis</i>, <i>Mitchellapis</i>, <i>Sayapis</i>, <i>Schrothkyapis</i></p> <p>Genus <i>Megachile</i>: <i>Addendella</i>, <i>Amegachile</i>, <i>Callochile</i>, <i>Delomegachile</i>, <i>Digitella</i>, <i>Eurymella</i>, <i>Eutricharaea</i>, <i>Litomegachile</i>, <i>Macromegachile</i>, <i>Megachile</i>, <i>Megella</i>, <i>Paracella</i>, <i>Platysta</i>, <i>Xanthosarus</i></p> <p>Genus <i>Megachiloidea</i>: <i>Argyropile</i>, <i>Derotropis</i>, <i>Megachiloidea</i>, <i>Phaenosa-</i> <i>rus</i>, <i>Xeromegachile</i></p> <p>Genus <i>Pseudocentron</i>: <i>Acentron</i>, <i>Grafella</i>, <i>Leptorachina</i>, <i>Leptorachis</i>, <i>Melanosarus</i>, <i>Moureana</i>, <i>Pseudocentron</i></p>	

Appendix 2. List of taxa included in the morphological and molecular analyses of the family Megachilidae and tribe Megachilini. We followed the classifications of Gonzalez *et al.* (2012) for the tribes of Megachilidae and that of Michener (2007) for the subgenera of *Megachile s.l.*, which also includes recently described taxa. In the combined analyses, we used closely related species to those used in the morphological analyses when molecular data were not available for the same species. We referred to those chimeric taxa by their generic name, and sometimes subgenus, followed by a combination of the first three letters of both specific epithets in square brackets. For example, the name for the operational taxonomic unit (OTU) resulting from *Trichothurgus wagenknechti* (Moure) and *T. herbsti* (Friese) is referred herein as *Trichothurgus [wagxher]* (see text for explanation). GenBank accession numbers for specimens of included species in the analyses are in Appendix 4. * = Type species of the particular subgenus indicated within *Megachile s.l.*, as recognized by Michener (2007). † = Extinct species. — = Species not included in the analysis.

Phylogeny of Megachilidae			
Morphological analysis	Molecular analysis	Combined analysis	
Outgroups			
Family MELITTIDAE Kawall			
<i>Macropis (Macropis) nuda</i> (Provancher) [USA]	<i>Macropis nuda</i>	<i>Macropis nuda</i>	
<i>Melitta (Melitta) leporina</i> (Panzer) [France, Spain, Iran]	<i>Melitta leporina</i>	<i>Melitta leporina</i>	
Family APIDAE Latreille			
<i>Apis mellifera</i> Linnaeus [USA]	<i>Apis mellifera</i>	<i>Apis mellifera</i>	
<i>Exomalopsis (Stilbomalopsis) solani</i> Cockerell [USA, Mexico]	<i>Exomalopsis</i> sp.	<i>Exomalopsis</i> [solxsp]	
<i>Diadasia (Coquilletapis) australis</i> (Cresson) [USA]	<i>Diadasia bituberculata</i> (Cresson)	<i>Diadasia</i> [ausxbit]	
<i>Nomada utahensis</i> Moalif [USA]	<i>Nomada maculata</i> Cresson	<i>Nomada</i> [utaxmax]	
<i>Ceratina calcarata</i> Robertson [USA]	<i>Ceratina calcarata</i>	<i>Ceratina calcarata</i>	
Ingroup			
Family MEGACHILIDAE Latreille			
Subfamily FIDELINAE Cockerell			
<i>Fidelia (Parafidelia) pallidula</i> (Cockerell) [South Africa]	<i>Fidelia pallidula</i>	<i>Fidelia pallidula</i>	
<i>F. (Fidelia) villosa</i> Brauns [South Africa]	<i>F. villosa</i>	<i>F. villosa</i>	
<i>F. (Fideliana) braunsiana</i> Friese [South Africa]	<i>F. braunsiana</i>	<i>F. braunsiana</i>	

Appendix 2. Continued.

Morphological analysis	Molecular analysis	Combined analysis
Subfamily PARARHOPHITINAE Popov		
<i>Pararhophites orobinus</i> (Morawitz) [Pakistan]	<i>Pararhophites orobinus</i>	<i>Pararhophites orobinus</i>
<i>P. quadratus</i> (Friese) [Egypt]	<i>P. quadratus</i>	<i>P. quadratus</i>
Subfamily LITHURGINAE Newman		
Tribe LITHURGINI Newman		
<i>Lithurgus</i> (<i>Lithurgopsis</i>) <i>apicalis</i> Cresson [USA]	<i>Lithurgus chrysurus</i> Fonscolombe	<i>Lithurgus</i> [api×chr]
<i>Microthurge corumbae</i> (Cockerell) [Bolivia]	<i>Microthurge</i> sp.	<i>Microthurge</i> [cor×sp]
<i>Trichothurgus aterrimus</i> (Cockerell) [Chile]	<i>Trichothurgus herbsti</i> (Friese)	<i>Trichothurgus</i> [atexher]
Tribe †PROTOLITHURGINI Engel		
† <i>Protolithurgus ditomeus</i> Engel		
Subfamily MEGACHILINAE Latreille		
Tribe ANTHIDIINI Ashmead		
<i>Afranthidium</i> (<i>Capanthidium</i>) <i>capicola</i> (Brauns) [South Africa]	<i>Afranthidium capicola</i>	<i>Afranthidium capicola</i>
<i>Anthidiellum</i> (<i>Loyolanthidium</i>) <i>robertsoni</i> (Cockerell) [USA]	<i>Anthidiellum robertsoni</i>	<i>Anthidiellum robertsoni</i>
<i>Anthidium</i> (<i>Anthidium</i>) <i>porterae</i> Cockerell [USA]	<i>Anthidium porterae</i>	<i>Anthidium porterae</i>
<i>Anthodioctes</i> (<i>Anthodioctes</i>) <i>calcaratus</i> (Friese) [Costa Rica]	<i>Anthodioctes</i> (<i>Anthodioctes</i>) <i>mapirensis</i> (Cockerell)	<i>Anthodioctes</i> [cal×map]
<i>Aztecathidium tenochtitlanicum</i> Snelling [Mexico]	<i>Aztecathidium tenochtitlanicum</i>	<i>Aztecathidium tenochtitlanicum</i>
<i>Cyphanthidium intermedium</i> Pasteels [Namibia]	<i>Cyphanthidium intermedium</i>	<i>Cyphanthidium intermedium</i>
<i>Dianthidium</i> (<i>Dianthidium</i>) <i>subparvum</i> Swenk [USA]	<i>Dianthidium subparvum</i>	<i>Dianthidium subparvum</i>
<i>Duckeanthidium thielei</i> Michener [Costa Rica: Heredia]	<i>Duckeanthidium thielei</i>	<i>Duckeanthidium thielei</i>
<i>Eoanthidium</i> (<i>Clistanthidium</i>) <i>rothschildi</i> (Vachal) [South Africa]	<i>Eoanthidium</i> (<i>Clistanthidium</i>) <i>turnericum</i> (Mavromoustakis)	<i>Eoanthidium</i> [rot×tur]

Appendix 2. Continued.

Morphological analysis	Molecular analysis	Combined analysis
<i>Epanthidium</i> (<i>Epanthidium</i>) <i>bicoloratum</i> (Smith) [Argentina]	<i>Epanthidium</i> <i>bicoloratum</i>	<i>Epanthidium</i> <i>bicoloratum</i>
<i>Euasps abdominalis</i> (Fabricius) [Zambia]	<i>Euasps abdominalis</i>	<i>Euasps abdominalis</i>
<i>Hoplostelis</i> (<i>Hoplostelis</i>) <i>bivittata</i> (Cresson) [Costa Rica]	<i>Hoplostelis bivittata</i>	<i>Hoplostelis bivittata</i>
<i>Hypanthioides</i> (<i>Michanthidium</i>) <i>ferrugineum</i> (Urban) [Argentina]	<i>Hypanthioides</i> (<i>Saranthidium</i>) <i>marginalata</i> (Moure & Urban)	<i>Hypanthioides</i> [ferxmar]
<i>Hypanthidium</i> (<i>Hypanthidium</i>) <i>mexicanum</i> (Cresson) [Mexico]	<i>Hypanthidium</i> (<i>Hypanthidium</i>) <i>obscurus</i> Schrottky	<i>Hypanthidium</i> [mexxobs]
<i>Icteranthidium ferrugineum</i> (Fabricius) [Egypt, Tunisia]	<i>Icteranthidium ferrugineum</i>	<i>Icteranthidium ferrugineum</i>
<i>Notanthidium</i> (<i>Notanthidium</i>) <i>stelooides</i> (Spinola) [Chile]	<i>Notanthidium stelooides</i>	<i>Notanthidium stelooides</i>
<i>Pachyanthidium</i> (<i>Pachyanthidium</i>) <i>katangense</i> Cockerell [Congo]	<i>Pachyanthidium</i> (<i>Pachyanthidium</i>) <i>cordatum</i> (Smith)	<i>Pachyanthidium</i> [katxcor]
<i>Plesianthidium</i> (<i>Spinanthidellum</i>) <i>rufocaudatum</i> (Friese) [South Africa]	<i>Plesianthidium rufocaudatum</i>	<i>Plesianthidium rufocaudatum</i>
<i>Pseudoanthidium</i> (<i>Micranthidium</i>) <i>lanificum</i> (Smith) [Cameroon, Congo]	<i>Pseudoanthidium</i> sp.	<i>Pseudoanthidium</i> [lanxsp]
<i>Rhodanthidium</i> (<i>Rhodanthidium</i>) <i>septemdentatum</i> (Latreille) [Greece]	<i>Rhodanthidium septemdentatum</i>	<i>Rhodanthidium septemdentatum</i>
<i>Serapista rufipes</i> (Friese) [South Africa]	<i>Serapista rufipes</i>	<i>Serapista rufipes</i>
<i>Stelis</i> (<i>Stelis</i>) <i>linsleyi</i> Timberlake [USA]	<i>Stelis</i> (<i>Stelis</i>) <i>lateralis</i> Cresson	<i>Stelis</i> [linxlat]
<i>Trachusa</i> (<i>Heteranthidium</i>) <i>larreae</i> (Cockerell) [USA]	<i>Trachusa larreae</i>	<i>Trachusa larreae</i>
Tribe ASPIDOSMINI Gonzalez & al.		
<i>Aspidosmia arnoldi</i> (Brauns) [South Africa]	<i>Aspidosmia arnoldi</i>	<i>Aspidosmia arnoldi</i>
<i>Aspidosmia volkmanni</i> (Friese) [South Africa]	<i>A. volkmanni</i>	<i>A. volkmanni</i>

Appendix 2. Continued.

Morphological analysis	Molecular analysis	Combined analysis
Tribe †CTENOPECTRELLINI Engel		
† <i>Ctenoplectrella cockerelli</i> Engel		
† <i>C. grimaldii</i> Engel		
† <i>C. viridiceps</i> Cockerell		
† <i>Glaesosmia genalis</i> Engel		
Tribe DIOXYINI Cockerell		
<i>Aglaopis tridentata</i> (Nylander) [Austria]	<i>Aglaopis tridentata</i>	<i>Aglaopis tridentata</i>
<i>Dioxys pomonae</i> Cockerell [USA]	<i>Dioxys moesta</i> Costa	<i>Dioxys</i> [pom×moe]
Tribe †GLYPTAPINI Cockerell		
† <i>Glyptapis densopunctata</i> Engel		
† <i>G. disareolata</i> Engel		
Tribe MEGACHILINI Latreille		
<i>Coelioxys (Boreocoelioxys) octodentata</i> Say [USA]	<i>Coelioxys octodentata</i>	<i>Coelioxys octodentata</i>
<i>Megachile (Chelostomoides) angularum</i> Cockerell [USA]	<i>Megachile (Chelostomoides) angularum</i>	<i>Megachile (Chelostomoides) angularum</i>
<i>M. (Creightonella) discolor</i> Smith [South Africa]	<i>M. (Creightonella) albisecta</i> Klug	<i>M. (Creightonella)</i> [dis×alb]
<i>M. (Sayapis) pugnata</i> Say [USA]	<i>M. (Sayapis) pugnata</i>	<i>M. (Sayapis) pugnata</i>
<i>Noteriades spinosus</i> Griswold & Gonzalez [Thailand]	<i>Noteriades</i> sp.	<i>Noteriades</i> [spi×sp]
<i>Radoszkowskiana rufiventris</i> (Spinola) [Egypt]	<i>Radoszkowskiana rufiventris</i>	<i>Radoszkowskiana rufiventris</i>
Tribe OSMIINI Newman		
<i>Afroheriades hyalinus</i> Griswold & Gonzalez [South Africa]	<i>Afroheriades prinnus</i> (Peters)	<i>Afroheriades</i> [hya×pri]
<i>Ashmeadiella (Ashmeadiella) aridula</i> Cockerell [USA]	<i>Ashmeadiella aridula</i>	<i>Ashmeadiella aridula</i>
<i>Atoposmia (Atoposmia) abjecta</i> (Cresson) [USA]	<i>Atoposmia (Eremosmia) mirifica</i> (Michener)	<i>Atoposmia</i> [abj×mir]

Appendix 2. Continued.

Morphological analysis	Molecular analysis	Combined analysis
<i>Chelostoma (Chelostoma) florissomme</i> (Linnaeus) [Hungry, Sweden]	<i>Chelostoma florissomme</i>	<i>Chelostoma florissomme</i>
<i>Haetosmia vechti</i> (Peters) [Israel, Pakistan]	<i>Haetosmia brachyura</i> (Morawitz)	<i>Haetosmia</i> [vec×bra]
<i>Heriades (Heriades) truncorum</i> (Linnaeus) [Austria, Sweden]	<i>Heriades crucifer</i> Cockerell	<i>Heriades</i> [trux×cru]
<i>Hofferia schmiedeknechti</i> (Schletterer) [Bulgaria, Greece]	<i>Hofferia schmiedeknechti</i>	<i>Hofferia schmiedeknechti</i>
<i>Hoplitis (Monumetha) albifrons</i> (Kirby) [USA: Utah]	<i>Hoplitis (Hoplitis) adunca</i> (Panzer)	<i>Hoplitis</i> [alb×adu]
<i>H. (Stenosmia) flavicornis</i> (Morawitz) [Mongolia, Uzbekistan]	<i>H. (Stenosmia) minima</i> (Schulthess)	<i>Hoplitis</i> [flax×min]
<i>Ochreriades fasciatus</i> (Friese) [Israel]	<i>Ochreriades fasciatus</i>	<i>Ochreriades fasciatus</i>
<i>Osmia (Osmia) lignaria</i> Say [USA]	<i>Osmia lignaria</i>	<i>Osmia lignaria</i>
<i>Othinosmia (Megaloheriades) globicola</i> (Stadelmann) [South Africa]	<i>Othinosmia globicola</i>	<i>Othinosmia globicola</i>
<i>Protosmia (Chelostomopsis) rubifloris</i> (Cockerell) [USA]	<i>Protosmia (Protosmia) humeralis</i> (Pérez)	<i>Protosmia</i> [rub×shum]
<i>Pseudoheriades moricei</i> (Friese) [Egypt]	<i>Pseudoheriades moricei</i>	<i>Pseudoheriades moricei</i>
<i>Stenoheriades asiaticus</i> (Friese) [Turkey]	<i>Stenoheriades asiaticus</i>	<i>Stenoheriades asiaticus</i>
<i>Wainia (Caposmia) elizabethae</i> (Friese) [South Africa]	<i>Wainia (Caposmia) eremoplana</i> (Mavromoustakis)	<i>Wainia</i> [elixer]
Phylogeny of Megachilini		
Outgroups		
Subfamily LITHURGINAE Newman		
Tribe LITHURGINI Newman		
<i>Microthurga friesei</i> (Ducke) [Argentina]	<i>Microthurga</i> sp.	<i>Microthurga</i> [fri×sp]
<i>Trichothurgus wagenknechti</i> (Moure) [Chile]	<i>Trichothurgus herbsti</i> (Friese)	<i>Trichothurgus</i> [wag×her]
Subfamily MEGACHILINAE Latreille		
Tribe ASPIDOSMINI Gonzalez & al.		
<i>Aspidosmia volkmanni</i> (Friese) [South Africa]	<i>A. volkmanni</i>	<i>A. volkmanni</i>

Appendix 2. Continued.

Morphological analysis	Molecular analysis	Combined analysis
Tribe ANTHIDIINI Ashmead		
<i>Aztecantidium tenochtitlanicum</i> Snelling [Mexico]	<i>A. tenochtitlanicum</i>	<i>A. tenochtitlanicum</i>
<i>Trachusa mitchelli</i> (Michener) [Mexico]	<i>T. larrae</i> (Cockerell)	<i>Trachusa</i> [mit×lar]
Tribe DIOXYINI Cockerell		
<i>Dioxys producta</i> (Cresson) [USA]	<i>Dioxys moesta</i> Costa	<i>Dioxys</i> [proxmoe]
Tribe OSMINI Newman		
<i>Chelostoma rapunculi</i> (Lepeletier) [USA]	<i>Chelostoma florissome</i> (Linnaeus)	<i>Chelostoma</i> [rap×flo]
<i>Hoplitis biscutellae</i> (Cockerell) [USA]	<i>Hoplitis adunca</i> (Panzer)	<i>Hoplitis</i> [rap×flo]
Ingroup		
Tribe MEGACHILINI Latreille		
<i>Coelioxys (Rhinocoelioxys) zapoteca</i> Cresson [Argentina, Bolivia, Brazil, Mexico]	—	—
<i>C. (Liothyrapis) decipiens</i> Spinola [India]	<i>Coelioxys decipiens</i>	<i>Coelioxys decipiens</i>
<i>C. (Torridapis) torrida</i> Smith [South Africa]	—	—
<i>Noteriades jenniferae</i> Griswold & Gonzalez [Thailand, Myanmar]	<i>Noteriades</i> sp.	<i>Noteriades</i> [jen×sp]
<i>Radoszkowskiana rufiventris</i> Spinola [Egypt]	<i>R. rufiventris</i>	<i>R. rufiventris</i>
Genus <i>Megachile</i> Latreille s.l.		
GROUP 1		
* <i>M. (Acentron) albataris</i> Cresson [USA]	<i>M. (Acentron)</i> sp.	<i>M. (Acentron)</i> [alb×sp]
<i>M. (Acentron) candida</i> Smith [Costa Rica]	—	—
<i>M. (Aethomegachile) lateiceps</i> Smith [India]	<i>M. (Aethomegachile) conjuncta</i> Smith	<i>M. (Aethomegachile)</i> [lat×con]
* <i>M. (Aethomegachile) trichorhysis</i> Engel [Thailand]	—	—
* <i>M. (Ameagachile) bituberculata</i> Ritsema [Cameroon]	<i>M. (Ameagachile) cf. bituberculata</i>	<i>M. (Ameagachile) bituberculata</i>

Appendix 2. Continued.

Morphological analysis	Molecular analysis	Combined analysis
<i>M. (Amegachile) ustulatifformis</i> Cockerell [Australia]	—	—
* <i>M. (Argyropile) parallela</i> Smith [USA]	<i>M. (Argyropile) parallela</i>	<i>M. (Argyropile) parallela</i>
<i>M. (Argyropile) sabinensis</i> Mitchell [USA]	—	—
<i>M. (Austromegachile) exaltata</i> Smith [Brazil]	—	—
* <i>M. (Austromegachile) montezuma</i> Cresson [Brazil]	<i>M. (Austromegachile) sp.</i>	<i>M. (Austromegachile) [mon×sp]</i>
* <i>M. (Chryosarus) guaranitica</i> Schrottky [Paraguay]	<i>M. (Chryosarus) sp.</i>	<i>M. (Chryosarus) [pse×sp]</i>
<i>M. (Chryosarus) parsonisiae</i> Schrottky [Argentina]	—	—
<i>M. (Chryosarus) pseudanthidioides</i> Moure [Brazil]	—	—
* <i>M. (Cressoniella) zapoteca</i> Cresson [Mexico]	<i>M. (Cressoniella) zapoteca</i>	<i>M. (Cressoniella) zapoteca</i>
<i>M. (Dasymegachile) schwimmeri</i> Engel [Argentina, Peru] (= <i>M. mitchelli</i> Raw, <i>nomen praeoccupatum</i>)	—	—
* <i>M. (Dasymegachile) saulcyi</i> Guérin-Méneville [Chile]	<i>M. (Dasymegachile) sp.</i>	<i>M. (Dasymegachile) [sau×sp]</i>
* <i>M. (Eumegachile) bombycina</i> Radoszkowski [Finland]	<i>M. (Eumegachile) bombycina</i>	<i>M. (Eumegachile) bombycina</i>
* <i>M. (Eutricharaea) argentata</i> Fabricius [USA]	—	—
<i>M. (Eutricharaea) digiticauda</i> Cockerell [Zimbabwe]	—	—
<i>M. (Eutricharaea) eurymera</i> Smith [Kenya, Nigeria]	<i>M. (Eutricharaea) aff. eurymera</i>	<i>M. (Eutricharaea) eurymera</i>
<i>M. (Eutricharaea) femorata</i> Smith [India]	—	—
<i>M. (Eutricharaea) leachella</i> Curtis [Slovakia]	—	—
<i>M. (Eutricharaea) rotundata</i> Fabricius [USA]	<i>M. (Eutricharaea) rotundata</i>	<i>M. (Eutricharaea) rotundata</i>
<i>M. (Eutricharaea) submetallica</i> Benoist [Madagascar]	—	—
* <i>M. (Grosapis) cockerelli</i> Rohwer [Mexico]	<i>M. (Grosapis) cockerelli</i>	<i>M. (Grosapis) cockerelli</i>
<i>M. (Leptorachis) crotalariae</i> Schwimmer [Brazil]	—	—
<i>M. (Leptorachis) laeta</i> Smith [Brazil]	—	—
* <i>M. (Leptorachis) petulans</i> Cresson [USA]	<i>M. (Leptorachis) petulans</i>	<i>M. (Leptorachis) petulans</i>

Appendix 2. Continued.

Morphological analysis	Molecular analysis	Combined analysis
*M. (<i>Litomegachile brevis</i> Say [USA]	M. (<i>Litomegachile texana</i> Cresson	M. (<i>Litomegachile</i>) [bre×tex]
M. (<i>Litomegachile gentilis</i> Cresson [USA]	—	—
*M. (<i>Megachile centuncularis</i> Linnaeus [USA]	—	—
M. (<i>Megachile montivaga</i> Cresson [USA]	—	—
M. (<i>Megachiloides integra</i> Cresson [USA]	M. (<i>Megachiloides nevadensis</i> Cresson	M. (<i>Megachiloides</i>) [int×nev]
*M. (<i>Megachiloides oenotherae</i> Mitchell [USA]	—	—
M. (<i>Megachiloides pascoensis</i> Mitchell [USA]	—	—
M. (<i>Melanosarus nigripennis</i> Spinola [Brazil]	—	—
*M. (<i>Melanosarus xylocopoides</i> Smith [USA]	M. (<i>Melanosarus</i>) sp.	M. (<i>Melanosarus</i>) [xy]×sp]
*M. (<i>Moureapis anthidioides</i> Radoszkowski [Brazil]	—	—
M. (<i>Neochelynia chichimeca</i> Cresson [Mexico]	M. (<i>Neochelynia?</i>) sp.	M. (<i>Neochelynia</i>) [chi×sp]
*M. (<i>Neochelynia paulista</i> Schrottky [Brazil]	—	—
*M. (<i>Neocressoniella carbonaria</i> Smith [India]	—	—
M. (<i>Paracella curta</i> Gerstaecker [Uganda]	—	—
*M. (<i>Paracella semivenusta</i> Cockerell [Malawi]	M. (<i>Paracella</i>) sp.	M. (<i>Paracella</i>) [sem×sp]
*M. (<i>Platysta platystoma</i> Pasteels [Congo]	—	—
M. (<i>Pseudocentron poeyi</i> Guérin-Méneville [Cuba]	—	—
*M. (<i>Pseudocentron pruina</i> Smith [USA]	M. (<i>Pseudocentron</i>) sp.	M. (<i>Pseudocentron</i>) [prux×sp]
*M. (<i>Ptilosaroides neoxanthoptera</i> Cockerell [Panama]	—	—
M. (<i>Ptilosarus microsoma</i> Cockerell [Trinidad and Tobago]	M. (<i>Ptilosarus microsoma</i>	M. (<i>Ptilosarus microsoma</i>
*M. (<i>Rhyssomegachile simillima</i> Smith [Brazil]	—	—
M. (<i>Sayapis planula</i> Vachal [Brazil, Paraguay]	—	—
*M. (<i>Sayapis pugnata</i> Say [USA]	M. (<i>Sayapis pugnata</i>	M. (<i>Sayapis pugnata</i>

Appendix 2. Continued.

Morphological analysis	Molecular analysis	Combined analysis
*M. (<i>Schrotkyapis</i>) <i>assumptionis</i> Schrottky [Brazil]	—	—
*M. (<i>Steloides</i>) <i>euzona</i> Pérez [Chile]	M. (<i>Steloides</i>) <i>euzona</i>	M. (<i>Steloides</i>) <i>euzona</i>
*M. (<i>Trichurochile</i>) <i>thygaterella</i> Schrottky [Peru, Brazil]	—	—
*M. (<i>Tylomegachile</i>) <i>orba</i> Schrottky [Mexico]	M. (<i>Tylomegachile</i>) sp.	M. (<i>Tylomegachile</i>) [orb×sp]
M. (<i>Tylomegachile</i>) <i>simplicipes</i> Friese [Mexico]	—	—
M. (<i>Xanthosarus</i>) <i>addenda</i> Cresson [USA]	—	—
M. (<i>Xanthosarus</i>) <i>fortis</i> Cresson [USA]	M. (<i>Xanthosarus</i>) <i>fortis</i>	M. (<i>Xanthosarus</i>) <i>fortis</i>
M. (<i>Xanthosarus</i>) <i>lagopoda</i> Linnaeus [Spain]	M. (<i>Xanthosarus</i>) <i>lagopoda</i>	M. (<i>Xanthosarus</i>) <i>lagopoda</i>
*M. (<i>Xanthosarus</i>) <i>latimanus</i> Say [USA]	—	—
*M. (<i>Zonomegachile</i>) <i>moderata</i> Smith [Brazil]	—	—
GROUP 2		
M. (<i>Alocanthedon</i>) <i>mamecylomae</i> (Engel) [Malaysia]	M. (<i>Alocanthedon</i>) sp.	M. (<i>Alocanthedon</i>) [mem×sp]
*M. (<i>Austrochile</i>) <i>resinifera</i> Meade-Waldo [Australia]	M. (<i>Austrochile</i>) sp.	M. (<i>Austrochile</i>) [res×sp]
M. (<i>Callomegachile</i>) <i>biseta</i> Vachal [Gabon]	—	—
M. (<i>Callomegachile</i>) <i>clotho</i> Smith [NE. Sulawesi]	—	—
M. (<i>Callomegachile</i>) <i>decemsignata</i> Radoszkowski [Uganda]	M. (<i>Callomegachile</i>) <i>decemsignata</i>	M. (<i>Callomegachile</i>) <i>decemsignata</i>
*M. (<i>Callomegachile</i>) <i>mysticema</i> Michener [Australia]	—	—
M. (<i>Callomegachile</i>) <i>sculpturalis</i> Smith [Japan, USA]	M. (<i>Callomegachile</i>) <i>sculpturalis</i>	M. (<i>Callomegachile</i>) <i>sculpturalis</i>
M. (<i>Callomegachile</i>) <i>torrida</i> Smith [Uganda]	—	—
*M. (<i>Cesacongoa</i>) <i>quadraticauda</i> Pasteels [Congo]	M. (<i>Cesacongoa</i>) sp.	M. (<i>Cesacongoa</i>) [qua×sp]
*M. (<i>Cestella</i>) <i>cestifera</i> Benoist [Madagascar]	—	—
M. (<i>Chalicodoma</i>) <i>asiatica</i> Morawitz [Turkey]	—	—
M. (<i>Chalicodoma</i>) <i>lefeborei</i> Lepeletier [Greece, Italy]	M. (<i>Chalicodoma</i>) <i>lefeborei</i>	M. (<i>Chalicodoma</i>) <i>lefeborei</i>

Appendix 2. Continued.

Morphological analysis	Molecular analysis	Combined analysis
<i>M. (Chalicodoma) manicata</i> Giraud [Kazakhstan]	<i>M. (Chalicodoma) manicata</i>	<i>M. (Chalicodoma) manicata</i>
* <i>M. (Chalicodoma) parietina</i> Geoffroy [Spain]	<i>M. (Chalicodoma) parietina</i>	<i>M. (Chalicodoma) parietina</i>
* <i>M. (Chalicodomoides) aethiops</i> Smith [Australia]	<i>M. (Chalicodomoides) aethiops</i>	<i>M. (Chalicodomoides) aethiops</i>
*† <i>M. (Chalicodomopsis) glaesaria</i> Engel [Dominican Republic]		
* <i>M. (Chelostomoda) spissula</i> Cockerell [China]	<i>M. (Chelostomoda) sp.</i>	<i>M. (Chelostomoda) [spi×sp]</i>
<i>M. (Chelostomoda) ulrica</i> Nurse [India]	—	—
<i>M. (Chelostomoides) campanulae</i> Robertson [USA]	<i>M. (Chelostomoides) angularum</i> Cockerell	<i>M. (Chelostomoides) [cam×ang]</i>
<i>M. (Chelostomoides) georgica</i> Cresson [USA]	—	—
* <i>M. (Chelostomoides) rugifrons</i> Smith [USA]	—	—
<i>M. (Chelostomoides) spinotulata</i> Mitchell [USA]	<i>M. (Chelostomoides) spinotulata</i>	<i>M. (Chelostomoides) spinotulata</i>
* <i>M. (Gronoceras) bombiformis</i> Gerstaecker [Tanzania]	<i>M. (Gronoceras) bombiformis</i>	<i>M. (Gronoceras) bombiformis</i>
<i>M. (Gronoceras) cincta combusta</i> (Smith) [Tanzania]	—	—
<i>M. (Hackeriapis) ferox</i> Smith [Australia]	—	—
<i>M. (Hackeriapis) heriadiiformis</i> Smith [Australia]	—	—
<i>M. (Hackeriapis) ignita</i> Smith [Australia]	—	—
* <i>M. (Hackeriapis) rhodura</i> Cockerell [Australia]	<i>M. (Hackeriapis) sp. 1</i>	<i>M. (Hackeriapis) [rho×sp]</i>
* <i>M. (Heriadopsis) striatulus</i> Cockerell [Zimbabwe]	<i>M. (Heriadopsis) sp.</i>	<i>M. (Heriadopsis) [str×sp]</i>
* <i>M. (Largella) semiovestita</i> Smith [C. Java]	<i>M. (Largella) floralis</i> (Fabricius)	<i>M. (Largella) [sem×flo]</i>
<i>M. (Lophanthedon) dimidiata</i> Smith [Malaysia]	<i>M. (Lophanthedon) dimidiata</i>	<i>M. (Lophanthedon) dimidiata</i>
* <i>M. (Matangapis) alticola</i> Cameron [Borneo]	<i>M. (Matangapis) alticola</i>	<i>M. (Matangapis) alticola</i>
* <i>M. (Maximegachile) maxillosa</i> Guérin-Méneville [Kenya, Natal, Tanzania]	<i>M. (Maximegachile) maxillosa</i>	<i>M. (Maximegachile) maxillosa</i>
* <i>M. (Megella) malimbana</i> Strand [Zaire]	—	—
<i>M. (Megella) pseudomonticola</i> Hedicke [Japan]	<i>M. (Megella) pseudomonticola</i>	<i>M. (Megella) pseudomonticola</i>

Appendix 2. Continued.

Morphological analysis	Molecular analysis	Combined analysis
*M. (<i>Mitchellapis</i>) <i>fabricator</i> Smith [Australia]	M. (<i>Mitchellapis</i>) <i>fabricator</i>	M. (<i>Mitchellapis</i>) <i>fabricator</i>
*M. (<i>Parachalicodoma</i>) <i>incana</i> Friese [Egypt]	M. (<i>Parachalicodoma</i>) sp.	M. (<i>Parachalicodoma</i>) [inc×sp]
M. (<i>Pseudomegachile</i>) <i>albocincta</i> Radoszkowski [Egypt]	—	—
M. (<i>Pseudomegachile</i>) <i>armatipes</i> Friese [Natal]	M. (<i>Pseudomegachile</i>) <i>laminata</i> Friese	M. (<i>Pseudomegachile</i>) [arm×lam]
*M. (<i>Pseudomegachile</i>) <i>ericetorum</i> Lepeletier [Spain]	M. (<i>Pseudomegachile</i>) <i>ericetorum</i>	M. (<i>Pseudomegachile</i>) <i>ericetorum</i>
M. (<i>Pseudomegachile</i>) <i>flavipes</i> Spinola [India]	—	—
M. (<i>Pseudomegachile</i>) <i>muansae</i> Friese [Tanzania]	M. (<i>Pseudomegachile</i>) <i>leucospilura</i> Cockerell	M. (<i>Pseudomegachile</i>) [muax×leu]
*M. (<i>Rhodomegachile</i>) <i>abdominalis</i> Smith [Australia]	M. (<i>Rhodomegachile</i>) sp.	M. (<i>Rhodomegachile</i>) [abd×sp]
*M. (<i>Schizomegachile</i>) <i>monstrosa</i> Smith [Australia]	—	—
*M. (<i>Stenomegachile</i>) <i>chelostomoides</i> Gribodo [Zaire]	M. (<i>Stenomegachile</i>) <i>chelostomoides</i>	M. (<i>Stenomegachile</i>) <i>chelostomoides</i>
M. (<i>Stenomegachile</i>) <i>dolichosoma</i> Benoist [Madagascar]	—	—
*M. (<i>Thaumatossoma</i>) <i>duboulaii</i> Smith [Australia]	M. (<i>Thaumatossoma</i>) <i>remeata</i> Cockerell	M. (<i>Thaumatossoma</i>) [dub×rem]
GROUP 3		
M. (<i>Creightonella</i>) <i>albisecta</i> Klug [Slovakia]	M. (<i>Creightonella</i>) <i>albisecta</i>	M. (<i>Creightonella</i>) <i>albisecta</i>
*M. (<i>Creightonella</i>) <i>cognata</i> Smith [Uganda]	M. (<i>Creightonella</i>) <i>cornigera</i> Friese	M. (<i>Creightonella</i>) [cog×cor]

Appendix 3. Continued.

Characters 47-92

	47	51	56	61	66	71	76	81	86	91
<i>M (Oligotropus) campanulae</i>	0	---	0	1	0	0	1	0	0	1
<i>M (Gnathodon) georgica</i>	0	---	0	1	0	0	1	0	0	1
<i>M (Chelostomoidella) spinotulata</i>	0	---	0	1	0	0	1	0	0	1
<i>M (Callomegachile) mystaceana</i>	0	---	0	1	0	0	1	0	0	1
<i>M (Callomegachile) sculpturalis</i>	0	---	0	1	0	0	1	0	0	1
<i>M (Eumegachilana) clotho</i>	0	---	0	1	0	0	1	0	0	1
<i>M (Carinula) torrida</i>	0	---	0	1	0	0	1	0	0	1
<i>M (Carinula) decemsignata</i>	0	---	0	1	0	0	1	0	0	1
<i>M (Morphella) biseta</i>	0	---	0	1	0	0	1	0	0	1
<i>M (Alocanthon) memecylonae</i>	0	---	0	1	0	0	1	0	0	1
<i>M (Cestella) cestifera</i>	0	---	0	1	0	0	1	0	0	1
<i>M (Chalicodoma) parietina</i>	0	---	0	1	0	0	1	0	0	1
<i>M (Euchalicodoma) asiatica</i>	0	---	0	1	0	0	1	0	0	1
<i>M (Allochalicodoma) lefebvrei</i>	0	---	0	1	0	0	1	0	0	1
<i>M (Katamegachile) manicata</i>	0	---	0	1	0	0	1	0	0	1
<i>M (Parachalicodoma) incana</i>	0	---	0	1	0	0	1	0	0	1
<i>M (Gronoceras) bombiformis</i>	0	---	0	1	0	0	1	0	0	1
<i>M (Digronoceras) cincta combusta</i>	0	---	0	1	0	0	1	0	0	1
<i>M (Largella) semivestita</i>	0	---	0	1	0	0	1	0	0	1
<i>M (Lophanthon) dimidiata</i>	0	---	0	1	0	0	1	0	0	1
<i>M (Maximegachile) maxillosa</i>	0	---	0	1	0	0	1	0	0	1
<i>M (Pseudomegachile) ericetorum</i>	0	---	0	1	0	0	1	0	0	1
<i>M (Archimegachile) flavipes</i>	0	---	0	1	0	0	1	0	0	1
<i>M (Neglectella) armatipes</i>	0	---	0	1	0	0	1	0	0	1
<i>M (Xenomegachile) albocincta</i>	0	---	0	1	0	0	1	0	0	1
<i>M (Dinavis) muansae</i>	?	?	?	?	?	?	?	?	?	?
<i>M (Cesacongoa) quadraticauda</i>	0	---	0	1	0	0	1	0	0	1

Appendix 3. Continued.

Characters 47-92

	47	51	56	61	66	71	76	81	86	91
<i>M (Eutricharaea) argentata</i>	0---	110110	-00021101100001012000002000100000001							
<i>M (Perezia) leachella</i>	0---	110110	-00021101100001012000002000100000001							
<i>M (Eurymella) eurymera</i>	0---	110100	-0102110110000101200000200000000101							
<i>M (Eurymella) submetallica</i>	0---	110100	-0102110110000101200000200000000101							
<i>M (Digitella) digiticauda</i>	0---	110100	-01021101100001012000002000100000101							
<i>M (Platysta) platystoma</i>	0---	110100	-1102110110000101200000200000000101							
<i>M (Neoeutricharaea) rotundata</i>	1010110110	-0102110110000101200000200000000101								
<i>M (Litomegachile) brevis</i>	1010110110	-01021101100000012000002000100000111								
<i>M (Litomegachile) gentilis</i>	1010110110	-01021101100000012000002000100020111								
<i>M (Megachile) centuncularis</i>	10100--110	-0102110110000101200000200000020111								
<i>M (Cyphopyga) montivaga</i>	0--0--110	-0102110110000101200000200000020001								
<i>M (Tylomegachile) orba</i>	1010110110	-0102110110000101200000200000000101								
<i>M (Tylomegachile) simplicipes</i>	1010110110	-01021101100001012000002000100000101								
<i>M (Chalicodomopsis) glaesaria</i>	0--0--???	???								

Appendix 3. Continued.

Characters 185-230

	185	189	194	199	204	209	214	219	224	229
<i>M (Neocressoniella) carbonaria</i>	0	--	000000	100101000000	111101100001	1011000002	100011			
<i>M (Aethomegachile) laticeps</i>	0	--	000000	100101000101	101101	--	110021	10110000	110000	110
<i>M (Aethomegachile) trichorhytisma</i>	1000	0000	1101101100	1100	--	110021	11001000	110000	110000	111
<i>M (Megella) malimbana</i>	0	--	000000	0000101100101101	--	110041	10110100	2000	00111	
<i>M (Megella) pseudomonticola</i>	0	--	000000	0000101201001111	10102001	10110100	1000	111		
<i>M (Austromegachile) montezuma</i>	0	--	000000	100101001001101	--	110001	10110100	0000	00111	
<i>M (Holcomegachile) exaltata</i>	0	--	001	--	0100101101001101	--	100001	10110100	0000	00111
<i>M (Cressoniella) zapoteca</i>	0	--	000000	10010100100211	10100001	1010010100	0000	111		
<i>M (Dasymegachile) saulcyi</i>	0	--	000000	0000101000101111	10100001	10110000	00100	111		
<i>M (Chaetochile) schwimmeri</i>	0	--	000000	0000101000101111	10112001	10110001	110000	110000	111	
<i>M (Neochelynia) paulista</i>	0	--	000000	000010100000100	--	100001	10110000	10000	00111	
<i>M (Neomegachile) chichimeca</i>	0	--	000000	000010100000100	--	110001	10100000	10000	00111	
<i>M (Ptilosaroides) neoxanthoptera</i>	0	--	000000	000010100000200	--	110001	1010010100	0000	111	
<i>M (Ptilosarus) microsoma</i>	0	--	000000	000010100000200	--	110001	1010010100	0000	111	
<i>M (Rhyssomegachile) simillima</i>	0	--	000000	000010100001100	--	110001	1010010100	0000	111	
<i>M (Trichurochile) thygaterella</i>	0	--	000000	000010100000100	--	100001	10110101	11000	111	
<i>M (Eumegachile) bombycina</i>	0	--	000000	10010100010111	10100000	10110101	1000	111		
<i>M (Grosapis) cockerelli</i>	0	--	000000	00001010000011	10110100	10110000	10000	00111		
<i>M (Argyropile) parallela</i>	0	--	000000	100101000102110	--	100001	10100000	12000	00111	
<i>M (Argyropile) sabinensis</i>	0	--	000000	100101000101110	--	101001	10100000	12000	00111	
<i>M (Megachilooides) oenotherae</i>	1000	0000	00010010110000	1111102001	10111001	1300	111			
<i>M (Xeromegachile) integra</i>	1100	0000	00000110110000	1111100000	10111100	3100	111			
<i>M (Derotropis) pascoensis</i>	1000	0000	00010010110000	0011111100	101101	1003100	111			
<i>M (Xanthosarus) latimanus</i>	1100	001	--	1001101000101111	1112001	10110000	10100	111		
<i>M (Addendella) addenda</i>	0	--	000000	100101000101101	--	100001	10110000	11000	00111	
<i>M (Macromegachile) lagopoda</i>	1010	0000	001011010001	011110112001	10110000	12000	00111			
<i>M (Phaenosarus) fortis</i>	1100	0000	00010110110000	0111111000	10111000	02100	111			

Appendix 3. Continued.

Characters 231-272

	231	235	240	245	250	255	260	265	270
M (<i>Chelostomoda</i>) <i>spissula parvula</i>	-	1100111000011010	-	0101010000000	---	10010000			
M (<i>Chelostomoda</i>) <i>ulrica</i>	11100111000011010	-	010111200	-	010	---	10010000		
M (<i>Creightonella</i>) <i>cognata</i>	11102100000211010	-	0100010111000	---	0	-	000100		
M (<i>Creightonella</i>) <i>albisecta</i>	-	1100111000011010	-	0100012011000	---	0	-	000100	
M (<i>Sayapis</i>) <i>pugnata</i>	11103101000011010	-	0100010001000	---	10010010				
M (<i>Sayapis</i>) <i>planula</i>	01100101000011010	-	0100010001200	---	0	-	010010		
M (<i>Schrottkyapis</i>) <i>assumptionis</i>	01100101000011010	-	0100010101000	---	0	-	010010		
M (<i>Mitchellapis</i>) <i>fabricator</i>	11100111010011010	-	0100010001000	---	10010100				
M (<i>Acentron</i>) <i>albitarsis</i>	01103101011011010	-	0100010001211	101010010010					
M (<i>Acentron</i>) <i>candida</i>	01103101011011010	-	0100010001211	101010010010					
M (<i>Leptorachis</i>) <i>petulans</i>	-	01031010011010	-	0100012001001000	10011000				
M (<i>Leptorachina</i>) <i>laeta</i>	-	0100101011011010	-	0110111100201010	10010100				
M (<i>Leptorachis</i>) <i>crotalariae</i>	0010010100011010	-	110001?010???	10010000					
M (<i>Melanosarus</i>) <i>xylocopoides</i>	01100101000011010	-	0100010100211	101010010000					
M (<i>Melanosarus</i>) <i>nigripennis</i>	11100101000011010	-	0100011100211	101010010000					
M (<i>Moureapis</i>) <i>anthidiodes</i>	11100101010001010	-	1100010001211	100010010000					
M (<i>Pseudocentron</i>) <i>pruina</i>	11100101011011010	-	0100010100211	10110	-	000000			
M (<i>Pseudocentron</i>) <i>poeyi</i>	11100101011011010	-	0100010100211	10110	-	000000			
M (<i>Chrysosarus</i>) <i>guaranitica</i>	-	0100101000110111	10100010000200	---	10010000				
M (<i>Chrysosarus</i>) <i>pseudanthidiodes</i>	-	0100101000110111	10100010001200	---	10010000				
M (<i>Dactylomegachile</i>) <i>parsonsiae</i>	-	0100101000110111	10100010000200	---	10010000				
M (<i>Stelodides</i>) <i>euzona</i>	10100101000110111	10100012001200	---	10000000					
M (<i>Zonomegachile</i>) <i>moderata</i>	1010010100011011001	1000100010001200	---	10010000					
M (<i>Amegachile</i>) <i>bituberculata</i>	0110010100011010	-	0100012001200	---	0	-	010000		
M (<i>Callochile</i>) <i>ustulatifformis</i>	0110010100011010	-	0110012101100	---	10010100				
M (<i>Paracella</i>) <i>semivenusta</i>	11100101100011010	-	0100012000210	---	10010100				
M (<i>Paracella</i>) <i>curtula</i>	10100101010011010	-	0111011001000000	---	0	-	010100		

Appendix 4. Quantitative descriptors of trees obtained from implied weighting (IW) analyses. F = total fit of characters to tree (Goloboff, 1993); K = concavity factor determining weighting strength; MPT = number of parsimonious trees; L = tree length; RI = retention index; GC Observed = average GC frequency-difference, as calculated from displayed support at each node in the resulting tree. Average value followed, in parentheses, by median, standard deviation, and number of nodes. * = a single node collapsed in the consensus tree. In all analyses, the Consistency Index was 13. Avg. SPR-dist. EW consensus = SPR distance between the resulting topology of each IW analysis and the topology obtained from the consensus tree of the equal weighting analysis. Avg. SPR-dist. Total evidence = SPR distance between the resulting topology of each IW analysis and the topology obtained from the Bayesian inference analysis of the full dataset. High values in bold face.

F	K	MPT	L	RI	GC Observed	Avg. SPR-dist EW consensus	Avg. SPR-dist Total Evidence
0.5	7.50	1	2434	56	50.24 (48.0, ± 35.11, n = 63)	0.5966	0.4538
0.54	8.81	1	2421	56	50.97 (54.5, ± 35.36, n = 60)	0.6134	0.4874
0.58	10.40	1	2415	56	51.03 (55.0, ± 35.87, n = 62)	0.6387	0.4622
0.62	12.20	1	2397	57	49.31 (42.0, ± 36.27, n = 65)	0.6891	0.4874
0.66	14.60	2*	2393	57	50.19 (46.5, ± 36.08, n = 64)	0.6807	0.4874
0.7	17.50	2*	2389	57	48.15 (40.0, ± 36.37, n = 67)	0.6639	0.4874
0.74	21.40	1	2378	57	48.03 (40.0, ± 35.79, n = 68)	0.7815	0.4790
0.78	26.60	1	2377	57	48.73 (41.0, ± 35.18, n = 67)	0.7899	0.4538
0.82	34.20	1	2377	57	47.38 (38.0, ± 35.43, n = 69)	0.7899	0.4538
0.86	46.10	1	2372	57	48.27 (38.5, ± 35.33, n = 66)	0.7563	0.4286
0.9	67.50	1	2366	57	49.67 (41.0, ± 34.88, n = 64)	0.8824	0.3782

Appendix 5. GenBank accession numbers for sequences used in this study.

Phylogeny of Megachilidae						
Taxa	EF1 α	Opsin	CAD	NAK	28S	
<i>Macropis nuda</i>	AY585155	DQ116686	DQ067171	HQ995917	HQ996008	
<i>Melitta leporina</i>	AY585158	DQ116688	DQ067174	EF646394	AY654529	
<i>Apis mellifera</i>	AF015267	AMU26026	DQ067178	XM_623142	AY703551	
<i>Exomalopsis</i> sp.	GU244989	HM211835	–	GU245110	GU244802	
<i>Diadasia bituberculata</i>	GU244927	AF344594	–	GU245074	GU244768	
<i>Nomada maculata</i>	GU245030	AF344609	–	GU245206	GU244890	
<i>Ceratina calcarata</i>	AY585108	AF344620	DQ067190	GU245213	HQ996011	
<i>Fidelia pallidula</i>	HQ995686	HQ995756	HQ995831	HQ995929	HQ996025	
<i>Fidelia villosa</i>	HQ995682	HQ995752	HQ995827	HQ995925	HQ996021	
<i>Fidelia braunsiana</i>	HQ995683	HQ995753	HQ995828	HQ995926	HQ996022	
<i>Fideliopsis major</i>	DQ141113	EU851628	HQ995833	HQ995931	HQ996027	
<i>Fidelia profuga</i>	GU244990	HQ995760	HQ995836	GU245151	HQ996030	
<i>Pararhophites orobinus</i>	HQ995679	HQ995749	HQ995823	HQ995922	HQ996018	
<i>Pararhophites quadratus</i>	EU851522	EU851627	HQ995824	GU245153	GU244841	
<i>Afranthidium (Capanthidium) capicola</i>	KX060937	KX060813	KX060879	KU976158	KU976218	
<i>Aspidosmia arnoldi</i>	HQ995701	HQ995773	HQ995850	HQ995945	HQ996042	
<i>Aspidosmia volkmanni</i>	HQ995702	HQ995774	HQ995851	HQ995946	HQ996043	
<i>Anthidiellum (Loyolanthidium) robertsoni</i>	KX060952	KX060830	KX060894	KU976175	KU976235	
<i>Anthidium (Anthidium) porterae</i>	GU244996	AF344619	–	GU245158	GU244846	
<i>Anthodioctes (Anthodioctes) mapirensis</i>	HQ995700	HQ995772	HQ995849	HQ995944	HQ996041	
<i>Dianthidium (Dianthidium) subparvum</i>	GU244993	KX060847	KX060909	GU245155	GU244843	
<i>Euasps abdominalis</i>	JX869703	JX869735	JX869627	JX869769	JX869662	

Appendix 5. Continued.

Taxa	EF1 α	Opsin	CAD	NAK	28S
<i>Hoplostelis bivittata</i>	JX869705	JX869737	—	JX869771	JX869671
<i>Pachyanthidium (Pachyanthidium) cordatum</i>	KX060971	KX060852	KX060915	KU976196	KU976257
<i>Serapista rufipes</i>	HQ995716	HQ995789	HQ995866	HQ995960	HQ996057
<i>Stelis lateralis</i>	JX869718	JX869751	JX869643	JX869784	JX869685
<i>Trachusa larreae</i>	HQ995719	HQ995791	HQ995868	GU245154	GU244842
<i>Notanthidium steloides</i>	HQ995712	HQ995784	HQ995861	HQ995956	HQ996053
<i>Plesianthidium (Spinanthidium) rufocaudatum</i>	KX060976	KX060857	KX060920	KU976201	KU976262
<i>Icteranthisidium ferrugineum flavum</i>	HQ995711	HQ995783	HQ995860	HQ995955	HQ996052
<i>Hypanthidium obscurius</i>	HQ995710	HQ995782	HQ995859	HQ995954	HQ996051
<i>Hypanthidioides marginata</i>	HQ995709	HQ995781	HQ995858	HQ995953	HQ996050
<i>Eoanthidium turnericum</i>	HQ995707	HQ995779	HQ995856	HQ995951	HQ996048
<i>Rhodanthidium septemdentatum</i>	HQ995715	HQ995788	HQ995865	HQ995959	HQ996056
<i>Epanthidium bicoloratum</i>	HQ995708	HQ995780	HQ995857	HQ995952	HQ996049
<i>Pseudoanthidium (Micranthidium) sp.</i>	KX060982	KX060862	KX060926	KU976206	KU976268
<i>Aztecanthidium tenochtitlanicum</i>	—	KX060844	KX060906	KU976189	KU976249
<i>Duckeanthidium thielei</i>	HQ995706	HQ995778	HQ995855	HQ995950	HQ996047
<i>Cyphanthidium intermedium</i>	KX060966	KX060845	KX060907	KU976190	KU976250
<i>Aglaopsis tridentata</i>	EU851524	EU851630	HQ995844	HQ995939	HQ996036
<i>Dioxys moesta</i>	HQ995696	HQ995768	HQ995845	HQ995940	HQ996037
<i>Lithurgus chrysurus</i>	EU851523	EU851629	HQ995837	HQ995934	HQ996031
<i>Microthurga sp.</i>	HQ995694	HQ995766	HQ995842	GU245161	GU244849
<i>Trichotheurgus herbsti</i>	HQ995695	HQ995767	HQ995843	GU245160	GU244848
<i>Afroheriades primus</i>	EU851532	EU851638	HQ995902	HQ995995	HQ996092

Appendix 5. Continued.

Taxa	EF1 α	Opsin	CAD	NAK	28S
<i>Ashmeadiella aridula</i>	EU851535	EU851641	HQ995903	GU245171	GU244858
<i>Atoposmia mirifica</i>	EU851541	EU851647	HQ995904	HQ995996	HQ996093
<i>Chelostoma florissomme</i>	EU851546	EU851652	HQ995905	HQ995997	HQ996094
<i>Haetosmia brachyura</i>	HQ995748	HQ995822	HQ995906	HQ995998	HQ996095
<i>Heriades crucifer</i>	EU851555	EU851661	DQ067194	GU245168	GU244855
<i>Hofferia schmidedeknechti</i>	EU851556	EU851662	HQ995907	HQ995999	HQ996096
<i>Hoplitis adunca</i>	EU851572	EU851678	HQ995908	HQ996000	HQ996097
<i>Ochroeriades fasciatus</i>	EU851590	EU851696	HQ995909	HQ996001	HQ996098
<i>Osmia lignaria</i>	EU851610	EU851715	HQ995910	GU245169	GU244856
<i>Othinosmia globicola</i>	EU851616	EU851721	HQ995911	HQ996002	HQ996099
<i>Protosmia humeralis</i>	EU851621	EU851726	HQ995913	HQ996004	HQ996101
<i>Pseudoheriades moricei</i>	EU851622	EU851727	HQ995914	HQ996005	HQ996102
<i>Stenoheriades asiaticus</i>	EU851623	EU851728	HQ995915	HQ996006	HQ996103
<i>Hoplitis minima</i>	EU851625	EU851730	EU851520	—	—
<i>Wainia eremoplana</i>	EU851626	EU851731	HQ995916	HQ996007	HQ996104
<i>Noteriades sp.</i>	EU851589	EU851695	HQ995900	HQ995993	HQ996090
<i>Coelioxys octodentata</i>	KX428310	KX428056	KX428226	KX428394	KX428151
<i>Megachile pugnata</i>	AY585147	HQ995818	DQ067196	HQ995990	HQ996087
<i>Megachile angelarum</i>	HQ995727	HQ995800	HQ995878	GU245163	GU244851
<i>Megachile albisecta</i>	EU851529	EU851635	HQ995881	HQ995974	HQ996071
<i>Radoszkowiskiana rufiventris</i>	HQ995747	HQ995821	HQ995901	HQ995994	HQ996091

Appendix 5. Continued.

Phylogeny of Megachilini						
Taxa	EF1 α	Opsin	CAD	NAK	28S	
<i>Trichothurgus herbsti</i>	HQ995695	HQ995767	HQ995843	GU245160	GU244848	
<i>Microthurge</i> sp.	HQ995694	HQ995766	HQ995842	GU245161	GU244849	
<i>Aspidosmia volkmanni</i>	HQ995702	HQ995774	HQ995851	HQ995946	HQ996043	
<i>Trachusa larreae</i>	HQ995719	HQ995791	HQ995868	GU245154	GU244842	
<i>Hoplitis adunca</i>	EU851572	EU851678	HQ995908	HQ996000	HQ996097	
<i>Chelostoma florissome</i>	EU851546	EU851652	HQ995905	HQ995997	HQ996094	
<i>Dioxys moesta</i>	HQ995696	HQ995768	HQ995845	HQ995940	HQ996037	
<i>Aztecantidium tenochtitlanicum</i>	—	KX060844	KX060906	KU976189	KU976249	
<i>Radoszkowskiana rufiventris</i>	HQ995747	HQ995821	HQ995901	HQ995994	HQ996091	
<i>Coelioxys decipiens</i>	KX428313	KX428059	KX428229	KX428397	KX428154	
<i>Noteriades</i> sp.	EU851589	EU851695	HQ995900	HQ995993	HQ996090	
<i>Megachile (Rhodomegachile)</i> sp.	HQ995744	HQ995817	HQ995897	HQ995989	HQ996086	
<i>M. (Matangapis) alticola</i>	—	—	—	—	KX580315	
<i>M. (Chelostomoda)</i> sp.	HQ995726	HQ995799	—	HQ995971	HQ996068	
<i>M. (Heriadopsis)</i> sp.	—	—	—	—	KX580316	
<i>M. (Hackeriapis)</i> sp. 1	KX428356	KX428102	KX428272	KX428438	KX428195	
<i>M. (Chelostomoidella) spinotulata</i>	HQ995728	HQ995801	HQ995879	HQ995972	HQ996069	
<i>M. (Chelostomoides) angularum</i>	HQ995727	HQ995800	HQ995878	GU245163	GU244851	
<i>M. (Thaumatoma) remeata</i>	HQ995745	HQ995819	HQ995898	HQ995991	HQ996088	
<i>M. (Stenomegachile) chelostomoides</i>	KX428383	KX428129	KX428299	KX428461	KX428218	
<i>M. (Maximegachile) maxillosa</i>	HQ995737	HQ995810	HQ995890	HQ995983	HQ996080	
<i>M. (Chalicodomoides) aethiops</i>	HQ995725	HQ995798	HQ995877	HQ995970	HQ996067	

Appendix 5. Continued.

Taxa	EFl α	Opsin	CAD	NAK	28S
<i>M. (Carinula) decemsignata</i>	KX428325	KX428071	KX428242	KX428409	KX428166
<i>M. (Callomegachile) sculpturalis</i>	HQ995724	HQ995797	HQ995875	HQ995968	HQ996065
<i>M. (Alocanthodon) sp.</i>	KX428318	KX428064	KX428235	KX428402	KX428159
<i>M. (Gronoceras) bombiformis</i>	HQ995733	HQ995806	HQ995886	HQ995979	HQ996076
<i>M. (Lophanthodon) dimidiata</i>	KX428359	KX428105	KX428275	KX428441	KX428198
<i>M. (Austrochile) sp.</i>	HQ995723	HQ995796	HQ995874	HQ995967	HQ996064
<i>M. (Parachalicodoma) sp.</i>	KX428370	KX428116	KX428286	KX428448	KX428205
<i>M. manicata</i>	KX428330	KX428076	KX428247	KX428413	KX428170
<i>M. (Chalicodoma) parietina</i>	EU851530	EU851636	HQ995876	HQ995969	HQ996066
<i>M. (Allochalicodoma) lefebvrei</i>	KX428329	KX428075	KX428246	KX428412	KX428169
<i>M. (Largella) floralis</i>	HQ995735	HQ995808	HQ995888	HQ995981	HQ996078
<i>M. (Pseudomegachile) ericetorum</i>	HQ995742	HQ995815	HQ995895	GU245165	GU244853
<i>M. (Neglectella) laminata</i>	KX428366	KX428112	KX428282	KX428444	KX428201
<i>M. (Dimais) leucospitura</i>	KX428336	KX428082	KX428252	KX428418	KX428175
<i>M. (Cesaongoa) sp.</i>	KX428328	KX428074	KX428245	KX428411	—
<i>M. (Creightonella) albisecta</i>	EU851529	EU851635	HQ995881	HQ995974	HQ996071
<i>M. (Creightonella) cornigera</i>	KX428334	KX428080	KX428250	KX428416	KX428173
<i>M. (Mitchellapis) fabricator</i>	HQ995740	HQ995813	HQ995893	HQ995986	HQ996083
<i>M. pugnata</i>	AY585147	HQ995818	DQ067196	HQ995990	HQ996087
<i>M. (Grosapis) cockerelli</i>	KX428355	KX428101	KX428271	KX428437	KX428194
<i>M. (Eumegachile) bombycina</i>	KX428337	KX428083	KX428253	KX428419	KX428176
<i>M. (Litomegachile) texana</i>	HQ995736	HQ995809	HQ995889	HQ995982	HQ996079
<i>M. (Neoneutrigharaea) rotundata</i>	XM003705302	XM003705921	XM012287299	XM012290255	—

Appendix 5. Continued.

Taxa	EFl α	Opsin	CAD	NAK	28S
<i>M. (Eurytmella) aff. eurymera</i>	KX428338	KX428084	KX428254	KX428420	KX428177
<i>M. (Argyropile) parallela</i>	HQ995722	HQ995795	HQ995873	HQ995966	HQ996063
<i>M. (Amegachile) cf. bituberculata</i>	KX428319	KX428065	KX428236	KX428403	KX428160
<i>M. (Xeromegachile) neoadensis</i>	HQ995739	HQ995812	HQ995892	HQ995985	HQ996082
<i>M. (Phaenosarus) fortis</i>	KX428371	KX428117	KX428287	KX428449	KX428206
<i>M. (Xanthosarus) lagopoda</i>	KX428390	KX428136	KX428306	—	—
<i>M. (Leptorachis) petulans</i>	KX428357	KX428103	KX428273	KX428439	KX428196
<i>M. (Pseudocentron) sp.</i>	KX428372	KX428118	KX428288	KX428450	KX428207
<i>M. (Melanosarus) sp.</i>	KX428365	KX428111	KX428281	KX428443	KX428200
<i>M. (Acentron) sp.</i>	KX428316	KX428062	KX428233	KX428400	KX428157
<i>M. (Paracella) sp.</i>	KX428368	KX428114	KX428284	KX428446	KX428203
<i>M. (Tylomegachile?) sp.</i>	KX428384	KX428130	KX428300	KX428462	KX428219
<i>M. (Aethomegachile) conjuncta</i>	HQ995720	HQ995793	HQ995871	HQ995964	HQ996061
<i>M. (Megella) pseudomonticola</i>	KX428364	KX428110	KX428280	KX428442	KX428199
<i>M. (Dasymegachile) sp.</i>	KX428335	KX428081	KX428251	KX428417	KX428174
<i>M. (Cressoniella) zapoteca</i>	HQ995730	HQ995803	HQ995882	HQ995975	HQ996072
<i>M. (Austromegachile) sp.</i>	KX428322	KX428068	KX428239	KX428406	KX428163
<i>M. (Ptilosarus) microsoma</i>	HQ995743	HQ995816	HQ995896	HQ995988	HQ996085
<i>M. (Neochelymia?) sp.</i>	KX428367	KX428113	KX428283	KX428445	KX428202
<i>M. (Stelodides) euzona</i>	KX428382	KX428128	KX428298	KX428460	KX428217
<i>M. (Chrysosarus) sp.</i>	HQ995729	HQ995802	HQ995880	HQ995973	HQ996070

Appendix 6. Organization of genera in tribe Megachilini, with synonyms indicated. For subgenera of *Megachile* refer to Appendix 7.

Genus † <i>Chalicodomopsis</i> Engel	Genus <i>Chelostomoides</i> Robertson
Genus <i>Noteriades</i> Cockerell	Subgenus <i>Chelostomoides</i> Robertson
Genus <i>Gronoceras</i> Cockerell	= <i>Oligotropus</i> Robertson
= <i>Berna</i> Friese	= <i>Gnathodon</i> Robertson
= <i>Digronoceras</i> Cockerell	= <i>Sarogaster</i> Robertson
Genus <i>Matangapis</i> Baker & Engel	Subgenus <i>Chelostomoidella</i> Snelling
Genus <i>Lophanthedon</i> Gonzalez & Engel	Genus <i>Chalicodoma</i> Lepeletier de Saint Fargeau
Genus <i>Coelioxys</i> Latreille	= <i>Euchalicodoma</i> Tkalčú
Genus <i>Radoszkowskiana</i> Popov	= <i>Allochalicodoma</i> Tkalčú
Genus <i>Carinula</i> Michener & al.	= <i>Parachalicodoma</i> Tkalčú, <i>nomen praeoccupatum</i>
= <i>Carinella</i> Pasteels, <i>nomen praeoccupatum</i>	= <i>Heteromegachile</i> Rebmann
Genus <i>Thaumatostoma</i> Smith	= <i>Katamegachile</i> Rebmann
Genus <i>Austrochile</i> Michener	= <i>Xenochalicodoma</i> Tkalčú
Genus <i>Rozenapis</i> Gonzalez & Engel, n. gen.	Genus <i>Megachile</i> Latreille (<i>vide</i> Appendix 7)
Genus <i>Rhodomegachile</i> Michener	
Genus <i>Chalicodomoides</i> Michener	<i>Incertae sedis</i>
Genus <i>Hackeriapis</i> Cockerell	Genus <i>Stellenigris</i> Meunier
Genus <i>Dinavis</i> Pasteels	
Genus <i>Cesacongoa</i> Koçak & Kemal	
= <i>Cuspidella</i> Pasteels, <i>nomen praeoccupatum</i>	
Genus <i>Neglectella</i> Pasteels	
= <i>Neochalicodoma</i> Pasteels	
Genus <i>Maximegachile</i> Guiglia & Pasteels	
Genus <i>Schizomegachile</i> Michener	
Genus <i>Callomegachile</i> Michener	
Subgenus <i>Alocanthedon</i> Engel & Gonzalez	
Subgenus <i>Callomegachile</i> Michener	
= <i>Orientocressonliella</i> Gupta	
Subgenus <i>Eumegachilana</i> Michener	
Subgenus <i>Morphella</i> Pasteels	
Genus <i>Saucrochile</i> Gonzalez & Engel, n. gen.	
Genus <i>Cremnochile</i> Gonzalez & Engel, n. gen.	
Genus <i>Stenomegachile</i> Pasteels	
Genus <i>Pseudomegachile</i> Friese	
Subgenus <i>Archimegachile</i> Alfken	
Subgenus <i>Cestella</i> Pasteels	
Subgenus <i>Largella</i> Pasteels	
Subgenus <i>Parachalicodoma</i> Pasteels	
Subgenus <i>Pseudomegachile</i> Friese	
= <i>Pseudomegalochila</i> Schulz, <i>nomen vanum</i>	
Subgenus <i>Xenomegachile</i> Rebmann	
Genus <i>Heriadopsis</i> Cockerell	

Appendix 7. Organization of genus *Megachile* Latreille, with synonyms of subgenera indicated.

Subgenus <i>Chelostomoda</i> Michener = <i>Neoashmeadiella</i> Gupta	Subgenus <i>Addendella</i> Mitchell
Subgenus <i>Mitchellapis</i> Michener	Subgenus <i>Digitella</i> Pasteels
Subgenus <i>Creightonella</i> Cockerell = <i>Creightoniella</i> Pasteels, <i>nomen vanum</i>	Subgenus <i>Tylomegachile</i> Moure
Subgenus <i>Sayapis</i> Titus = <i>Gnathocera</i> Provancher, <i>nomen praeoccupatum</i> = <i>Ceratias</i> Robertson = <i>Schrottkyapis</i> Mitchell, n. syn.	Subgenus <i>Austromegachile</i> Mitchell = <i>Holcomegachile</i> Moure
Subgenus <i>Paracella</i> Michener = <i>Paracella</i> Pasteels, <i>nomen invalidum</i>	Subgenus <i>Neochelynia</i> Schrottky = <i>Neomegachile</i> Mitchell
Subgenus <i>Amegachile</i> Friese = <i>Callochila</i> Michener = <i>Platychile</i> Michener, <i>nomen nudum</i>	Subgenus <i>Zonomegachile</i> Mitchell
Subgenus <i>Eurymella</i> Pasteels = <i>Platysta</i> Pasteels	Subgenus <i>Chaetochile</i> Mitchell
Subgenus <i>Argyropile</i> Mitchell	Subgenus <i>Rhyssomegachile</i> Mitchell
Subgenus <i>Phaenosarus</i> Mitchell	Subgenus <i>Chalepochile</i> Gonzalez & Engel
Subgenus <i>Megachiloides</i> Mitchell = <i>Xeromegachile</i> Mitchell = <i>Derotropis</i> Mitchell	Subgenus <i>Aporiochile</i> Gonzalez & Engel
Subgenus <i>Moureapis</i> Raw = <i>Moureana</i> Mitchell, <i>nomen praeoccupatum</i> = <i>Willinkella</i> Laroca <i>et al.</i> , <i>nomen nudum</i> = <i>Acentrina</i> Schlindwein, <i>nomen nudum</i>	Subgenus <i>Ptilosarus</i> Mitchell
Subgenus <i>Leptorachis</i> Mitchell = <i>Grafella</i> Mitchell	Subgenus <i>Ptilosaroides</i> Mitchell
Subgenus <i>Leptorachina</i> Mitchell	Subgenus <i>Chrysosarus</i> Mitchell = <i>Dactylomegachile</i> Mitchell = <i>Stelodides</i> Moure
Subgenus <i>Acentron</i> Mitchell	Subgenus <i>Dasymegachile</i> Mitchell
Subgenus <i>Pseudocentron</i> Mitchell	Subgenus <i>Trichurochile</i> Mitchell
Subgenus <i>Melanosarus</i> Mitchell	Subgenus <i>Cressionella</i> Mitchell
Subgenus <i>Neocressoniella</i> Gupta	Subgenus <i>Grosapis</i> Mitchell
Subgenus <i>Megella</i> Pasteels	Subgenus <i>Eumegachile</i> Friese
Subgenus <i>Eutricharaea</i> Thomson = <i>Paramegachile</i> Friese = <i>Paramegalochila</i> Schulz, <i>nomen vanum</i> = <i>Andrygonella</i> Cockerell = <i>Perezia</i> Ferton = <i>Fertonella</i> Cockerell = <i>Neoeutricharaea</i> Rebmann = <i>Melanoeutricharaea</i> Tkalcü = <i>Anodonteutricharaea</i> Tkalcü	Subgenus <i>Megachile</i> Latreille = <i>Megalochila</i> Schulz, <i>nomen vanum</i> = <i>Anthemois</i> Robertson = <i>Cyphopyga</i> Robertson
Subgenus <i>Aethomegachile</i> Engel & Baker	
Subgenus <i>Litomegachile</i> Mitchell	
Subgenus <i>Xanthosarus</i> Robertson = <i>Delomegachile</i> Viereck = <i>Macromegachile</i> Noskiewicz	



Journal of Melittology

A Journal of Bee Biology, Ecology, Evolution, & Systematics

The *Journal of Melittology* is an international, open access journal that seeks to rapidly disseminate the results of research conducted on bees (Apoidea: Anthophila) in their broadest sense. Our mission is to promote the understanding and conservation of wild and managed bees and to facilitate communication and collaboration among researchers and the public worldwide. The *Journal* covers all aspects of bee research including but not limited to: anatomy, behavioral ecology, biodiversity, biogeography, chemical ecology, comparative morphology, conservation, cultural aspects, cytogenetics, ecology, ethnobiology, history, identification (keys), invasion ecology, management, melittopalynology, molecular ecology, neurobiology, occurrence data, paleontology, parasitism, phenology, phylogeny, physiology, pollination biology, sociobiology, systematics, and taxonomy.

The *Journal of Melittology* was established at the University of Kansas through the efforts of Michael S. Engel, Victor H. Gonzalez, Ismael A. Hinojosa-Díaz, and Charles D. Michener in 2013 and each article is published as its own number, with issues appearing online as soon as they are ready. Papers are composed using Microsoft Word® and Adobe InDesign® in Lawrence, Kansas, USA.

Interim Editor

Victor H. Gonzalez
University of Kansas

Assistant Editors

Victor H. Gonzalez
University of Kansas

Claus Rasmussen
Aarhus University

Cory S. Sheffield
Royal Saskatchewan Museum

Founding Editor & Editor Emeritus

Michael S. Engel
University of Kansas

Journal of Melittology is registered in ZooBank (www.zoobank.org), and archived at the University of Kansas and in Portico (www.portico.org).

<http://journals.ku.edu/melittology>
ISSN 2325-4467